

**DOKUZ EYLÜL UNIVERSITY  
GRADUATE SCHOOL OF NATURAL AND APPLIED  
SCIENCES**

**PRODUCTION AND INDUSTRIAL  
APPLICATION OF NANOSTRUCTURED FLAME  
RETARDANT REINFORCED COMPOSITE  
MATERIALS**

**by  
Serdar YILDIRIM**

**July, 2013  
İZMİR**

**PRODUCTION AND INDUSTRIAL  
APPLICATION OF NANOSTRUCTURED FLAME  
RETARDANT REINFORCED COMPOSITE  
MATERIALS**

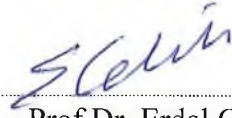
**A Thesis Submitted to the  
Graduate School of Natural and Applied Sciences of Dokuz Eylül University  
In Partial Fulfillment of the Requirements for the Degree of Master of Science  
in Metallurgical and Material Science Engineering**

**by  
Serdar YILDIRIM**

**July, 2013  
İZMİR**

## M.Sc THESIS EXAMINATION RESULT FORM

We have read the thesis entitled **PRODUCTION AND INDUSTRIAL APPLICATION OF NANOSTRUCTURED FLAME RETARDANT REINFORCED COMPOSITE MATERIALS** completed by **SERDAR YILDIRIM** under supervision of **PROF.DR. ERDAL ÇELİK** and we certify that in our opinion it is fully adequate, in scope and in quality, as a thesis for the degree of Master of Science.



Prof.Dr. Erdal ÇELİK

Supervisor



Prof. Dr. Kadriye Ertekin

(Jury Member)



Yrd. Doç. Dr. Aylin Z.  
Albayrak

(Jury Member)



Prof.Dr. Ayşe OKUR

Director

Graduate School of Natural and Applied Sciences

## ACKNOWLEDGMENTS

First of all, I would like to express my deepest gratitude to my advisor Prof. Dr. Erdal elik for his constructive ideas and scientific guidance throughout the course of this thesis. I am proud to have had such an excellent advisor.

I wish to extend special thanks to Metin Yurddařkal, Tuncay Dikici and E. Burak Ertuř for sincere assistance and support at all times. I would like to thank Fatma Bakal, Mustafa Erol and Savař ztürk for their kind friendship and helps. I would like to thank Teknobim Company and my boss Tuncer Sigalı supplying of materials used in my study and to support financial and moral. I would like to thank my home friends Fikri Emek, Nihat zcan, Furkan nlü and Ramazan Erdoęan for their kind friendship and helps. I would also like to express my gratitude to each person that it would be impossible to name all here.

Finally, I reserve my most sincere thanks to my family for their concern, confidence and support.

**Serdar Yıldırım**

# PRODUCTION AND INDUSTRIAL APPLICATION OF NANOSTRUCTURED FLAME RETARDANT REINFORCED COMPOSITE MATERIALS

## ABSTRACT

Paints used in many areas of daily life are utilized with the aim of creating in surface protection and decorative designs of materials. These paints contain material susceptible to fire such as polymeric binders, organic solvents. Because of this reason, paints easily burn. In this study, flame retardant properties of plastic paint material were investigated and tried to be developed. In this context, composite materials were obtained by adding different amounts of environmentally friendly (hologen-free) and nanosized flame retardant materials such as huntite/hydromagnesite, antimony (III) oxide and boric acid to paint material. And then these composite materials were characterized by XRD, XPS, FT-IR, DTA-TG, SEM, surface roughness and hardness testing machines. Candle flame test standards were also performed to examine flame retardant properties of these composite materials. After the results of the performed tests, composite materials were determined to exhibit excellent flame retardant properties.

**Keywords:** Flame retardant, paints, polymer, nanocomposites

# NANOYAPILI ALEV GECİKTİRİCİ TAKVİYE EDİLMİŞ KOMPOZİT MALZEMELERİN ÜRETİMİ VE ENDÜSTRİYEL UYGULAMASI

## ÖZ

Boyalar, çeşitli malzemelerin yüzeylerini korumak ve dekoratif tasarımlar oluşturmak amacıyla ile günlük hayatta yaygın olarak kullanılmaktadır. Bu boyalar aleve karşı dayanıksız polimerik bağlayıcılar, organik çözücüler vb. malzemeler içermektedir. Dolayısıyla bu boyalar kolayca tutuşabilmektedir. Bu çalışmada plastik boya malzemesinin alev geciktiricilik özellikleri incelendi ve geliştirilmeye çalışıldı. Bu kapsamda boya malzemelerine çevre dostu (halojen içermeyen), nanoboyutlu huntit/hidromanyezit, antimon oksit ve borik asit bileşikleri farklı miktarlarda ilave edilerek kompozit malzemeler elde edildi. Üretilen kompozit malzemelerin karakterizasyon çalışmaları; XRD, XPS, FT-IR, DTA-TG, SEM, yüzey profilometre ve nanoindentasyon cihazları ile yapıldı. Ayrıca bu kompozit malzemelere çalışma konumuzun amacı olan alev geciktiricilik özelliklerinin belirlenmesi için mum alevi testi yapıldı. Yapılan testler sonucunda kompozit malzemelerin mükemmel alev geciktirici özellik sergilediği belirlendi.

**Anahtar Kelimeler:** Alev geciktirme, boyalar, polimer, nanokompozit

## CONTENTS

	Page
M.Sc THESIS EXAMINATION RESULT FORM .....	ii
ACKNOWLEDGEMENTS .....	iii
ABSTRACT .....	iv
ÖZ .....	v
LIST OF FIGURES .....	ix
LIST OF TABLES .....	xi
<b>CHAPTER ONE – INTRODUCTION .....</b>	<b>1</b>
1.1 General .....	1
1.2 Organization of the Thesis .....	6
<b>CHAPTER TWO – THEORITICAL BACKGROUND .....</b>	<b>8</b>
2.1 Polymers .....	8
2.1.1 Polymer Combustion .....	8
2.2 Flame Retardant Materials and Mechanisms .....	11
2.2.1 Halogen-Containing Flame Retardants .....	13
2.2.2 Antimony (III) oxide (Sb <sub>2</sub> O <sub>3</sub> ) .....	16
2.2.3 Phosphorus-Based Flame Retardants .....	20
2.2.4 Nitrogen-Based Flame Retardants .....	21
2.2.5 Silicon-Containing Flame Retardants .....	23
2.2.6 Intumescent Coatings .....	24
2.2.7 Boron-Containing Flame Retardants .....	25
2.2.8 Inorganic Hydroxides Flame Retardants .....	27
2.2.8.1 Hydroxycarbonates .....	32
2.2.9 Synergism .....	34
2.2.10 Criteria for Selection of Flame Retardants .....	35
2.3 Environmental Concerns .....	36

2.4 Nanocomposites.....	40
2.5 Fire Tests and Standards.....	41
2.5.1 Limited Oxygen Index (LOI).....	42
2.5.2 UL 94 Vertical Test.....	43
2.5.3 Cone Calorimeter.....	45
2.6 Potential Applications of Flame Retardant Materials.....	47
<b>CHAPTER THREE-EXPERIMENTAL PROCEDURE.....</b>	<b>50</b>
3.1 Purpose.....	50
3.2 Materials.....	51
3.2.1 Matrix Material.....	51
3.2.2 Reinforcing Materials.....	52
3.3 Ball Milling of Reinforcing Materials.....	53
3.4 Production of Composite Coatings/Paints.....	54
3.5. Characterization of Reinforcing Materials and Composites.....	56
3.5.1 Particle Size Distribution.....	56
3.5.2 X-Ray Diffractometer (XRD).....	56
3.5.3 X-Ray Photoelectron Spectroscopy (XPS).....	58
3.5.4 Fourier Transform Infrared Spectroscopy (FT-IR).....	59
3.5.5 Scanning Electron Microscopy (SEM).....	61
3.5.6 Differential Thermal Analysis-Thermogravimetry (DTA-TG).....	61
3.5.7 Surface Profilometer (Roughness).....	62
3.5.8 Mechanical Tests.....	62
3.6 Flame Retardant Test.....	66
<b>CHAPTER FOUR-RESULTS AND DISCUSSION.....</b>	<b>68</b>
4.1 Particle Size Distribution.....	68
4.2 Phase Analysis.....	69
4.3 Elemental Analysis.....	73
4.4 FT-IR Analysis.....	75



4.5 SEM Analysis.....	78
4.6 DTA-TG Analysis.....	81
4.7 Surface Roughness.....	85
4.8 Mechanical Properties.....	86
4.9 Flame Retardant Properties.....	89
<b>CHAPTER FIVE-CONCLUSIONS AND FUTURE PLANS.....</b>	<b>98</b>
5.1 General Results.....	98
5.2 Future Plans.....	101
<b>REFERENCES.....</b>	<b>103</b>

## LIST OF FIGURES

	<b>Page</b>
Figure 1.1 CO formation of PP compounds with different flame retardants.....	5
Figure 2.1 Principle of the combustion cycle.....	9
Figure 2.2 Schematic representation of a burning polymer.....	11
Figure 2.3 Dependence of total flaming time of polypropylene measured in a UL-94 test on bromine content for an aliphatic brominated flame retardant and an aromatic brominated flame retardant.....	15
Figure 2.4 Reaction scheme occurring between antimony oxide and halogen compounds.....	18
Figure 2.5 Thermal decomposition of melamine phosphate.....	22
Figure 2.6 Char and intumescence formation.....	25
Figure 2.7 Thermogravimetry of commercial zinc borates.....	26
Figure 2.8 Thermogravimetry of ATH and Mg(OH) <sub>2</sub> .....	30
Figure 2.9 Differential scanning calorimetry of ATH and Mg(OH) <sub>2</sub> .....	31
Figure 2.10 Smoke emissions from selected polypropylene compounds filled with 50wt % of filler.....	31
Figure 2.11 Experimental set-up for LOI measurement.....	42
Figure 2.12 Experimental set-up for the UL94 V flammability test.....	44
Figure 2.13 Experimental set-up for a cone calorimetry measurement.....	46
Figure 3.1 The high energy ball milling machine.....	54
Figure 3.2 Diffraction of x-rays by planes of atoms (A-A' and B-B').....	57
Figure 3.3 Schematic diagram of an x-ray diffractometer; T: x-ray source, S: specimen, C: detector, and O: the axis around which the specimen and detector rotate.....	58
Figure 3.4 Rough schematic of XPS physics.....	59
Figure 3.5 Schematic representation of an ATR system.....	60
Figure 3.6 SEM images of the tips of (a) Berkovich, (b) Knoop, and (c) cube-corner indenters used for nanoindentation testing. The tip radius of a typical diamond pyramidal indenter is in the order of 100 nm.....	64

Figure 3.7 A schematic representation of load versus displacement during nanoindentation.....	65
Figure 3.8 Nanoindentation system.....	65
Figure 3.9 Needle flame test machine.....	66
Figure 3.10 (a) Flame adjustment and (b) test position.....	67
Figure 4.1 Particle size distribution of huntite/hydromagnesite mineral after and before milling process.....	68
Figure 4.2 Particle size distribution of antimony (III) oxide mineral after and before milling process.....	69
Figure 4.3 XRD pattern of huntite/hydromagnesite mineral.....	70
Figure 4.4 XRD pattern of antimony (III) oxide mineral.....	70
Figure 4.5 XRD patterns of pure, 10H, 10B and 10A samples.....	71
Figure 4.6 XRD patterns of 3A3B, 3A7H, 3B7H and 1A2B7H samples.....	72
Figure 4.7 XPS results of (a) huntite/hydromagnesite mineral and (b) antimony (III) oxide powders.....	73
Figure 4.8 XPS results of (a) pure, (b) 10%H, (c) 10%B, (d) 10%A, (e) 3B7H, (f) 3A7H, (g) 3A3B and (h) 1A2B7H samples.....	74
Figure 4.9 FT-IR analysis of (a) 10%H, (b) 10%B, (c) 10%A, (d) 3B7H, (e) 3A7H, (f) 3A3B and (g) 1A2B7H composite samples.....	76
Figure 4.10 SEM micrographs of (a) pure dye, (b) 10%H, (c) 10%B, (d) 10%A, (e) 3B7H, (f) 3A7H, (g) 3B3A and (h) 1A2B7H samples.....	78
Figure 4.11 Thermal behaviours of (a) pure, (b) 10%H, (c) 10%B, (d) 10%A, (e) 3B7H, (f) 3A7H, (g) 3A3B and (h) 1A2B7H samples.....	82
Figure 4.12 Elasticity modulus of (a) pure dye, (b) 10%H, (c) 10%B, (d) 10%A, (e) 3B7H, (f) 3A7H, (g) 3B3H and (h) 1A2B7H samples.....	88
Figure 4.13 Hardness of (a) pure dye, (b) 10%H, (c) 10%B, (d) 10%A, (e) 3B7H, (f) 3A7H, (g) 3B3H and (h) 1A2B7H samples.....	88

## LIST OF TABLES

	<b>Page</b>
Table 2.1 The advantages and disadvantages of halogen-containing flame retardants.....	14
Table 2.2 The advantages and disadvantages of phosphorus-containing flame retardants.....	21
Table 2.3 Principle candidate flame retardant fillers.....	28
Table 2.4 The advantages and disadvantages of inorganic hydroxides flame retardants.....	33
Table 2.5 REACH status for the main halogenated flame retardants.....	39
Table 2.6 Flash-ignition temperatures, self-ignition temperatures and correlated LOI values for selected representative polymers.....	43
Table 2.7 Classification of materials for the UL 94 V flammability test.....	45
Table 2.8 Flame retardant (FR) market application.....	47
Table 2.9 Examples of flame resistance standards.....	48
Table 3.1 Formulas and properties of huntite & hydromagnesite.....	53
Table 3.2 Classified of sample names, code and properties of prepared composite coatings/paints.....	55
Table 4.1 Surface roughness values of pure and reinforced composite coatings/paints.....	86
Table 4.2 Mechanical properties of pure and reinforced composite coatings/paints.....	87
Table 4.3 Flame retardancy results of pure and composite coatings/paints.....	90

# CHAPTER ONE

## INTRODUCTION

### 1.1 General

Together with numerous advantages that synthetic polymeric materials provide to society in everyday life, there is one obvious disadvantage related to the high flammability of many synthetic polymers. Polymers are used in manufacturing not only bulk parts but also films, fibers, coatings, and foams, and these thin objects are even more combustible than molded parts (Alexander & Charles, 2007). Polymers, being hydrocarbons, combust through a process that begins as heat in the pre-ignition phase and progresses to fire, which breaks down their long-chain structure into volatile hydrocarbons, hydrogen, and hydroxyl-free radicals. These elements formed during decomposition are high in energy and react with oxygen, releasing heat and causing fire to spread (Joseph & Serbaroli, 2006).

Fire is a unique destructive force of nature; what it touches cannot easily be repaired, rebuilt, or restored to its original form (Charles & Alexander, 2010). Fires frequently happen all over the world every day. It kills people, causes huge peculiarly losses for the economy and destroys unique goods such as art works (Weber, 1999). According to fire statistics, more than 12 million fires break out every year in the United States, Europe, Russia, and China, killing some 166,000 people and injuring several hundreds of thousands. Even though calculating the direct worldwide losses and costs of fire is difficult, \$500 million is an estimate based on some national data (Manor-Orit, 2005). According to Turkish Statistical Institute, in Turkey, the fire occurred over 9,000 between 1988 and 2008 and as a result of these fires, 3,237 people lost their lives. In many applications, areas risk of fire cannot be ruled out, therefore products should be well-protected against fire. The open question in a lot of cases is how to ensure such levels of protection against fire attacks. Flame retardant materials play an important role in this issue. This research reviews these materials, especially plastics and their functions (Yılmaz, 2007).

Flame retardancy means that something has been done to a material so that when exposed to a flame, either the material will retard the growth and propagation of that flame, or it will retard (slow) the growth and propagation of any flames that may come from the material once it has been ignited. Fire retardant does not mean that the material will not burn, but rather that it will be harder to burn. In some cases, the flame-retardant material may self-extinguish after being ignited if the external flame is removed, but in other cases the flame-retardant approach assumes the material will stay lit once ignited, and will instead just burn slowly (Charles & Alexander, 2010).

Flame retardants are added to polyolefins, polycarbonate, polyamides, polyester, and other polymers to increase resistance to ignition, reduce flame spread, suppress smoke formation, and prevent a polymer from dripping. The primary goal is to delay the ignition and burning of materials, allowing people more time to escape the affected area. A secondary consideration is to limit property damage. Plastics containing flame retardants are found in homes and office buildings, cars and mass transit vehicles, furnishings, fibers, household appliances, and many other areas and applications (Joseph & Serbaroli, 2006).

All flame retardants act either in the vapour phase or the condensed phase through a chemical and/or physical mechanism to interfere with the combustion process during heating, pyrolysis, ignition or flame spread. Once the flame retardant materials are looked at related markets, they are classified as two main categories; halogenated and halogen free flame retardants. The most commercially viable flame retardants include brominated and chlorinated types, phosphorus based types, and metallic oxides. To illustrate, the incorporation of fillers mainly acts to dilute the polymer and reduce the concentration of decomposition gases. Hydrated fillers also release non-flammable gases or decompose endothermically to cool the pyrolysis zone at the combustion surface. Halogen, phosphorus and antimony act in the vapour phase by a radical mechanism to interrupt the exothermic processes and to suppress combustion. Phosphorus can also act in the condensed phase promoting char formation on the surface, which acts as a barrier to inhibit gaseous products from diffusing to the flame and to shield the polymer surface from heat and air. Another

major category of flame retarding mechanism is that known as 'intumescent', in which materials swell when exposed to fire or heat to form a porous foamed mass, usually carbonaceous, which in turn acts as a barrier to heat, air and pyrolysis product (Shui-Yu & Ian, 2002).

Looking at the studies in the literature, for example, Song et al. (2004), examined preparation and properties of non-halogen flame-retarded polyamide6/organoclay nanocomposite. Halogen-free flame-retarded polyamide6/organoclay (PA6/OMT) nanocomposite was prepared by using magnesium hydroxide (MH) and red phosphorus (RP) as a flame retardant and organoclay (OMT) as synergist via a melt blend technique. The effects of organoclay on the mechanical properties and flammability of the PA6 were investigated. The results showed higher mechanical and flame-retarded properties of the nanocomposite as compared with flame-retarded PA6 and a synergistic effect among OMT, MH and RP.

Sain et al. (2004), studied by horizontal burning rate and oxygen index tests flammability of polypropylene, sawdust/rice husk filled polypropylene composites and flame retarding effect of magnesium hydroxide for these composites. Effect of flame-retardants such as boric acid or zinc borate in combination with magnesium hydroxide also studied. Characterization of composites was determined by XRD, SEM and the wetting angle. LOI of polyethylene was obtained 32.5% by addition 60% Mg(OH)<sub>2</sub>. It was found that magnesium hydroxide can effectively reduce the flammability (almost 50%) of natural fibre filled polypropylene composites. No synergetic effect was observed when magnesium hydroxide was used in combination with boric acid and zinc borate.

Martin et al. (2006), synthesized and copolymerized to test the influence of boron on the properties of two novel difunctional styrenic monomers – 2,2-bis(4-vinylbenzyl)propane-1,3-diol and 5,5-bis(4-vinylbenzyl)-2-phenyl-[1,3,2] dioxaborin materials. Materials were characterized by elemental analysis, mass spectrometry, FT-IR and <sup>1</sup>H, <sup>13</sup>C NMR spectroscopy. The copolymers with boron showed higher thermal stability and char yields than polystyrene or homologous copolymers without

boron. The thermal degradation of boron-containing styrenic polymers was studied by FT-IR and boric acid was detected at high temperatures. LOI values increased with boron content.

Kuan et al. (2008), in themselves work; silane was grafted on expandable graphite via a free-radical reaction. The modified expandable graphite has an -OEt functional group which reacts with TEOS and PMMA that was modified via a sol-gel reaction using a coupling agent that contains silicon. Synergism between silicon flame retardant and expandable graphite increased the flame retardance of the materials. Expandable graphite was functionalized using a coupling agent to increase the interactive force between the organic and inorganic phases. It enhanced the thermal stability of the composites.

Fang et al. (2008), prepared by melt nanocomposites based on polypropylene (PP) and fullerene C<sub>60</sub> (in the range of 0.5–2 wt %). It was observed that C<sub>60</sub> could not only significantly enhanced the thermal stability in nitrogen but also considerably delayed the oxidation decomposition in air of polypropylene. The incorporation of C<sub>60</sub> greatly reduced the heat release rate of PP and resulted in a longer time to ignition. And the free radicals-trapping mechanism of C<sub>60</sub> was proposed for explaining the enhanced thermal properties and improved flame retardancy of PP.

Yılmaz (2007), H. investigated flame retardancy properties of huntite/hydromagnesite mineral in plastic compounds for electrical applications. Phase and microstructural analysis of huntite/hydromagnesite mineral powders were indentified using XRD and SEM-EDS before fabrication of composite materials. The ground minerals with different particle size and content levels were added to the plastic compounds to produce composite materials. After fabrication of hydromagnesite/huntite reinforced plastic composite samples, they were characterized by using DTA-TG and SEM-EDS. Flame retardancy test were performed according to UL94 standards. The more of them were determined as V0 featured.



Besides, P, Si, B, N, Br, Sb and some of these mixed oxides are used as flame retardant agents. These materials delay the fire when incorporated in the polymeric material as the reinforcing material. As a result of the different contributions in the light of the data obtained from the literature search was determined to restricted flammability of polymers. As fire-retardant materials are usually inert materials such as  $\text{SiO}_2$ ,  $\text{CaCO}_3$ , carbon black and clay, on the other hand  $\text{Al}(\text{OH})_2$ ,  $\text{Mg}(\text{OH})_2$  and huntite-magnesite are known as the active reinforcement elements (Horrocks & Price, 2001).

Although halogen atoms (e.g. bromine or chlorine) form some of the most widely applied flame retardant materials, in particular for polymers used in composite organic matrices or in electronic equipment, they do have clear disadvantages: not least the potential to corrode metal components and, more pressingly, the toxicity of the hydrogen halide formed during combustion (Shui-Yu & Ian, 2002). Halogen containing flame retardants act in the gas phase and constitute incomplete burned substances like black smoke and toxic CO. Thus, for the increasing percentage of people killed by smoke inhalation in North America, halogenated systems, especially brominated systems, play an important.

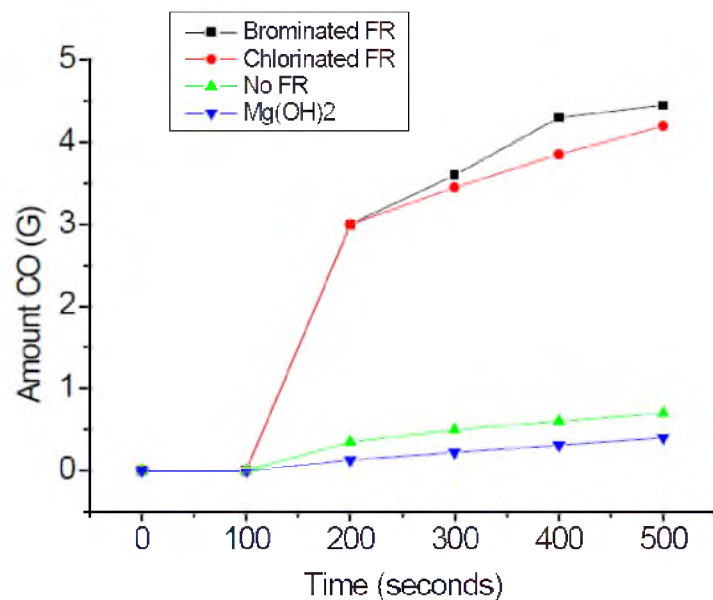


Figure 1.1 CO formation of PP compounds with different flame retardants (Weber, 1999).

In a real fire many toxic gases are found. The most serious one is carbon monoxide (CO), it is a highly toxic and non-irritating gas. As CO blocks the oxygen transport of the blood, it can disturb the respiration process immediately. Again, traditional solutions based on halogens have many disadvantages compared to mineral flame retardants. Figure 1.1 depicts a comparison of flame retardant materials (Weber, 1999).

## **1.2 Organization of the Thesis**

In this study, we developed flame retardant composite coatings/paints which are easier and cheaper the production process be used in all areas where fire hazard instead modify the structure of polymer materials, which is an expensive method. Another important aspect of this project is halogen-free, environmentally friendly and cheap flame-retardant materials. Huntite/hydromagnesite mineral which was used as a reinforcing material has flame retardant properties, which is in Turkey and Greece a large part of the world. In addition, due to the synergistic effects of boric acid and antimony (III) oxide was used as the auxiliary materials and flame resistant composite paint materials were developed. Before creating composite material due to the smooth surface quality and high efficiency, micron-sized huntite/hydromagnesite and antimony (III) oxide minerals were reduced to nanosized by grinding process. Composite material was prepared mixed with different amounts of the flame retardant materials and plastic paint used as matrix material and then it was applied on plastic materials by a paint gun. The used minerals before and after grinding were characterized as particle size, phase analysis and elemental analysis. After fabrication of nanosized flame retardant materials reinforced composite samples, they were characterized by using XRD, XPS, FT-IR, DTA-TG, SEM, surface roughness and hardness testing machines. In addition, candle flame tests measuring flame retardancy properties were performed as a main objective of this research. In this way, flame retardancy properties of composite materials were determined. After the results of performed tests, it was observed that the fire resistance of the reinforced composite materials was very good.

With this context, chapters can be explained in details. Chapter one provides a brief introduction to the area of research and the research objectives of this thesis. In Chapter two, a comprehensive literature reviews concerning properties/behaviours and mechanisms of flame retardant paints/coatings in details. Chapter three, the experimental procedures of polymeric paints/coatings with huntite/hydromagnesite minerals, antimony (III) oxide and boric acid are explained. Besides, the performed fire tests and characterizations are explained in this chapter. In Chapter four, the results concerning pure polymeric dye and effect of reinforcing materials on the stability of coating structure are demonstrated and discussed in details. Characterization of pure and reinforced dye coatings is also analyzed in the same chapter. The conclusion and future plans are summarized in Chapter five.

## CHAPTER TWO

### THEORETICAL BACKGROUND

#### 2.1 Polymers

Now, in the 21st century, polymer materials are used in ever more areas and under ever more demanding environmental conditions (Shui-Yu & Ian, 2002). Polymers can be classified in a variety of ways, several of which are worth considering. Firstly, they have often simply been classified as natural or synthetic (and sometimes as synthetic modifications of natural polymers). Nevertheless, a classification based on their physical/mechanical properties can also be used, in particular their elasticity and degree of elongation. Under these criteria, polymers can be classified into elastomers, plastics and fibres. Elastomers (rubbers) are characterised by having a high extensibility and recovery; plastics have intermediate properties, whilst fibres can have very high tensile strength but low extensibility. Plastics are often further subdivided into thermoplastics (whose deformation at elevated temperature is reversible) and thermosets (which undergo irreversible changes when heated) (Horrocks & Price, 2001). Together with numerous advantages that polymeric materials provide to society in everyday life, there is one obvious disadvantage related to the high flammability of many polymers (Alexander & Charles, 2007). The use of flame retardants to reduce combustibility of the polymers, and smoke or toxic fume production, therefore becomes a pivotal part of the development and application of new materials. Flame retardant materials play an important role in this point.

##### *2.1.1 Polymer Combustion*

Due to their chemical structure, made up mainly of carbon and hydrogen, polymers are highly combustible (Pal & Macskasy, 1991). The life span of the combustion cycle depends on the quantity of heat liberated during the combustion of the fuel. When the amount of heat liberated reaches a certain level, new decomposition reactions are induced in the solid phase, and therefore more

combustibles are produced. The combustion cycle is thus maintained, and called a fire triangle as presented in Figure 2.1 (Laoutid et al. 2009).

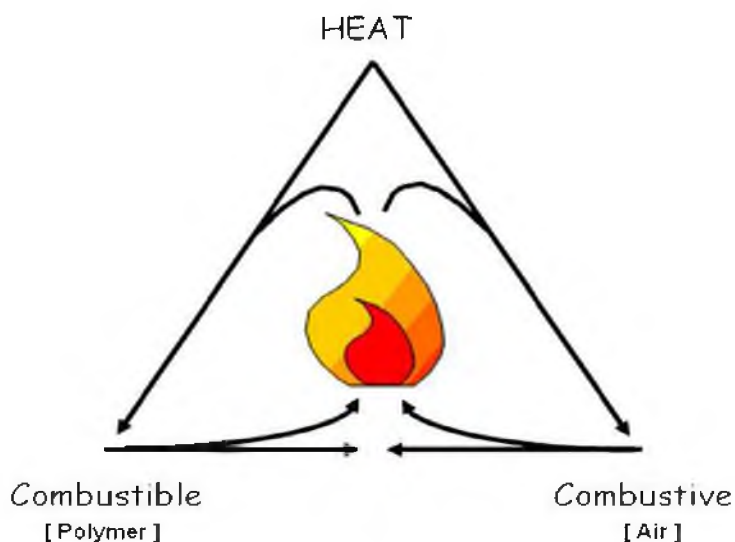


Figure 2.1 Principle of the combustion cycle (Laoutid et al. 2009).

All polymer fires start with an ignition event, where a source of heat comes into contact with a fuel generated by the heating of the polymer. This event initiates a flow of flammable degradation products, which react with oxygen from the air to produce a flame and heat. Some of the heat is transferred back to the surface of the fuel, maintaining the flow of flammable volatile degradation products. Low ignitability of the polymers is the first line of defence against fire. In spite of the fact that all organic polymers do ignite, the higher the temperature that a material has to reach before it ignites, the safer it is. For most materials, the ignition temperature is in the range 275 to 475 °C (Alexander & Charles, 2007).

The thermal decomposition of a polymer (i.e. covalent bond dissociation) is an endothermic phenomenon, which requires an input of energy. The energy provided to the system must be higher than the binding energy between the covalently linked atoms (200–400 kJ/mol for most C–C polymers). The decomposition mechanism is highly dependent on the weakest bonds, and also on the presence or absence of oxygen in the solid and gas phases. Generally speaking, thermal decomposition is the result of a combination of the effects of heat and oxygen (Pal & Macskasy, 1991).

The possibility of extinguishing a polymer flame depends on the mechanism of thermal decomposition of the polymer. Whereas ignition of a polymer correlates primarily with the initial temperature of decomposition, steady combustion is related to the tendency of the polymer to yield a char, which is produced at the expense of combustible volatile fragments. Therefore, the dependence of steady combustion on the amount of char seems to be simple, and in an early study it was established that the oxygen index shows a very good correlation with the char yield (Van, 1975). In reality, char also serves as a physical barrier for heat flux from the flame to the polymer surface, as well as a diffusion barrier for gas transport to the flame (Levchik & Wilkie, 2000). Therefore, the contribution of the char can be more significant than is expected from a simple reduction in combustible gases.

Four general mechanisms are important for thermal decomposition of polymers: (1) random chain scission, in which the polymer backbone is randomly split into smaller fragments; (2) chain-end scission, in which the polymer depolymerises from the chain ends; (3) elimination of pendant groups without breaking of the backbone; and (4) cross-linking. Only a few polymers decompose predominantly through one mechanism; in many cases a combination of two or more mechanisms is in effect (Hirschler, 2000). In terms of flammability, random scission and depolymerisation polymers are usually more flammable than polymers that cross-link or remove pendant groups. Cross-linking leads to precursors of char and as a result, to lower flammability. Elimination of pendant groups results in double bonds, which can also give cross-links or lead to aromatization (Alexander & Charles, 2007).

Figure 2.2 denotes a schematic cross-section of a polymer fire indicating the important reaction zones. The flame is fuelled by combustible pyrolysis products escaping from the polymer surface owing to heat being conducted from the flame in contact with the polymer surface and also that radiated from the flame (Charles & Alexander, 2010). The latter is the significant cause of flame spread and this process is modelled by the cone calorimeter. The oxygen required to sustain the flame combustion diffuses in from the air environment. Various solid particles escape from the flame as smoke that is accompanied by gaseous species, some of which can be

toxic (Hull, 2008). The significant polymer degradation reactions occur within a millimeter or so of the interface between the flame and the solid polymer. Here, the temperature is high enough for condensed-phase degradation reactions to occur. These involve the polymer and any additive systems included in the polymer formulations. Volatile species formed escape into the flame, while heavier species remain to undergo further reaction and may eventually degrade leaving a char. This is where the significant condensed-phase chemistry occurs. Experimental studies of this region have been undertaken by Price and Szabo et al. (1999).

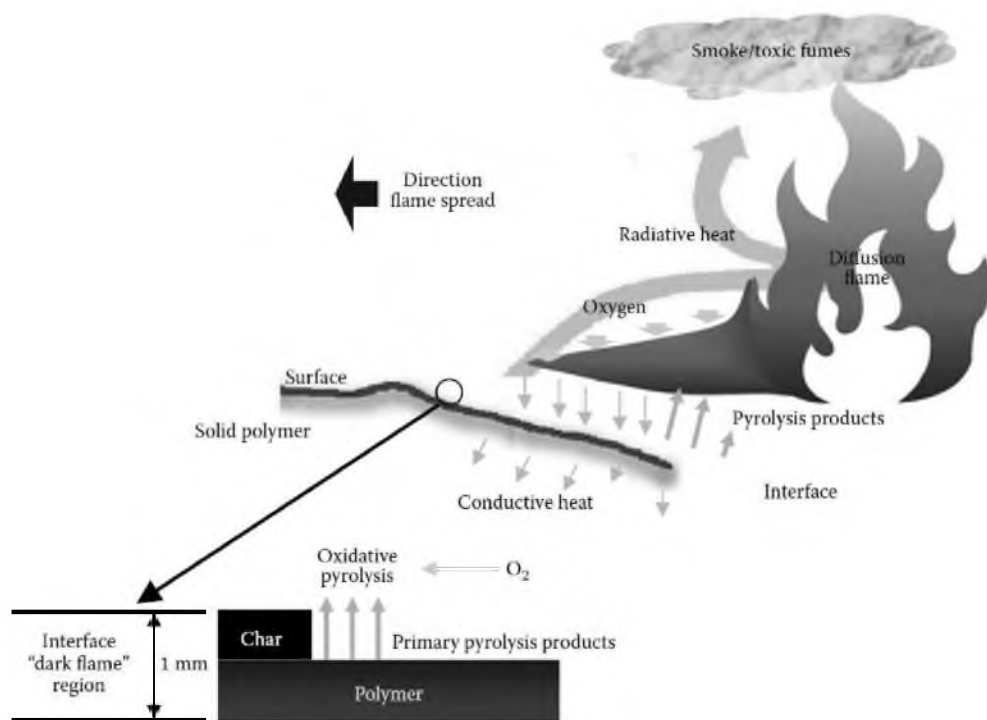


Figure 2.2 Schematic representation of a burning polymer (Charles & Alexander, 2010).

## 2.2 Flame Retardant Materials and Mechanisms

This term is used for any additives that allow a polymer to retard a flame, or for any polymer that shows the ability to slow fire growth when ignited. It does not mean non-combustible or ignition resistant—these are very different terms and should not be used to describe a flame-retardant material. A material that is truly non-combustible or ignition resistant either cannot be combusted (no thermo-oxidative decomposition can occur) or cannot be ignited with a particular size

flame/heat source. A material could be flame retarded so that under a test that measures aspects of ignition or combustibility, the material is measured/assessed to be non-combustible/ignition resistant, but under another set of conditions it burns with ease (Charles & Alexander, 2010). Protection against fire by the employment of flame retardants in plastics formulations must achieve at least one of several tasks during the course of a fire. These can briefly be stated as:

- Raising of the ignition temperature,
- Reduction of the rate of burning,
- Reduction of flame spread, and
- Reduction, if not elimination, of smoke generation (Dufton, 2003).

Flame retardants can be classified in two categories:

- Additive flame retardants: these are generally incorporated during the transformation process and do not react at this stage with the polymer but only at higher temperature, at the start of a fire; they are usually mineral fillers, hybrids or organic compounds, which can include macromolecules.
- Reactive flame retardants: unlike additive flame retardants, these are usually introduced into the polymer during synthesis (as monomers or precursor polymers) or in a post-reaction process (e.g. via chemical grafting). Such flame retardants are integrated in the polymer chains (Laoutid, 2009).

Although flame retardants may differ from one another in terms of chemical structure, certain general mechanisms of action are applicable to various classes of flame retardants. The first line of separation normally distinguishes gas-phase-active and condensed-phase-active flame retardants. Gas-phase-active flame retardants act primarily through scavenging free radicals responsible for the branching of radical chain reactions in the flame. This is the chemical mechanism of action in the gas phase. Other flame retardants generate large amounts of non-combustible gases, which dilute flammable gases, sometimes dissociate endothermically, and decrease the temperature by absorbing heat. This slows combustion and may eventually result



in extinguishment of the flame. This is the physical mechanism of action in the gas phase.

Condensed-phase mechanisms of action are more numerous than the gas-phase mechanisms. Charring, discussed briefly above, is the most common condensed phase mode of action. Again, charring could be promoted either by chemical interaction of the flame retardant and the polymer or by physical retention of the polymer in the condensed phase. Charring could also be promoted by catalysis or oxidative dehydrogenation. Some flame retardants show almost exclusively a physical mode of action. Examples are aluminum hydroxide and magnesium hydroxide. On the other hand, there is no single flame retardant that will operate exclusively through a chemical mode of action. Chemical mechanisms are always accompanied by one or several physical mechanisms, most commonly endothermic dissociation or dilution of fuel. Combinations of several mechanisms can often be synergistic (Alexander & Charles, 2007).

### ***2.2.1 Halogen-Containing Flame Retardants***

Halogen-containing flame retardants represent the most diversified class of retardants (Georlette, Simons & Costa, 2000). To be effective, halogen-containing flame retardants need to release halogen in the form of radical or halogen halide at the same temperature range or below the temperature of decomposition of the polymer (Horrocks & Price (Eds) 2001). Theoretically, four classes of chemical compounds can be used as halogenated flame retardants: those containing fluorine, chlorine, bromine, or iodine. Fluorinated organics are normally more stable than any other polymers and do not release fluorine radicals or hydrogen fluoride. Nonetheless, there are a few examples of the commercial use of fluorinated flame retardants operating differently from all other halogenated flame retardants. By contrast, iodinated organics have very low thermal stability and cannot be processed with most commercial polymers. In addition, fluorine and iodine are more expensive than chlorine or bromine, which also limits development of flame retardants based on these two halogens (Alexander & Charles, 2007).

Chlorinated aromatic products are relatively stable and therefore not very efficient, but chlorinated aliphatic and cycloaliphatic flame retardants are well known. The chlorine content in some chlorinated paraffins can reach 70%, and some improved grades can be used in polyolefins and in high-impact polystyrene (HIPS) (Stevenson et al. 2002). A broad range of brominated flame retardants are commercially available brominated flame retardants help maintain a good balance of physical properties, such as good impact and tensile strength and a high heat distortion temperature. These flame retardants are generally suitable for many plastics; however, their principal use is in engineering plastics and epoxy resins (Bie, 2002). In this case the emphasis is on aromatic products. Although aliphatic brominated flame retardants are often more efficient than aromatics, their use has been limited to certain polymers. For similar structures there is usually a correlation between degree of bromination and thermal stability. Fully brominated aromatics have low volatility and are used in engineering resins with a relatively high processing temperature. Polymeric and oligomeric brominated aromatic flame retardants are also widely used (Alexander & Charles, 2007). The advantages and disadvantages of this class of materials can be summarised as Table 2.1.

Table 2.1 The advantages and disadvantages of halogen-containing flame retardants (Dufton, 2003).

<b>Advantages</b>	<b>Disadvantages</b>
<ul style="list-style-type: none"> <li>• Effective at low concentration</li> <li>• Relatively little detrimental effect on physical properties</li> <li>• Easy incorporation and processing</li> <li>• Moderately priced materials</li> </ul>	<ul style="list-style-type: none"> <li>• Generally require a synergist</li> <li>• May be a skin and eye irritant during handling and processing</li> <li>• Release of toxic combustion products</li> </ul>

Figure 2.3 compares the flame retardant efficiency of aliphatic brominated flame retardant and aromatic brominated flame retardant. Because the thermal decomposition of the aliphatic flame retardant starts at temperatures below the thermal decomposition of polypropylene, it shows very good performance in polypropylene. In contrast, because the aromatic brominated fire retardant is

significantly more stable, optimum debromination is not achieved at the temperature of decomposition of polypropylene, and this flame retardant shows inferior performance.

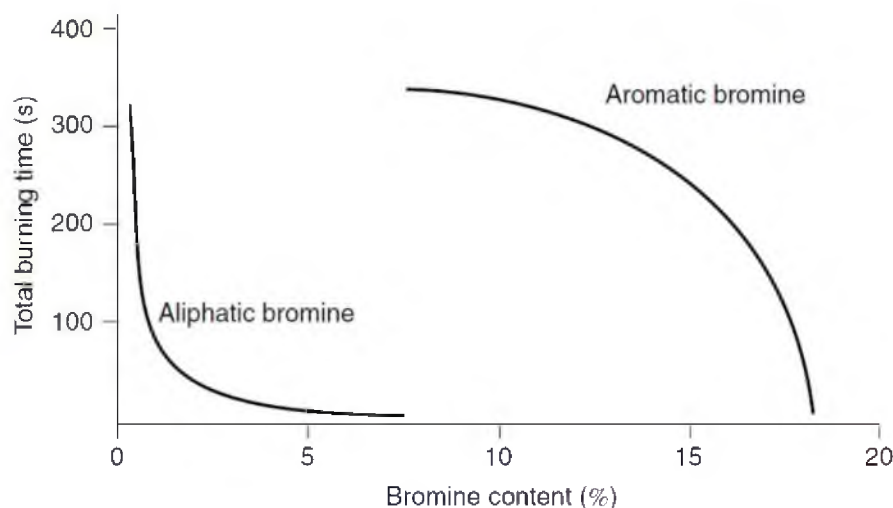


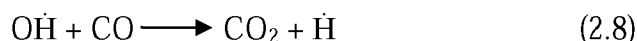
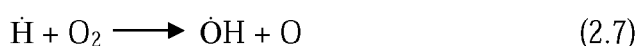
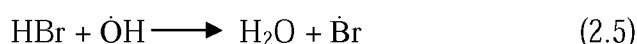
Figure 2.3 Dependence of total flaming time of polypropylene measured in a UL-94 test on bromine content for an aliphatic brominated flame retardant and an aromatic brominated flame retardant (Alexander & Charles, 2007).

It is generally accepted that the main mechanism of flame retardant action of halogenated flame retardants is in the gas phase, and it is primarily the chemical mode of action. The reaction begins with the abstraction of halogen radical from the flame retardant. This halogen immediately abstracts hydrogen from either the flame retardant additive or the polymer. An example of such a sequence of reactions, with the participation of bromine and an aliphatic polymer, is



In the absence of a synergist, hydrogen halides volatilize and enter the flame. Hydrogen halides will quickly react with hydrogen or hydroxyl radicals and regenerate the halogen. Examples of such reactions with HBr are shown below in Reactions 2.4 and 2.5. Further bromine radicals will react with hydrocarbons in the

gas phase and regenerate HBr as shown in Reaction 2.6, with the process repeating until bromine leaves the flame. Atomic hydrogen and hydroxyl radicals are very important for sustaining combustion. The hydrogen radical is responsible for the chain-branching free-radical reactions in the flame (Reaction 2.7), whereas the hydroxyl radical is responsible for the oxidation of CO to CO<sub>2</sub> (Reaction 2.8), which is a highly exothermic reaction and is responsible for the larger part of the heat generation in the flame (Alexander & Charles, 2007).



In some other reactions, the more reactive radicals ( $\dot{\text{H}}$ ,  $\dot{\text{O}}\text{H}$ ,  $\dot{\text{C}}\text{H}_3$ ) are replaced by the less active  $\dot{\text{Br}}$  radicals (Boryniec & Przygocki, 2001). If  $\dot{\text{Br}}$  meets with  $\dot{\text{H}}$  in the presence of a neutral molecule (third body), HBr is regenerated. It has been found by spectroscopy that the introduction of halogen-containing inhibitors into the flame clearly reduces the concentration of  $\dot{\text{H}}$ ,  $\dot{\text{O}}\text{H}$ , and  $\dot{\text{H}}\text{C}\text{O}$  radicals, whereas there is an increase in the content of the diradicals  $\text{C}_2^{\cdot\cdot}$  and soot. As the concentration of inhibitor is increased, the flame temperature decreases. Small additions of halogen inhibitors (on the order of a few mole%) can reduce the rate of flame propagation up to 10- fold and have a marked effect on the ignition limits. On the other hand, halogens accelerate the formation of soot in the flame (Alexander & Charles, 2007).

### 2.2.2 Antimony (III) oxide ( $\text{Sb}_2\text{O}_3$ )

It is well established that  $\text{Sb}_2\text{O}_3$  is synergistic with halogen-containing flame retardants because it facilitates delivery of halogen atoms in the gas phase and prolongs residence of the halogens in the flame zone so that more “hot” radicals can be scavenged. Antimony trioxide reacts with HCl or HBr in the condensed phase,

forming  $\text{SbCl}_3$  or  $\text{SbBr}_3$ , respectively, both of which are relatively volatile (Pitts, Scott & Powell, 1970).

On the other hand, some involvement of antimony in decomposition of the solid phase is indicated by the fact that char formation may be enhanced in antimony-containing systems. The synergistic action clearly involves interaction of  $\text{Sb}_2\text{O}_3$  with either the halogenated compound or a decomposition product of the halogenated material, presumably HX, in fact optimum conditions for retardancy depend on the ratio of antimony to chlorine and on the ease of decomposition of the halogenated species (Lyons, 1970).

Studies on antimony oxides/fire-retardant compounds containing chlorine/bromine confirm formation of gaseous species containing antimony and halides. It is believed that first some hydrogen halide is released from the halogen compound due to interaction with antimony trioxide or with polymer. The HX reacts with  $\text{Sb}_2\text{O}_3$  producing  $\text{SbX}_3$ . Even though it is clear that the final product of halogenated additives/antimony reaction is antimony trihalide, which is volatile at the temperature of the burning polymer, different mechanisms have been proposed for its formation. Literature data favour the formation of  $\text{SbX}_3$  through intermediate oxyhalides as compared to direct complete halogenations, for example, in the case of  $\text{Sb}_2\text{O}_3$  reacting with chlorinated or brominated compounds as shown in Figure 2.4 (Lum, 1977).

It can be seen that chemical halogenations of  $\text{Sb}_2\text{O}_3$  leads to progressively halogen richer oxyhalides up to the trihalide while the oxyhalides undergo thermal disproportionation with evolution of the trihalide and formation of the halogen-poorer oxyhalide. Therefore, the mechanism of the process depends on the temperature and on the interplay between thermal stability and chemical reactivity of the oxyhalides (Camino, 1987).

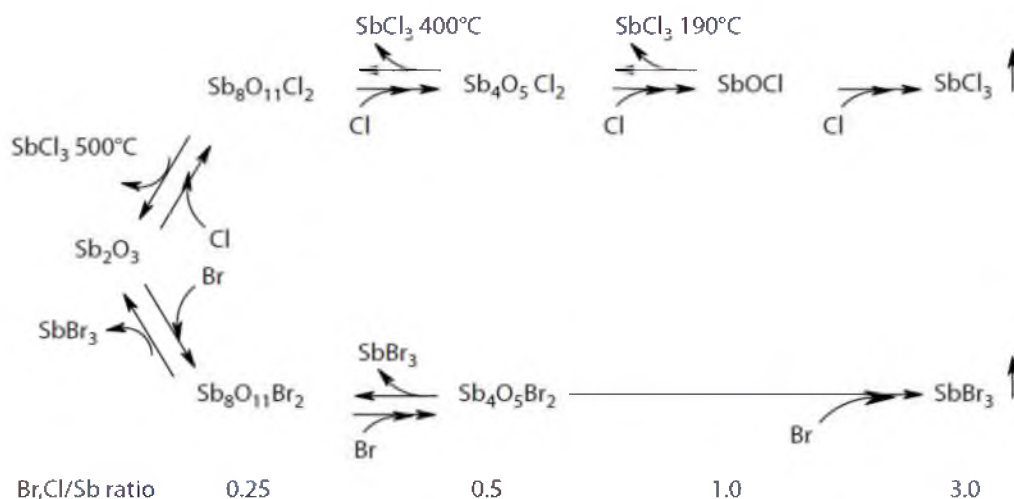
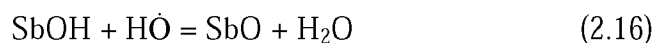
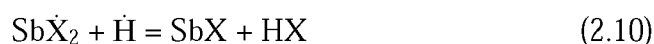
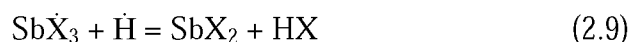


Figure 2.4 Reaction scheme occurring between antimony oxide and halogen compounds (Charles & Alexander, 2010).

In the case of chlorinated additives, independent of whether or not they release HCl on heating,  $\text{Sb}_4\text{O}_5\text{Cl}_2$  was the dominant oxychloride found in conditions close to those of polymer burning, although  $\text{Sb}_8\text{O}_{11}\text{Cl}_2$  was expected to be the most stable oxychloride under these conditions (Costa et al. 1990). This was explained assuming that  $\text{Sb}_8\text{O}_{11}\text{Cl}_2$  is formed first but does not accumulate because it is a highly reactive dechlorinating agent and gives  $\text{Sb}_4\text{O}_5\text{Cl}_2$ . This last would give  $\text{SbCl}_3$  at a relatively lower rate either through thermal disproportionation or direct complete chlorination.  $\text{Sb}_4\text{O}_5\text{Cl}_2$  and  $\text{Sb}_8\text{O}_{11}\text{Cl}_2$  might also undergo chlorination to  $\text{SbOCl}$  which then rapidly disproportionates. It is not possible to demonstrate whether  $\text{SbOCl}$  is an intermediate in the process because of its high thermal instability under these conditions. In the case of brominated additives the process is less studied, for decabromodiphenyl oxide, a widely used brominated fire-retardant additive,  $\text{Sb}_8\text{O}_{11}\text{Br}_2$  is the dominant oxybromide, whereas  $\text{Sb}_4\text{O}_5\text{Br}_2$  was not detected in measurable amounts. It was assumed that, if this last is formed by bromination of  $\text{Sb}_8\text{O}_{11}\text{Br}_2$ , it eliminates  $\text{SbBr}_3$  relatively rapidly either by thermal disproportionation or by chemical reaction with decabromodiphenyl oxide (Bertelli et al. 1988).

The role of antimony halides as flame-retardant species in the gaseous phase is well established: when  $\text{SbX}_3$  ( $\text{X} = \text{chlorine or bromine}$ ) is introduced into premixed methane–oxygen flames, atomic antimony and antimony monoxide are found in the

flame.  $\text{Sb}_2\text{O}_3$  was shown by mass spectrometry to be present only in the preflame zone and no antimony–halogen species could be detected in the flame itself (Hastie, 1973). The proposed sequence of reactions taking place in the flame includes the following steps, where  $\text{X}^\bullet$  is a halogen atom:



Antimony halides are believed to have two functions in the flame. The first is to provide a ready source of hydrogen halide early on and the second is to produce a “mist” of fine particles of solid  $\text{SbO}$  in the middle of the flame region. The function of  $\text{SbO}$  as an inhibitor independent of the presence of halogen species is verified by the effect on fire retardancy of triphenylantimony in the absence of halogen compounds. Triphenylantimony is an efficient flame retardant for epoxy resins, even in the absence of halogen (Martin & Price, 1968). This can be explained in terms of the low volatility but ready oxidizability of triphenylantimony so that it forms particles of antimony oxides in the gaseous phase. It is supposed by Hastie that antimony monoxide is sufficiently stable in the flame to catalyze the recombination of  $\text{H}$ ,  $\text{O}$ , and  $\text{OH}$  via the formation of transient species (Equation 2.9 through 2.16) such as  $\text{SbOH}$  analogous to what suggested to explain the catalytic effect of other oxides such as  $\text{SnO}$  (Bulewicz & Padley, 1971).

As mentioned earlier, the halogen radicals evolved from the flame retardant in the condensed phase abstract the hydrogen from the polymer and produce unsaturation (Reactions 2.2 and 2.3). The double bonds are known to be precursors of char formation through either cross-linking or aromatization (Levchik & Wilkie, 2000). If

hydrogen is abstracted from the aromatic ring, this ring has a chance to couple with another ring and start forming polyaromatic structures, which are precursors of graphitic domains in the char. This char formation is an important condensed-phase contribution of halogen-based flame retardants, which is often overlooked (Pearce, Shalaby & Barker, 1975).

### ***2.2.3 Phosphorus-Based Flame Retardants***

Phosphorus-containing flame retardants include inorganic phosphates, insoluble ammonium phosphate, organophosphates and phosphonates, halophosphates and chlorophosphonates, phosphine oxides, and red phosphorus. The mechanism for flame retardancy varies with the phosphorus compound and the polymer type. A phosphorus containing flame retardant can function in the condensed phase, the gas phase, or concurrently in both phases. Important categories are the phosphate esters, extensively used in flexible PVC, modified polyphenylene oxide and some cellulosic polymers; and chlorinated phosphates, commonly used in polyurethane formulations.

Some phosphorus compounds decompose in the condensed phase to form phosphoric or polyphosphoric acids. These can act as dehydration catalysts, reacting with cellulose for example, to form a good char. Char yield is also increased with rigid polyurethanes. The polyphosphoric acid can also form a viscous molten surface layer or surface glass. This layer can shield the polymeric substrate from the flame (heat) and oxygen. Intumescence, which requires an acid such as phosphoric acid, results in a dense carbon char on the polymer surface protecting the substrate from heat and oxygen.

Red phosphorus is also used as a flame retardant – disadvantages include high flammability and in the presence of heat and/or friction it can explode. In the presence of moisture it releases phosphine. However, red phosphorus has a number of advantages as a flame retardant – the material need only be added in fairly low concentrations of around 6-10%. At this addition level, the phosphorus has a negligible effect on physical properties. An overview of the advantages and



disadvantages of the phosphorus-containing flame retardants is given in Table 2.2 (Dufton, 2003).

Table 2.2 The advantages and disadvantages of phosphorus-containing flame retardants (Dufton, 2003).

<b>Advantages</b>	<b>Disadvantages</b>
<ul style="list-style-type: none"> <li>• Effective at low concentration</li> <li>• Relatively little detrimental effect on physical properties</li> <li>• Easy incorporation and processing</li> <li>• Moderately priced materials</li> </ul>	<ul style="list-style-type: none"> <li>• Generally require a synergist</li> <li>• May be a skin and eye irritant during handling and processing</li> <li>• Release of toxic combustion products</li> </ul>

#### ***2.2.4 Nitrogen-Based Flame Retardants***

Melamine is a thermally stable crystalline product characterized by a melting point as high as 345 °C that contains 67 wt% nitrogen atoms. Melamine sublimates at about 350 °C. Upon sublimation, a significant amount of energy is absorbed, decreasing the temperature. At high temperature, melamine decomposes with the elimination of ammonia, which dilutes oxygen and combustible gases and leads to the formation of thermally stable condensates, known as melam, melem and melon.

The formation of melam, melem and melon generates residues in the condensed phase and results in endothermal processes, also effective for flame retardancy. In addition, melamine can form thermally stable salts with strong acids: melamine cyanurate, melamine phosphate, and melamine pyrophosphate. Melamine and melamine salts are characterized by various flame retardant mechanisms. Upon heating, melamine based salts dissociate and the re-formed melamine volatilizes, like neat melamine, but a large proportion of the melamine undergoes more progressive condensation than in the case of pure melamine. The action of salts in the condensed phase is therefore significantly higher (Costa et al. 1990).

The thermal decomposition of melamine phosphate (see Figure 2.5 for details) leads to the formation of melamine polyphosphate, with the release of melamine and

phosphoric acid. The phosphoric acid released is known to phosphorylate many polymers and produce flame retardant effects similar to phosphorus-based flame retardant additives.

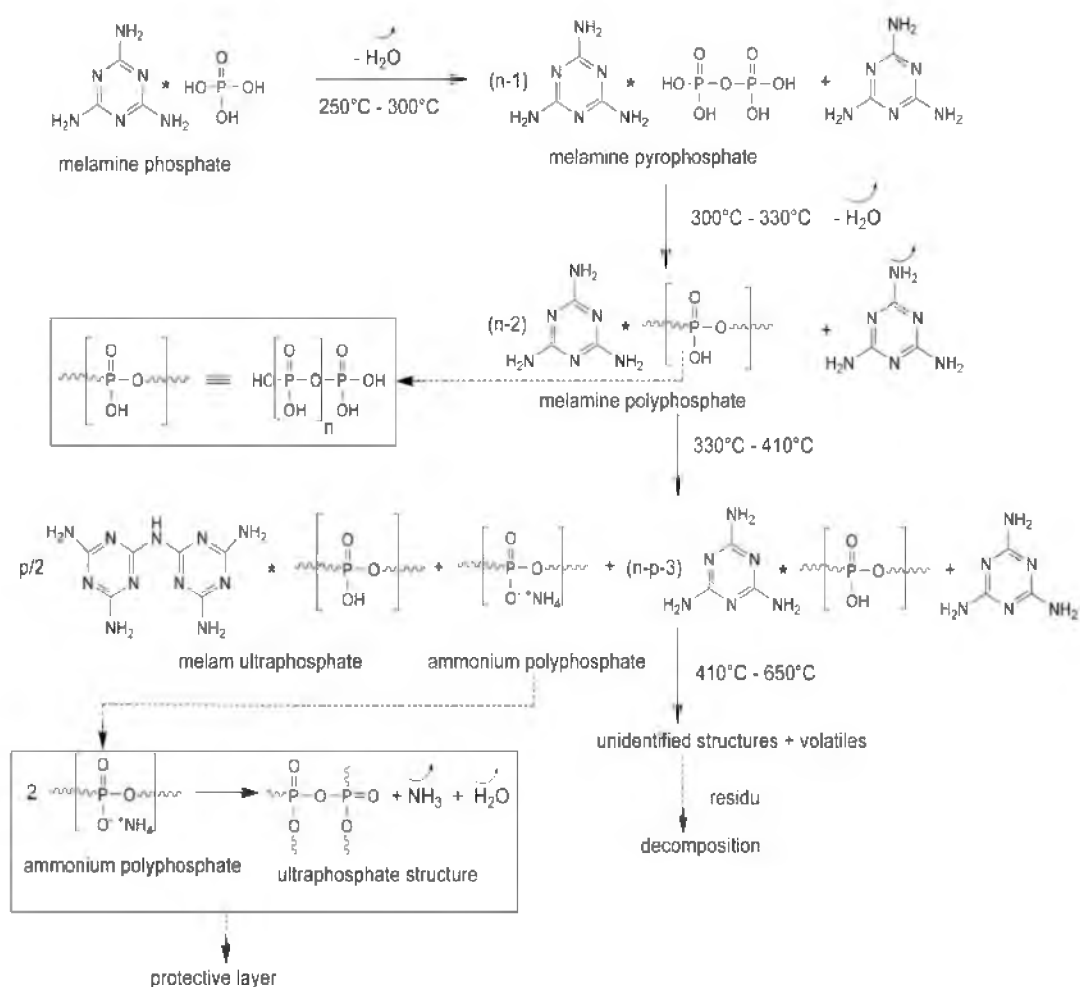


Figure 2.5 Thermal decomposition of melamine phosphate (Laoutid et al. 2009).

The thermal decomposition of melamine polyphosphate leads to the formation of melam ultraphosphate and ammonium polyphosphate, with the release of melamine. However, the melamine in the gaseous phase competes with the formation of its condensation products, such as melam ultraphosphate. The condensation of melamine is thus accompanied by the formation of polyphosphoric structures.

Ammonium polyphosphate can also be formed from melamine polyphosphate. In addition, ammonium polyphosphate tends to dissociate and release ammonia above

300 °C and the free condensed hydroxyl groups give crosslinked structures (ultraphosphate) with water elimination. The hydrolysis of the melam ultraphosphate generates a melam phosphate derivative or melam polyphosphate. Above 410 °C, the thermal degradation of the ultraphosphate is limited and is followed around 650 °C by the formation of a relatively stable residue.

The melamine pyrophosphate evolves to melamine during thermal decomposition but its thermal performances are different from those of melamine and its other salts; the formation of carbonaceous structures is more significant here and its action mode is similar to that of ammonium polyphosphate (Laoutid et al. 2009).

### ***2.2.5 Silicon-Containing Flame Retardants***

Under the heading here we include any chemical compound containing Si. For a long time silicons were considered as useful coadditives in flame retardant systems, but recent developments, especially with polycarbonates have again drawn significant attention to silicon.

Talc is a naturally occurring magnesium silicate which is finding broad application as a filler in polyolefins. Apparently, it provides a moderate flame retardant effect, but because talc is inexpensive, it is used as a partial substitute for more expensive flame retardants. Fumed silica is used as a filler in epoxy resins for the encapsulation of electronic devices at a relatively high loading, up to 80 to 90 wt%. Thanks to the relatively small amount of combustible resin, this composition can be flame retarded by the addition of a very small amount of a conventional flame retardant. It is not clear if the silica contributes to the flame retardancy by any mechanism other than heat dispersion (Alexander & Charles, 2007).

Octaphenylcyclotetrasiloxane in combination with potassium of sulfonated diphenylsulfone is used commercially in polycarbonate, where clarity of the polymer is important. Recently, some specific branched methylphenylsiloxanes were found particularly effective in polycarbonate (PC) and in PC/acrylonitrile–butadiene–

styrene (ABS) blends with a low (ABS) content (Iji & Serizawa, 1998). It is believed that due to the inclusion of aromatic groups in the siloxane, it becomes significantly more soluble and more easily dispersed in PC than straight polydimethylsiloxane. It was shown that these siloxanes tend to migrate from the inside of the PC resin to the surface during combustion and accumulate quickly on the surface. Such movement resulted from differences in viscosity and solubility between the siloxane and the PC at high temperatures. The branched methylphenylsiloxanes showed a higher thermal stability than that of linear dimethylsiloxanes and a greater tendency to induce charring. In contrast, Nishihara et al. showed that linear polysiloxanes are more advantageous flame retardants in PC than are branched polysiloxanes because of higher mobility in the molten plastic (Nishihara, Suda & Sakuma, 2003).

### ***2.2.6 Intumescent Coatings***

Intumescent coatings are fire protection systems which are used to protect materials such as wood or plastic from fire (prevent burning), but also to protect steel and other materials from the high temperatures of fires (thus preventing or retarding structural damage during fires). The coatings are made of a combination of products, applied to the surface like paint, which are designed to expand to form an insulating and fire-resistant covering when subject to heat. The products involved contain a number of essential interdependent ingredients: spumific compounds, which (when heated) release large quantities of non-flammable gas (such as nitrogen, ammonia, CO<sub>2</sub>) a binder, which (when heated) melts to give a thick liquid, thus trapping the released gas in bubbles and producing a thick layer of froth an acid source and a carbon compound. On heating, the acid source releases phosphoric, boric or sulphuric acid which chars the carbon compound, causing the layer of bubbles to harden and giving it a fire-resistant coating. Often the binder can also serve as this carbon compound (Efra, 2012).

Flame-retarding polymers by intumescence are essentially a special case of a condensed phase activity without apparent involvement of radical trap mechanisms in the gaseous phase. Intumescence involves an increase in volume of the burning

substrate as a result of network or char formation. For ingress of oxygen to the fuel, this char serves as a barrier and also as a medium in which heat can be dissipated (Figure 2.6).

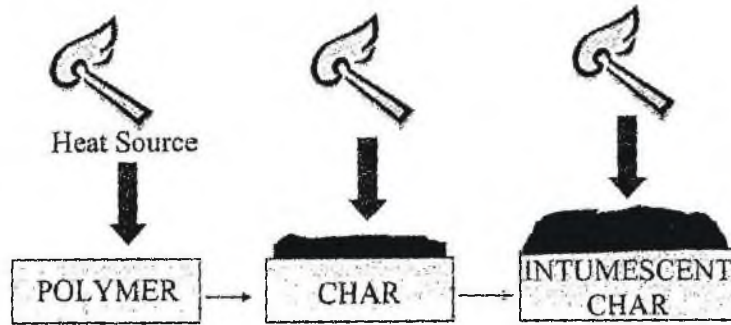


Figure 2.6 Char and intumescence formation (Xanthos, 2004).

The produced fuel amount is greatly diminished in intumescence and char rather than combustible gases is formed. The char constitutes a two-way barrier, both for hindering the passage of combustible gases and molten polymer to the flame as well as for shielding the polymer from the heat of the flame (Xanthos, 2004).

In a fire, the coating expands to a thick non-flammable layer of bubbles, offering good insulation protection to the material coated. As well as being used to protect flammable materials and structural elements, intumescent systems are now being incorporated into certain plastics, thus providing inherent fire protection capacity materials (Efra, 2012).

### ***2.2.7 Boron-Containing Flame Retardants***

Water-soluble borates such as sodium borate (borax) and boric acid have long been used to flame-retard cellulosic materials (e.g., paper boards, wood, and some technical textiles). On the other hand, water-insoluble and more thermally stable zinc borates have found use in thermoplastics. The mechanism of fire retardant action of these two types of borates is quite different (Alexander & Charles, 2007).

It is believed that soluble borates can esterify the OH groups of cellulose and promote char formation similar to that of phosphorus. For instance, a comparison of the performance of ammonium pentaborate, which decomposes and releases boric acid, and ammonium polyphosphate, which releases polyphosphoric acid, showed some similarity (Levchik et al. 1995). Borates and boric acid also release some water, which provides a heat sink. Sodium borate and boric acid or anhydride or their mixtures are low-melting solids. Their viscous glassy melts can cause intumescence by evolved decomposition gases, mostly water, or they can just cover the surface of the pyrolyzing polymer or char, healing cracks and providing a barrier to heat and decomposition products (Alexander & Charles, 2007).

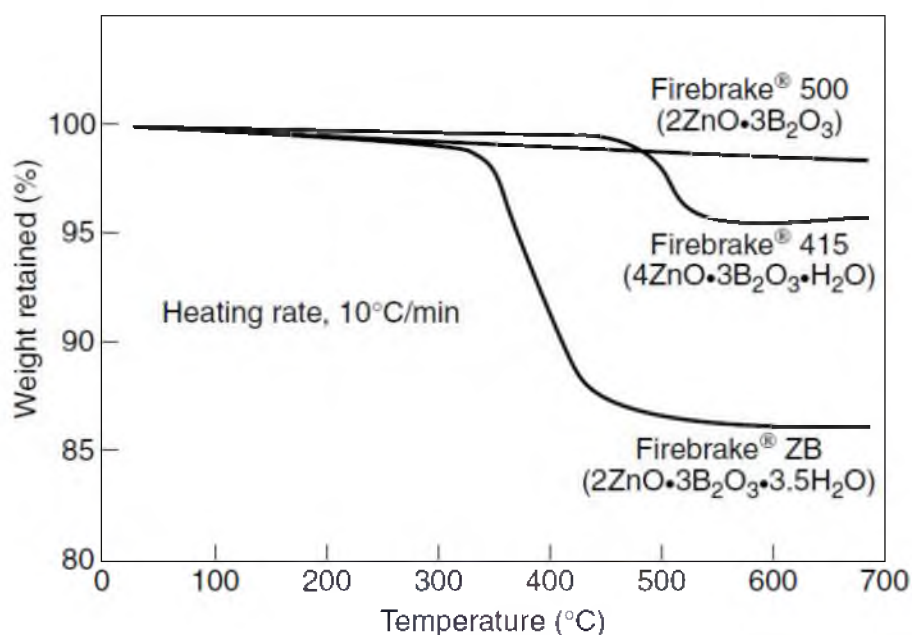


Figure 2.7 Thermogravimetry of commercial zinc borates (Alexander & Charles, 2007).

Several grades of zinc borates are commercially available, which release different amounts of water. Although in formulas for borates, water is often shown as a water of hydration, in fact, borates are rather complex hydroxide salts. Upon heating and polymer combustion, zinc borates dehydrate endothermically, and vaporized water absorbs heat and dilutes oxygen and gaseous flammable components (Yang, Shi & Zhao, 1999). For example, zinc borate  $2\text{ZnO}\cdot 3\text{B}_2\text{O}_3\cdot 3.5\text{H}_2\text{O}$ , known as Firebrake ZB (U.S. Borax), loses about 13.5 wt% water at 290 to 450 °C and absorbs 503 J/g.

Thermogravimetric curves of thermal decomposition of various borates are shown in Figure 2.7. Zinc borates are often used in halogen-containing systems and most often in PVC. In PVC, zinc borates significantly increase the amount of char formed during combustion. Zinc borates react with hydrogen chloride released from the thermal decomposition of PVC. Then zinc chloride catalyzes dehydrohalogenation and promotes cross-linking. This leads to an increase in char yield and even more important, a significant decrease in smoke formation. At sufficiently high temperatures, zinc borate can melt to produce a glassy layer, but this usually does not happen in small flames. Instead, zinc borate sinters and helps improve the insulating properties of the char and inhibits afterglow combustion.

Zinc borate can also change the oxidative decomposition pathway of halogen-free polymers. It is not completely clear if this is happening because of an inhibition effect of boron oxides toward the oxidation of hydrocarbons or the oxidation of graphite structures in the char, or is due purely to the formation of a protective sintered layer. In combination with Aluminium hydroxide (ATH), zinc borate creates a porous ceramic like residue, which has much better insulative properties than those of pure anhydrous alumina. It was shown that zinc borate accelerates dehydration of magnesium hydroxide and creates a ceramic like structure with dehydrated MgO (Alexander & Charles, 2007).

### ***2.2.8 Inorganic Hydroxides Flame Retardants***

Any type of inorganic filler, even inert, can influence the reaction of polymers to fire for several reasons:

- it reduces the content of combustible products;
- it modifies the thermal conductivity of the resulting material and all its thermophysical properties;
- it changes the viscosity of the resulting material;

Table 2.3 Principle candidate flame retardant fillers (Rothon, 2003)

Candidate material (common names and formula)	Approximate onset of decomposition (°C) *	Approximate enthalpy of decomposition (kJ.kg <sup>-1</sup> )	Volatile content		
			% w/w		
			H <sub>2</sub> O	CO <sub>2</sub>	Total
Nesquehonite MgCO <sub>3</sub> .3H <sub>2</sub> O	70-00	1750	39	32	71
Calcium sulfate dihydrate, Gypsum CaSO <sub>4</sub> .2H <sub>2</sub> O	60-130	Not available	21	0	21
Magnesium phosphate octahydrate, Mg <sub>3</sub> (PO <sub>4</sub> ) <sub>2</sub> .8H <sub>2</sub> O	140-150	Not available	35.5	0	35.5
Alumina trihydrate, Aluminium hydroxide, Al(OH) <sub>3</sub>	180-200	1,300	34.5	0	34.5
Basic magnesium carbonate, Hydromagnesite 4MgCO <sub>3</sub> .Mg(OH) <sub>2</sub> .4H <sub>2</sub> O	220-240	1,300	19	38	57
Dawsonite (sodium form) NaAl(OH) <sub>2</sub> CO <sub>3</sub>	240-260	Not available	12.5	30.5	43
Magnesium hydroxide , Mg(OH) <sub>2</sub>	300-320	1,450	31	0	31
Magnesium carbonate sub- hydrate (MCS), MgO.CO <sub>2</sub> (0.96)H <sub>2</sub> O(0.30)	340-350	Not available	9	47	56
Boehmite, AlO(OH)	340-350	560	15	0	15
Calcium hydroxide, Ca(OH) <sub>2</sub>	430-450	1,150	24	0	24

\*The decomposition temperatures are only approximate, as they are usually determined under dynamic conditions and depend on heating rate and sample conditions.

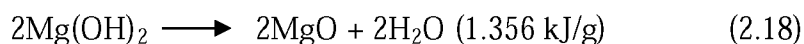
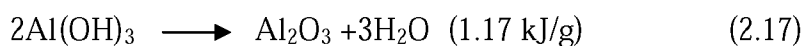
All these actions have an indirect incidence on the polymer's fire performance. Nevertheless, some minerals are more specifically used as flame retardants owing to their behaviour at high temperature. The most commonly used mineral flame retardants are metal hydroxides (especially of aluminium and magnesium),



hydroxycarbonates and zinc borates. Besides the aforementioned general effects, these inorganic fillers have a direct physical flame retardant action. As the temperature rises, these fillers decompose endothermically and therefore absorb energy. Moreover, they release non-flammable molecules (H<sub>2</sub>O, CO<sub>2</sub>), which dilute combustible gases, and can also promote the formation of a protective ceramic or vitreous layer (Laoutid et al. 2009). The flame retardant materials in Table 2.3 are seen to cover a wide range of decomposition temperatures, and to include release of carbon dioxide as well as water (Rothon, 2003, Yılmaz Atay & Çelik, 2010). Those materials remove a good deal of the heat evolved in degradation and thus can prevent further degradation.

Inorganic hydroxides or mixed hydroxide–inorganic salts that can release water upon heating above 200 °C can be used as flame retardants in many types of polymers. The two most commonly used products are aluminium hydroxide (ATH) and magnesium hydroxide (MH). In fact, ATH is, by weight, the largest commercially manufactured flame retardant, its main use being in wire and cable insulation and other elastomeric products, synthetic marble and synthetic onyx, latex for carpet back-coatings, phenolics, epoxies, and unsaturated polyesters (Fink, 2004).

ATH begins to release water at about 220 °C with an endotherm of 1.17 kJ/g, whereas MH starts releasing water at about 330 °C with an endotherm of 1.356 kJ/g. Thermogravimetric and differential scanning calorimetry curves obtained on heating of ATH and MH are shown in Figures 2.8 and 2.9, respectively.



There is little doubt that the main mechanism of fire retardant action of these hydroxides is heat absorption and dilution of the flame with water vapors (Equations 2.17 and 2.18). Another mechanism could be the catalytic effect of anhydrous alumina, which will help acid-catalyzed dehydration of some polymers and as a result can enhance charring (Lewin & Weil, 2001). Since both anhydrous alumina

and magnesia are white highly refractory powders, they provide heat insulation by reflecting heat when they accumulate on a surface.

ATH and MH are used primarily in wire and cables in poly(vinyl chloride) (PVC), polyethylene, and various elastomers. There is also some limited application of MH in polyamide-6. To pass flame retardancy tests, 35 to 65 wt% of metal hydroxide is required. Decreasing the loading of metal hydroxides will result in a significant gain in physical properties, especially low-temperature flexibility; therefore, combinations with red phosphorus, silicones, boron compounds, nanoclays (treated montmorillonites), and charring agents have been explored. Surface treatment of metal hydroxides also helps to improve physical properties and sometimes improves flame retardancy, due to better dispersion (Alexander & Charles, 2007).

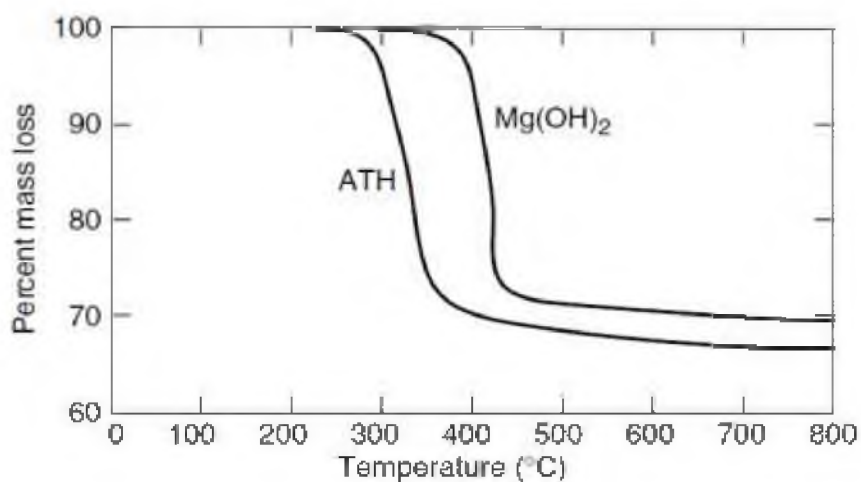


Figure 2.8 Thermogravimetry of ATH and Mg(OH)<sub>2</sub> (Alexander & Charles, 2007).

However, the fire properties of ATH-filled polymers are only interesting at high loading levels. For instance, the Limiting Oxygen Index (LOI) can reach values higher than 50% for EVA containing 75% (w/w) of ATH. The use of ATH also decreases the HRR peak in the cone calorimeter test and considerably reduces smoke production (Figure 2.10). Owing to its relatively low degradation temperature, ATH is limited to polymers with low processing temperatures, such as EVA and LDPE (Laoutid et al. 2009).

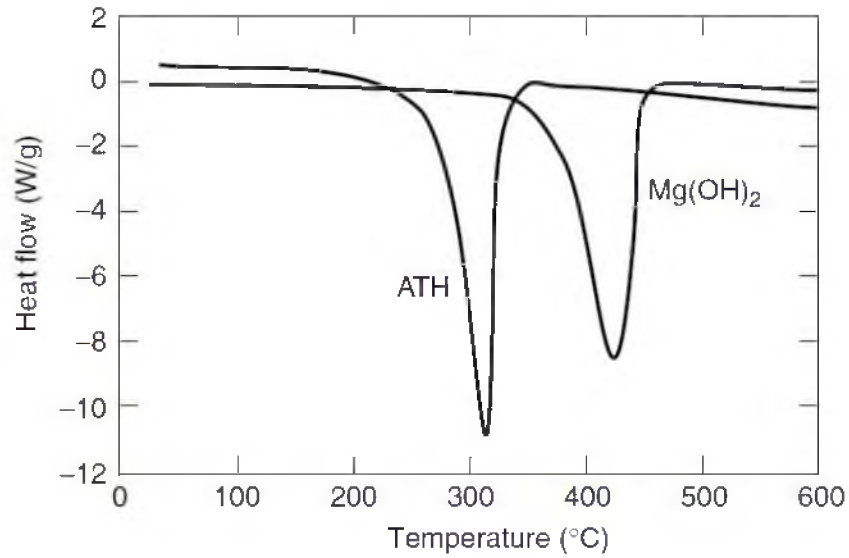


Figure 2.9 Differential scanning calorimetry of ATH and Mg(OH)<sub>2</sub> (Alexander & Charles, 2007).

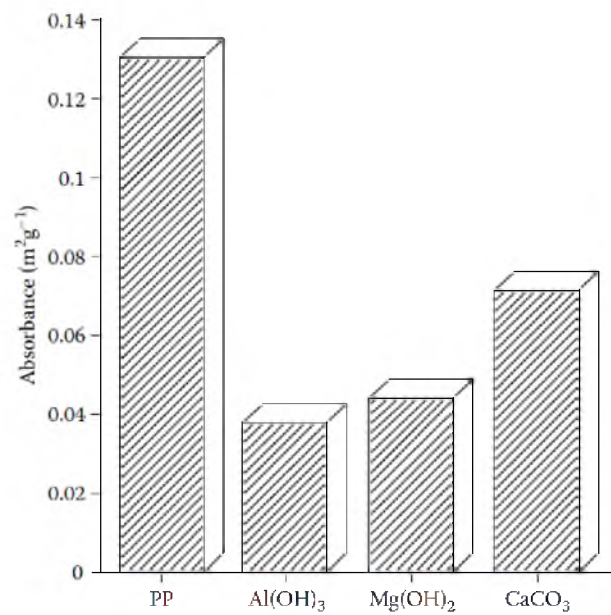


Figure 2.10 Smoke emissions from selected polypropylene compounds filled with 50 wt % of filler (Charles & Alexander, 2010).

Many other reports have demonstrated the smoke suppressing tendencies of hydrated fillers in various polymers including ethylene-propylene-diene elastomers, PP, polystyrene, modified polyphenylene oxide, polybutylene terephthalate, and ABS. In addition to suppressing smoke generation, a delay in the onset of smoke evolution is also achievable. Figure 2.10 illustrates smoke reductions obtained in PP. The analysis of smoke and soot formation from polymers during combustion has

been extensively studied; however, less is understood on how hydrated fillers influence this mechanism. It is likely that smoke reduction results from the deposition of carbon onto the high surface area oxide surface, produced on the decomposition of the filler. The volatilization of carbonaceous residue as carbon oxides then occurs, reducing obscuration effects from the smoke (Charles & Alexander, 2010).

Interestingly, magnesium di-hydroxide nanoparticles have also been considered as flame retardant additives. Such nanoparticles can be obtained by several methods, via a sol-gel technique followed by a hypercritical drying procedure, a hydrothermal reaction using various precursors and solvents or by precipitation of magnesium salts with an alkaline solution (Henrist et al. 2003). This last method allows for the control of the nanoparticle morphology by fine tuning of the experimental parameters such as the chemical nature of the base used as precipitant, the type of counter-ion, the temperature and the hydrothermal treatment. For example, simply changing the base precipitant (NaOH or NH<sub>4</sub>OH) leads to the formation of nanometric magnesium di-hydroxide with needle- or lamella-like morphologies, respectively.

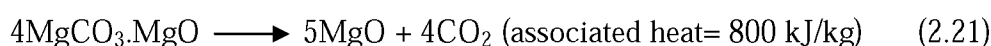
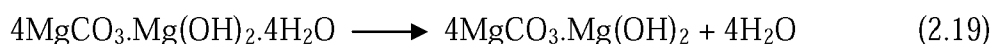
The use of nanosized MH can enable interesting fire performances to be achieved at lower loading levels. It has been shown that the LOI obtained with EVA containing 50% (w/w) of magnesium di-hydroxide increases from 24% to 38.3% when micronic magnesium di-hydroxide (2–5 mm) is replaced by nanometric Mg(OH)<sub>2</sub>. The enhancement of EVA flame retardancy by nanosized Mg(OH)<sub>2</sub> was attributed to the good dispersion of the nanoparticles, which leads to the formation of more compact and cohesive char during the combustion test.

#### *2.2.8.1 Hydroxycarbonates*

All carbonates release CO<sub>2</sub> at high temperatures but only magnesium and calcium carbonates release it below 1000 °C, with magnesium carbonate presenting the lowest release temperature (550 °C). Even though hydroxycarbonates are less widely used than other conventional flame retardants, they remain an alternative to metal

hydroxides. In addition to the release of water, natural magnesium carbonate (magnesite) and synthetic magnesium hydroxycarbonate (hydromagnesite) also break down endothermically due to the liberation of CO<sub>2</sub> at high temperature.

The thermal decomposition of hydromagnesite (4MgCO<sub>3</sub>.Mg(OH)<sub>2</sub>.4H<sub>2</sub>O or 5MgO.4CO<sub>2</sub>.5H<sub>2</sub>O) in air can be described by the following reactions:



Hydromagnesite releases water and carbon dioxide over a wider temperature range than aluminum tri-hydrate and magnesium di-hydroxide. This material has been used as a flame retardant in polypropylene and an LDPE/EVA polymer blend (3:1 blend). While aluminum tri-hydroxide and magnesium di-hydroxide have water release temperatures around 180–200 °C and 300–340 °C, respectively, hydromagnesite releases both water and carbon dioxide between 200 and 550 °C, which suggests that it may have similar or better flame retardancy effectiveness than ATH and MDH (Laoutid et al. 2009). The advantages and disadvantages of this class of materials can be summarised as Table 2.4:

Table 2.4 The advantages and disadvantages of inorganic hydroxides flame retardants (Dufton, 2003).

<b>Advantages</b>	<b>Disadvantages</b>
<ul style="list-style-type: none"> <li>• Combined filler and flame retardant functions</li> <li>• Does not require halogens</li> <li>• Does not produce toxic gases</li> <li>• Suppresses smoke formation</li> <li>• Non-volatile and unaffected by water</li> <li>• Low cost</li> <li>• Non-toxic</li> </ul>	<ul style="list-style-type: none"> <li>• Requires high loadings</li> <li>• Affects physical properties and processing behaviour</li> <li>• Relatively low decomposition temperature</li> </ul>

### ***2.2.9 Synergism***

The concept of synergism is very often used in the optimization of flame retardant formulations; however, synergism is sometimes misinterpreted. By definition, synergism means enhanced performance of the mixture of two or more components compared to the simple additive performance of the components at the same concentration (Weil, 1975).

The two mostly common examples of synergism, halogens with antimony and phosphorus with nitrogen, were discussed earlier. Apart from  $\text{Sb}_2\text{O}_3$ , halogen containing flame retardants are synergistic with other metal oxides, including  $\text{Bi}_2\text{O}_3$ ,  $\text{SnO}_2$ ,  $\text{MoO}_3$ ,  $\text{Fe}_2\text{O}_3$ , and  $\text{ZnO}$ . In some formulations these metal oxides can substitute for  $\text{Sb}_2\text{O}_3$  partially or completely. Zinc borates or zinc sulphide can be used in the same role of partial substitution of  $\text{Sb}_2\text{O}_3$ . In many instances these metal oxides also provide additional advantages of smoke suppression.

In spite of the fact that different speculative mechanisms of catalysis of charring (e.g., by zeolites), or thermal oxidative promotion of charring by manganese dioxide were proposed, these mechanisms probably play a minor role. The principal mechanism appears to be interaction of polyphosphoric acid formed during thermal decomposition of ammonium polyphosphate (APP) and metal-containing compounds. Inasmuch as only divalent and higher-valency metals show this effect, it is reasonable to assume that metal cations assist to cross-link polyphosphoric acid and increase its viscosity. This, in turn, helps to create a more thermally insulative char structure. If the mineral compound is added in large quantities, solid crystalline phosphates are formed, and this results in cracking of the char and the loss of insulating properties. This also explains why this synergistic effect is observed in a very narrow concentration range (Alexander & Charles, 2007).

Because of increased attention to halogen-free systems in recent years, there has also been a significant effort to enhance the fire retardant performance of aluminum hydroxide (ATH) and magnesium hydroxide (MH), because these additives are used

at very high loading levels. It is interesting that just a simple combination of ATH and MH can be synergistic (Weil, 1999). This probably relates to the extension of the temperature interval for the elimination of water. Combinations of MH and zinc borate were found to be synergistic in poly(ethylene-co-vinyl acetate), (EVA) according to a cone calorimeter study. It was found that zinc borate catalyzes dehydration of MH. In addition, zinc borate helps to sinter particles of MgO together, which, in turn, leads to better retention of combustible polymer in the condensed phase and eventual charring (Weil et al. 2004).

### ***2.2.10 Criteria for Selection of Flame Retardants***

Criteria for the selection of flame retardants are usually based on:

- The efficiency of a particular type of flame retardant in a particular polymer system
- The processing conditions of the polymer
- Compatibility and the ability to preserve valuable physical properties
- The cost–performance trade-off

As mentioned above, halogenated flame retardants are more universal than phosphorus-based flame retardants because the halogenated retardants are effective primarily in the flame zone, which is chemically similar for many polymers. Nevertheless, other criteria listed above require halogenated flame retardants to be tailored to specific polymers. To illustrate this, aliphatic halogenated flame retardants are used primarily in thermoset resins or in expandable polystyrene, in terms of their limited thermal stability. Flame retardants that are soluble in polystyrene are not good for HIPS, because solubility results in plasticization and a dramatic decrease in the heat distortion temperature. On the other hand, partially soluble additives (e.g., decabromodiphenyl oxide) are very suitable for HIPS because they help keep an acceptable heat distortion temperature and good impact properties. Even though ABS is chemically similar to HIPS, additives that are soluble in polystyrene (e.g., tetrabromobisphenol A or brominated epoxy oligomers) are preferable. Now that

ABS has a higher rubber content than HIPS, the use of insoluble additives is detrimental for polymer toughness.

Phosphorus-based flame retardants are usually more suitable for engineering plastics that undergo charring than for commodity polymers. In some plastics, such as PC-ABS or poly (phenylene oxide)-HIPS blends, phosphorus-based flame retardants are more effective than halogenated flame retardants. Antimony trioxide, which is a part of halogen-containing formulations, is a Lewis acid and may destabilize some condensation polymers. Furthermore, the impact properties of engineering polymers may suffer due to the presence of powdery antimony trioxide.

Inorganic hydroxides are used at very high loading levels. Only certain polymers, e.g., polyolefins, can tolerate such high loading without a significant loss of physical properties. Furthermore, relatively low thermal stability, especially of ATH, significantly limits the use of inorganic hydroxides. Other polymeric systems in which ATH is used are PVC, unsaturated polyesters, and latex back coatings of polyamide or polyester carpets (Alexander & Charles, 2007).

### **2.3 Environmental Concerns**

A campaign of national and international environmental and consumers agencies against the use of halogen-based fire retardants, which is due to growing concern for possible side effects of these compounds when they perform the fire-retardant action, has been ongoing for about two decades. Indeed, halogen-based fire retardants are very effective in reducing fire risk, i.e., the probability of occurrence of a fire, but they show a high fire hazard, that is, the probability of producing toxic, corrosive, obscuring smokes while performing the fire-retardant action or when involved in a fully developed fire, beyond flashover, when the fire can no longer be extinguished.

Indeed, radical trapping in the gas phase performed by HX is bound to increase production of CO which would otherwise be oxidized by OH radicals. Furthermore, restriction of oxidation increases the amount of nonoxidized products which may



condense into droplets or particles when they leave the flame, increasing the optical density of the smoke. Finally HX and metal halides are highly corrosive. The ensuing threat to people, structures, and goods involved in the fire may discourage the use of these fire retardants in spite of their high effectiveness and versatility which is far ahead of any other system developed so far. Moreover, the environmental impact of halogenated fire retardants during their entire life cycle, including end of life disposal, has been of growing concern since planetary contamination by bioaccumulation of synthetic halogenated compounds.

Toxicity and environmental concerns led to submission of a proposal to European Union to ban the use of polybromo biphenyl ethers (PBDPE) in 1989 (111-4301-89 EN Draft). The proposal was rejected on the basis of recommendations issued by a thorough debate between scientists, regulators, producers, and users of fire retardants, stating that banning would involve an unacceptable fire risk since alternatives were not available to replace halogen-based fire retardants with comparable effectiveness. Ever since, fire retardant research has been mostly devoted to the development of nonhalogenated replacements for the halogen fire retardants (Charles & Alexander, 2010).

Over the years directives on usage/waste and recycling on halogenated flame retardants were more and more restrictive with the accumulation of evidences on their environmental effects (Lomakin & Zaikov, 2003). In February 2003, the Restriction of Hazardous Substances Directive or RoHS was adopted by the European Union. This directive is on the restriction of the use of certain hazardous substances in electrical and electronic equipments. The RoHS directive took effect on 1 July 2006, and is required to be enforced and become law in each member state. This directive restricts the use of six hazardous materials, included brominated flame retardants, in the manufacture of various types of electronic and electrical equipment. It is closely linked with the Waste Electrical and Electronic Equipment Directive (WEEE) 2002/96/EC which sets collection, recycling, and recovery targets for electrical goods and is part of a legislative initiative to solve the problem of huge amounts of toxic e-waste. The RoHS restricts the use of PBBs and PBDPEs. The

maximum concentrations allowed are 0.1 wt % of homogeneous material. The WEEE directive imposes separated collection of polymer materials fire retarded with brominated aromatics unless the size is below 10 cm<sup>2</sup> for printed circuits (Castrovinci, Lavaselli & Camino, 2008).

The RoHS procedure has now combined with European Union Registration, Evaluation, Authorisation and restriction of Chemicals (REACH), which is a new European Union Regulation (EC/2006/1907 of 18 December 2006). Four additional substances are listed that will be assessed as a priority, among these substances is hexabromocyclododecane, a brominated flame retardant widely used in expanded polystyrene for which no alternatives have been found so far. REACH addresses the production and use of chemical substances and their potential impacts on both human health and the environment; it has been described as the most complex legislation in the Union's history and the most important in the last 20 years. It is the strictest law to date regulating chemical substances and will impact industries throughout the world. REACH entered into force in June 2007, with a phased implementation over the next decade.

The aims of the proposed new regulations are to improve the protection of human health and the environment whilst maintaining the competitiveness and enhancing the innovative capability of the EU chemicals industry. REACH would furthermore give greater responsibility to industry to manage the risks from chemicals and to provide safety information on the substances. This information would be passed down the chain of production.

The brominated flame retardants were one of the first categories investigated by REACH and at the end of 2008 the registration was practically complete. The results of REACH for the main halogenated flame retardants are summarized in Table 2.5. Mechanistic studies described above show that halogenated fire-retardant systems can act by a condensed phase mechanism that in some cases could be induced by a halogen-free compound (Charles & Alexander, 2010).

Table 2.5 REACH status for the main halogenated flame retardants (Charles & Alexander, 2010).

Molecule	Status
Pentabromodiphenyl ether	The risk assessments was unfavorable
Octabromodiphenyl ether	The risk assessment indicates some risks. Production was stopped on the basis of precautionary principles.
Decabromodiphenyl ether	Risk assessment closed. No restrictions due to the lack of risks identified for the use of this substance.
Hexabromocyclododecane	Review of RoSH published on 10 December 2008 will impose a review with REACH directive
Short chain chlorinated paraffin	The risk assessment for short chain (C10–C13) chloroparaffins (SCCPs) was completed with the conclusion that the use of SCCPs in metal working and leather processing poses a risk to the aquatic environment. As a consequence, risk reduction measures have been implemented (EU Directive 2002/45). No significant risks to human health were identified. In all applications where they are used as flame retardants, no risk of secondary poisoning through accumulation in the environment or the food chain was found. Further studies of SCCPs have been specified by EU Regulation 642/2005: emissions and biodegradation in marine environment.
Medium-long-chain chlorinated paraffin	The EU Risk Assessment (Part I—Environment was completed in 2005) identifies a risk of accumulation in the food chain, and suggests risk reduction measures for all applications. Part II—Human Health are under evaluation
Tetrabromobisphenol A	EU human health risk assessment, completed on May 2005, concluded that TBBPA presents no risk to human health. Therefore TBBPA is not subject to any classification for health.

## 2.4 Nanocomposites

Since the early 1990s, the subject of polymer nanocomposites has expanded greatly, to its current status as a major field of polymer materials research. It is now realized that polymer nanocomposites, as a class of materials, were in use long before this field of research was officially named in the early 1990s. Indeed, work published as early as 1961, and patents going back to the 1940s, have shown that layered silicates (or clays) can be combined with polymers in low amounts to produce new materials with greatly improved properties. Nonetheless, it was the work in the 1990s that properly identified these clay-containing materials as polymer nanocomposites and kindled today's interest in these materials. One could argue that polymer nanocomposites are just part of the nanotechnology boom, but there is more to it. The fundamental understanding of how two dissimilar materials interface at the nanometer scale has tremendous implications for performance and properties at the macro scale. Therefore, the study of polymer nanocomposites is not just about capturing the buzz from nanotechnology; it is about understanding structure–property relationships and interfacial science at the molecular and macromolecular scale.

With the recent understanding that the addition of clays or other nanoparticles to a polymer forms a polymer nanocomposite, these materials have been investigated for many potential applications. Flammability applications for polymer clay nanocomposites were discovered a little later, and only recently has the material found its way into commercial use. Polymer nanocomposites for flammability applications are attractive because the formation of a nanocomposite not only improves the fire properties but can also improve other properties (e.g., mechanical properties), and it has the potential to bring true multifunctionality to materials.

Multifunctionality has the great potential to simplify materials science and engineering by having one material do the work of several. For instance, a plastic case for an electronic device can have several requirements. It will require particular mechanical properties (e.g., modulus, impact strength), thermal properties (not melt or sag under normal use conditions), flammability properties (meet regulations

depending on the fire risk scenario), and electromagnetic properties (frequency shielding). Also, cost, density, colour, and recyclability will need to be considered if it is a commercial product. With such a long list of requirements, it can be very difficult to find one material that can meet all needs. The class of materials that has the greatest chance of obtaining true multifunctionality is that of polymer nanocomposites.

Polymer nanocomposites have shown great improvements over traditional composites in mechanical, thermal, gas barrier, conductivity, flammability, electromagnetic shielding, and other properties, and this has spawned a huge amount of research. Inasmuch as a polymeric material can reduce flammability and improve mechanical and thermal properties and possibly other properties as well, there is a great deal of promise that polymeric nanocomposites will not just meet this need for flammability reduction, but also exceed it, thus providing fire safety and improved properties for a wide range of consumer goods (Alexander & Charles, 2007). In this study, we have focused on the improvements in paint materials flammability using nanocomposites technology.

## **2.5 Fire Tests and Standards**

The flammability of polymers can be characterized by their ignitability, flame-spread rate and heat release. Depending on the targeted application of the polymeric material, one or more of these flammability criteria need to be measured by appropriate flammability tests. There are numerous small-, intermediate- or full-scale flammability tests used in industrial or academic laboratories for either screening materials during product development or testing manufactured products (Laoutid et al. 2009). We will review to three of the most commonly used laboratory test methods.

### 2.5.1 Limited Oxygen Index (LOI)

This test was first proposed in 1966 by Fenimore and Martin (Fenimore & Martin, 1966) and is used to indicate the relative flammability of materials. Standardized in France (NF T 51-071) and in the United States (ASTM D 2863), the LOI test is now subject to an international standard (ISO 4589). The value of the LOI is defined as the minimal oxygen concentration  $[O_2]$  in the oxygen/nitrogen mixture  $[O_2/N_2]$  that either maintains flame combustion of the material for 3 min or consumes a length of 5 cm of the sample, with the sample placed in a vertical position (the top of the test sample is inflamed with a burner). The LOI is expressed as:  $LOI = 100 \frac{[O_2]}{[O_2] + [N_2]}$ .

According to ISO 4589, the LOI is measured on  $(80 \times 10 \times 4 \text{ mm}^3)$  specimens placed vertically at the center of a glass chimney (Figure 2.11). The mixture of gases flows upstream through this chimney and is homogenized by being passed through layers of glass beads. After a 30s purge of the column, the top of the specimen is ignited, like a candle.

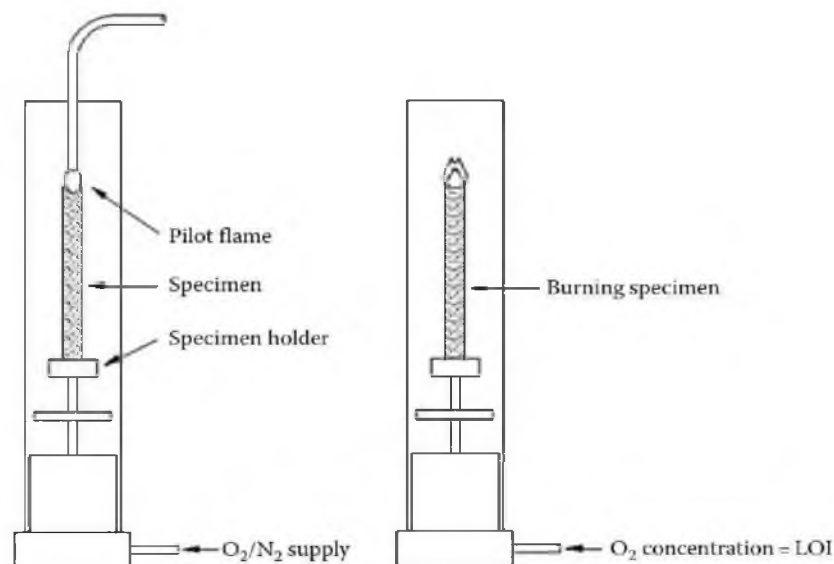


Figure 2.11 Experimental set-up for LOI measurement (Charles & Alexander, 2010).

As air contains 21% oxygen, materials with an LOI below 21% are classified as ‘‘combustible’’ whereas those with an LOI above 21% are classified as ‘‘self-

extinguishing'', because their combustion cannot be sustained at ambient temperature without an external energy contribution. The higher the LOI is the better the flame retardant property.

Although this test is nowadays considered to be relatively unsophisticated due to the development and standardization of more elaborate methods, it remains one of the most important screening and quality control methods used in the plastics industry (Laoutid et al. 2009). Table 2.6 lists flash ignition and self-ignition temperatures for various polymers, together with their LOI values.

Table 2.6 Flash-ignition temperatures, self-ignition temperatures and correlated LOI values for selected representative polymers (Laoutid et al. 2009).

<b>Polymer</b>	<b>Flash-ignition temperature (°C)</b>	<b>Self-ignition temperature (°C)</b>	<b>LOI (%)</b>
Polyethylene	340	350	18
Polypropylene	320	350	18
Polystyrene	350	490	18
Poly(vinyl chloride)	390	450	42
Poly(tetrafluoroethylene)	560	580	95
Poly(methyl methacrylate)	300	430	18
Poly(acrylonitrile)	480	560	27
Polyamide 6	420	450	25
Polymaide 66	490	530	24

### ***2.5.2 UL 94 Vertical Test***

The set of UL94 tests has been approved by the ‘‘Underwriters’ Laboratories’’ as tests of the flammability of plastic materials for parts in devices and appliances. It includes a range of flammability tests (small and large flame vertical tests, horizontal tests for bulk and foamed materials, radiant panel flame-spread test). In terms of practice and usage, the most commonly used test is UL94 V for measuring the ignitability and flame-spread of vertical bulk materials exposed to a small flame. This test is the subject of an international standard (IEC 60695-11-10) for small

flames (50W). It is a simple test of vertical combustion that classifies materials as V0, V1 or V2. The corresponding experimental device is shown in Figure 2.12.

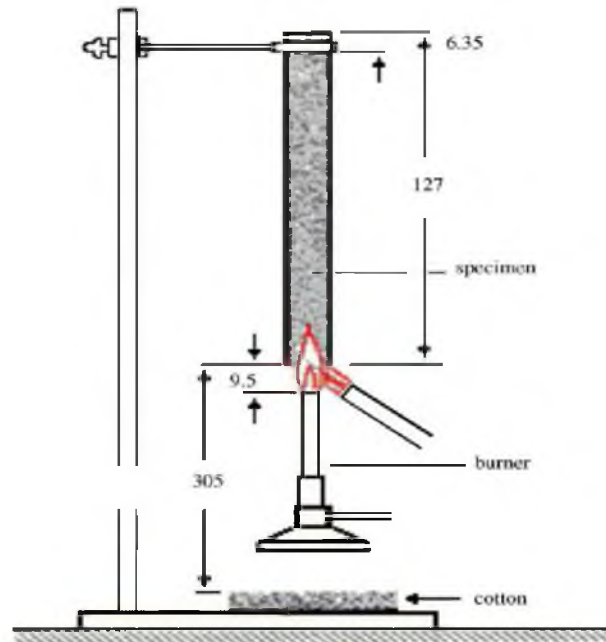


Figure 2.12 Experimental set-up for the UL94 V flammability test (Laoutid et al. 2009).

The burner is controlled to produce a blue flame with a 20 mm high central cone and a power of 50 W. The flame is applied to the bottom of the specimen and the top of the burner has to be located at 10 mm from the bottom edge of the specimen. The flame is applied for 10 s and removed. The after flame time  $t_1$  (the time required for the flame to extinguish) is noted. After extinction, the flame is applied for another 10 s. The after flame time  $t_2$  is noted, together with the afterglow time  $t_3$  (the time required for the fire glow to disappear).

During the application of the flame, the distance between burner and specimen must remain constant. If drops fall, the burner must be tilted through a maximum angle of  $45^\circ$  or slightly isolated from the specimen flame. During the test, the presence of burning drops, causing a piece of cotton located under the sample to ignite, must be noted (Laoutid et al. 2009).



The standard specifies that five specimens must be tested. The specimen is classified as V0, V1 or V2 according to the criteria listed in Table 2.7.

Table 2.7 Classification of materials for the UL 94 V flammability test (Laoutid et al. 2009).

<b>Fire classification</b>	<b>Description</b>
V0	<p><math>t_1</math> and <math>t_2</math> less than 10 s for each specimen,  <math>t_1 + t_2</math> less than 50 s for the five specimens,  <math>t_2 + t_3</math> less than 30 s for each specimen,            No after flame or afterglow up to the holding clamp, No burning drops.</p>
V1	<p><math>t_1</math> and <math>t_2</math> less than 30 s for each specimen,  <math>t_1 + t_2</math> less than 250 s for the five specimens,  <math>t_2 + t_3</math> less than 60 s for each specimen,            No after flame or afterglow up to the holding clamp, No burning drops.</p>
V2	<p><math>t_1</math> and <math>t_2</math> less than 30 s for each specimen,  <math>t_1 + t_2</math> less than 250 s for the five specimens,  <math>t_2 + t_3</math> less than 60 s for each specimen,            No after flame or afterglow up to the holding clamp, Burning drops allowed.</p>

### ***2.5.3 Cone Calorimeter***

Cone calorimetry is one of the most effective medium-sized polymer fire behaviour tests. The principle of cone calorimeter experiments is based on the measurement of the decreasing oxygen concentration in the combustion gases of a sample subjected to a given heat flux (in general from 10 to 100 kW/m<sup>2</sup>). Figure 2.13 illustrates the experimental set-up of a cone calorimeter. Standardized in the United States (ASTM E 1354), the cone calorimeter test is also the subject of an international standard (ISO 5660). The sample (100 x 100 x 4 mm<sup>3</sup>) is placed on a load cell in order to evaluate the evolution of mass loss during the experiment. A conical radiant electrical heater uniformly irradiates the sample from above. The combustion is triggered by an electric spark.

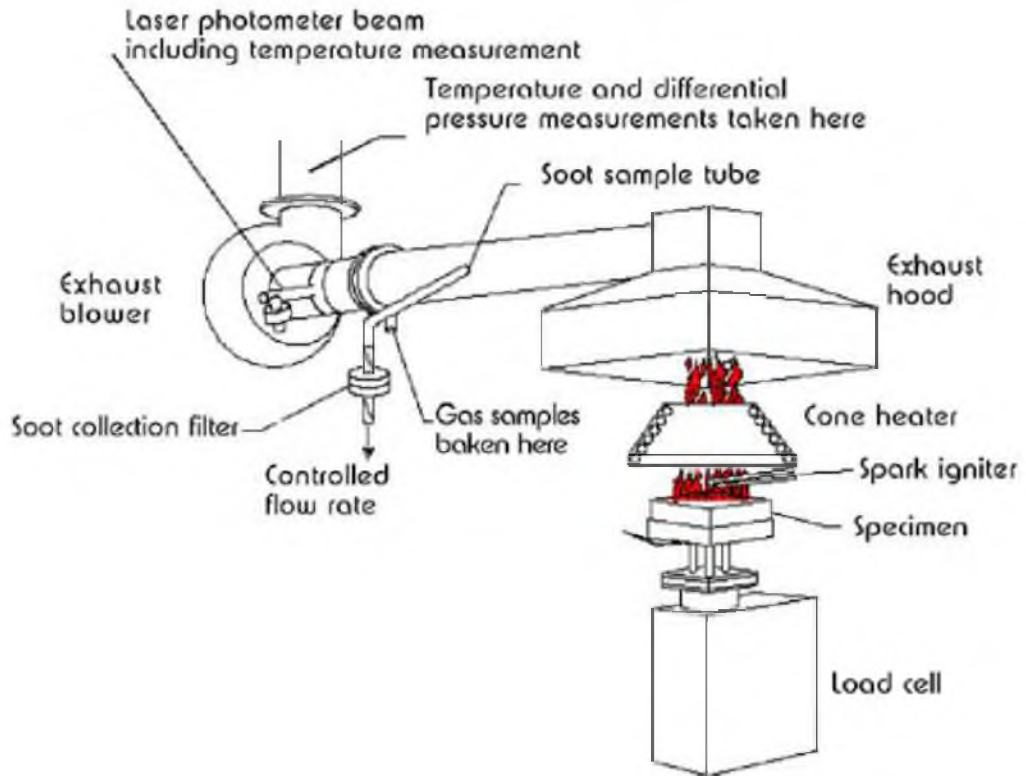


Figure 2.13 Experimental set-up for a cone calorimetry measurement (Laoutid et al. 2009).

The combustion gases produced pass through the heating cone and are captured by means of an exhaust duct system with a centrifugal fan and a hood. The gas flow, oxygen, CO and CO<sub>2</sub> concentrations and smoke density are measured in the exhaust duct (Laoutid et al. 2009).

The measurements of the gas flow and oxygen concentration are used to calculate the quantity of heat released per unit of time and surface area: HRR (heat release rate) expressed in kW/m<sup>2</sup>. The evolution of the HRR over time, in particular the value of its peak/maximum (pHRR or HRRmax), is usually taken into account in order to evaluate the fire properties. The calculation is based on Huggett's observation that most organic materials release a quantity of heat practically proportional to the quantity of oxygen consumed while burning. The proportionality factor is constant from one material to another and is equal to 13.1 kJ/g consumed oxygen (Huggett, 1980). Integration of the HRR vs. time curve gives the total heat released (THR) expressed in kJ/m<sup>2</sup>. In addition, the cone calorimeter test also enables characterization of the time to ignition (TTI), time of combustion or extinction

(TOF), mass loss during combustion, quantities of CO and CO<sub>2</sub>, and total smoke released (TSR) (Laoutid et al. 2009).

## 2.6 Potential Applications of Flame Retardant Materials

The use of flame retardants to reduce combustibility of the polymers, and smoke or toxic fume production, therefore becomes a pivotal part of the development and application of new materials. Amongst the major markets where flame retardants are required, the industries dealing with construction, electrical and electronics components and transportation are the three of greatest importance (Table 2.8) (Innes, 1996).

For instance, in the aerospace industry, advanced composite materials are developed to displace metals in response to a strong economic imperative to save weight while at the same time increasing the payload. These new materials require properties such as thermo-oxidative stability, low flammability and retention of material strength at elevated temperatures, low corrosion and better fatigue resistance, lower tooling costs and relative ease of fabrication. Of course, at the same time it is important that the structural materials are cost competitive with metals (Shui & Ian, 2002).

Table 2.8 Flame retardant (FR) market application (Shui & Ian, 2002).

<b>Market area</b>	<b>Subgroup</b>	<b>FR requirements</b>
Building construction and contents	Building	Containment
	Interior finishing	Flame spread
	Furnishings	Ignition resistance
Electrical and electronics	Appliances	Ignition resistance
	Electronic devices	Flame spread
	Wire and cable	
Transportation	Automobile	Escape time
	Rail	Containment
	Aviation and aerospace	

Each one of these sectors has established its own FR standards and specifications over the past decades, often with reference to local government regulations. As a result, every market segment has a large number of regulations and test procedures forcing materials developers to adapt their formulations to match customer requirements in order to meet the safety legislation of each relevant authority. In Germany, for example, these can differ from one Land to another. Currently, attempts are being made to harmonise standards, with the construction industry farthest along the route to finalise such procedures. Examples of standards are shown in Table 2.9.

Table 2.9 Examples of flame resistance standards (Dufton, 2003).

<b>Sector</b>	<b>Test</b>	<b>Evaluation</b>
Construction	DIN 4102 (Germany)	B1, B2 (vertical chimney)
Electrical and appliance	UL94 (USA), IEC 65 (Europe)	V-0, V-1, V-2, HB (vertical test), (horizontal test), pass or fail
Others	e.g., Mining tests	e.g., tunnel test

Fire protection requirements exist in the fields of E&E engineering, the construction industry, transportation, textiles and upholstery for furniture. More than 40% of FRs are utilised by the E&E sector and cables, especially for consumer electronics, business machines, household appliances and industrial applications.

In the wake of European harmonisation, national fire requirements in the construction industry and rail-transport sector are gradually being replaced. A new classification system and new test procedures for the fire behaviour of construction products replaced existing national systems within the EU. This means there was more stringent requirements overall, calling for a reassessment of the plastics currently utilised. All the construction products introduced on a national basis have to be tested according to the new test procedures, particularly the Single Burning Item (SBI) Test, involving a higher outlay on material and higher expenditure, since there are not generally any correlations with the existing national tests. The same applies for railway rolling stock, whose test procedures are currently harmonised on

a national level and will become so at European level in future. In the case of international test procedures already introduced, changes are pointing towards an increasing level of fire protection (Dufton, 2003).

## CHAPTER THREE

### EXPERIMENTAL PROCEDURE

#### 3.1 Purpose

The aim of this thesis is to develop flame retardant coatings/paints which are easier and cheaper as a production process be used in all areas due to the fact that a modification of structure of polymer materials is an expensive method. Another important aspect of the thesis, the used reinforcing materials are halogen-free, environmentally friendly and cheap flame-retardant materials. From this point of view, in this research, the new approach is to explore both the science and technology of how reinforced materials affect structures of water-based dye as composite coatings and connect the results to materials properties, and show the engineering concepts that can be used to produce or improve flame retardant paints by several applications. This work will be a guide for the future researches followed by the researches.

In this context, huntite/hydromagnesite mineral was used as a reinforcing material has flame retardant properties. In addition, thanks to the synergistic effects of boric acid and antimony (III) oxide was used as the auxiliary materials and flame resistant composite paint materials were developed. Before creating composite material due to the smooth surface quality and high efficiency micron-sized huntite/hydromagnesite and antimony oxide minerals were reduced to nanosized by grinding process. Composite material was prepared by mixing with different amounts of the flame retardant materials and plastic paint used as matrix material and then it was applied on plastic materials by a paint gun. The used minerals before and after grinding process were characterized as particle size, phase analysis and elemental analysis. After fabrication of nanosized flame retardant materials reinforced composite samples, they were characterized through XRD, XPS, FT-IR, DTA-TG, SEM, surface roughness and hardness testing machines. In addition, flame retardancy tests were performed as a main objective of this research. In this way, flame retardancy properties of composite materials were determined. With the results of tests that were

done, it was determined that the composite materials exhibit excellent flame retardant properties. After we aimed to reduce the surface roughness of coatings in the thesis, flame resistance time increased because of getting a more uniform coating.

## **3.2 Materials**

### ***3.2.1 Matrix Material***

In this study, water-based white dye which is purchased from DYO Inc., Izmir was used as matrix material. Paints and/or coatings are used to protect substrates against mechanical, chemical, and atmospheric influences. At the same time, they serve to decorate and colour buildings, industrial plants, and utensils. Paints or coatings are liquid, paste, or powder products which are applied to surfaces by various methods and equipment in layers of given thickness. These form adherent films on the surface of the substrate.

Paints are made of numerous components, depending on the method of application, the desired properties, the substrate to be coated, and ecological and economic constraints. Paint components can be classified as volatile or non-volatile. Volatile paint components include organic solvents, water, and coalescing agents. Non-volatile components include binders, resins, plasticizers, paint additives, dyes, pigments and extenders. In some types of binder, chemical hardening can lead to condensation products such as water, alcohols and aldehydes or their acetals, which are released into the atmosphere, thus being regarded as volatile components.

All components fulfill special functions in the liquid paint and in the solid coating film. Solvents, binders, and pigments account for most of the material, the proportion of additives being small. Low concentrations of additives produce marked effects such as improved flow behaviour, better wetting of the substrate of pigment, and catalytic acceleration of hardening.

Solvents and pigments need not always be present in a coating formulation. Solvent-free paints and pigment-free varnishes are also available. The most important component of a paint formulation is the binder. The binders essentially determine the application method, drying and hardening behaviour, adhesion to the substrate, mechanical properties, chemical resistance, and resistance to weathering (Dieter, 1998).

### ***3.2.2 Reinforcing Materials***

In the experiment, huntite/hydromagnesite, antimony (III) oxide, boric acid minerals were used as flame retardant reinforced minerals.

#### *3.2.2.1 Huntite/Hydromagnesite*

Natural hydromagnesite has been discovered in mixed deposits with huntite which is the reason such mixtures have generated interest as fire retardants. Mixtures of natural hydromagnesite and huntite have been commercially exploited as fire retardants since the late 1980's. The world's largest known reserves of mixed hydromagnesite and huntite are in Turkey, operated commercially by Minelco. Huntite/hydromagnesite used in this study was commercially purchased from Minelco Company.

The deposit normally consists of physical blends of two minerals huntite and hydromagnesite with varying ratios in between 40-30% huntite and 60-70% hydromagnesite. The level of impurities is very low; the most important ones are other white carbonate minerals such as aragonite, calcite and dolomite. An average mineralogical composition, based on XRD and chemical analysis data of current ores is as follows: huntite (46%), hydromagnesite (46%), magnesite (4%), aragonite (3%) and calcite (1%). A typical chemical analysis of the ore is MgO (38.0%), CaO (9.5%), H<sub>2</sub>O (9.1%), CO<sub>2</sub> (43.4%) and LOI (52.5%). In contrast to the other mineral flame retardants mentioned above, huntite/hydromagnesite has no simple metal hydroxide structure, but consists of two distinct carbonates (Table 3.1) Physical



densities of huntite ( $\text{Mg}_3\text{Ca}(\text{CO}_3)_4$ ) and hydromagnesite ( $\text{Mg}_4(\text{OH})_2(\text{CO}_3)_3 \cdot 3\text{H}_2\text{O}$ ) minerals are  $2,70 \text{ g/cm}^3$  and  $2,24 \text{ g/cm}^3$  respectively (Kirschbaum, 2001).

Table 3.1 Formulas and properties of huntite & hydromagnesite (Kirschbaum, 2001).

<b>Name</b>	<b>Formula</b>	<b>Physical Density</b>	<b>Temp. Stability</b>
Huntite	$\text{Mg}_3\text{Ca}(\text{CO}_3)_4$	$2,70 \text{ g/cm}^3$	$>400 \text{ }^\circ\text{C}$
Hydromagnesite	$\text{Mg}_4(\text{OH})_2(\text{CO}_3)_3 \cdot 3\text{H}_2\text{O}$	$2,24 \text{ g/cm}^3$	$240-250 \text{ }^\circ\text{C}$

The advantages of this mineral can be arranged in order such as being non-corrosive to processing equipments, low smoke generation, no acid gas emission, halogen free, environmentally safe, recyclable, no combustion gas corrosion, no limitation in colouring and low combustion. In addition, huntite/hydromagnesite offers a good cost/performance relationship in flame retardant applications (Weber, 1999). Detailed information about boric acid and antimony (III) oxide was explained in Chapter 2.

### **3.3 Ball Milling of Reinforcing Materials**

The most important parameters in the intended production of nanocomposite materials are particle size distribution and homogeneous dispersion in the polymeric matrix since the total particle surface increased with decreasing particle size. Therefore surfaces interactions of nanoparticles with each other will increase so that the polymer matrix composites will have a higher efficiency than larger grained powders.

In this context, Fritsch Premium line Pulverisette 7 model High Energy Ball milling machine which is shown in Figure 3.1 was used for milling huntite/hydromagnesite (Minelco) and antimony (III) oxide (Aldrich) minerals. The minerals were milled at rate of 750 rpm at room temperature for 120 minutes in air. For milling, tungsten carbide bowls and balls were employed.



Figure 3.1 The high energy ball milling machine (Nanotechnology Lab., DEU-EMUM)

### **3.4 Production of Composite Coatings/Paints**

Composite coatings/paints were prepared by reinforcing flame retardant nanoparticles at different ratios into the water-based white dye as single, binary and ternary component. Materials were stirred for 30 minutes and at 1000 rpm with the magnetic stirrer to homogenize of dye-mineral mixture. Prepared composite materials were applied on plastic substrate (TV cabinet material) by a paint gun and were dried at 60 °C for 90 minutes in oven. Sample names, code and properties of prepared the flame retardant composite coatings were classified in Table 3.2.

Table 3.2 Classified of sample names, code and properties of prepared composite coatings/paints

Sample Name	Sample Code	Sample properties
Pure	P	Coating with pure dye
Huntite/Hydromagnesite	1H	Paint + 1% Huntite/Hydromagnesite
	3H	Paint + 3% Huntite/Hydromagnesite
	5H	Paint + 5% Huntite/Hydromagnesite
	10H	Paint + 10% Huntite/Hydromagnesite
	15H	Paint + 15% Huntite/Hydromagnesite
Antimony (III) Oxide ( $Sb_2O_3$ )	1A	Paint + 1% Antimony (III) Oxide
	3A	Paint + 3% Antimony (III) Oxide
	5A	Paint + 5% Antimony (III) Oxide
	10A	Paint + 10% Antimony (III) Oxide
	15A	Paint + 15% Antimony (III) Oxide
Boric Acid ( $H_3BO_3$ )	1B	Paint + 1% Boric Acid
	3B	Paint + 3% Boric Acid
	5B	Paint + 5% Boric Acid
	10B	Paint + 10% Boric Acid
	15B	Paint + 15% Boric Acid
Huntite/Hydromagnesite + Antimony (III) Oxide ( $Sb_2O_3$ )	3A1H	Paint + 1% Hun. + 3% Ant.
	3A3H	Paint + 3% Hun. + 3% Ant.
	3A5H	Paint + 5% Hun. + 3% Ant.
	3A7H	Paint + 7% Hun. + 3% Ant.
Huntite/Hydromagnesite + Boric Acid ( $H_3BO_3$ )	3B1H	Paint + 1% Hun. + 3% Bor.
	3B3H	Paint + 3% Hun. + 3% Bor.
	3B5H	Paint + 5% Hun. + 3% Bor.
	3B7H	Paint + 7% Hun. + 3% Bor.
Antimony (III) Oxide ( $Sb_2O_3$ ) + Boric Acid ( $H_3BO_3$ )	3A1B	Paint + 3% Bor. + 3% Ant.
	3A2B	Paint + 3% Bor. + 3% Ant.
	3A3B	Paint + 3% Bor. + 3% Ant.
Huntite/Hydromagnesite + Antimony (III) Oxide ( $Sb_2O_3$ ) + Boric Acid ( $H_3BO_3$ )	1A2B1H	Paint + 1% Hun. + 1% Ant. + 2% Bor.
	1A2B3H	Paint + 3% Hun. + 1% Ant. + 2% Bor.
	1A2B5H	Paint + 5% Hun. + 1% Ant. + 2% Bor.
	1A2B7H	Paint + 7% Hun. + 1% Ant. + 2% Bor.
	1A2B10H	Paint + 10% Hun. + 1% Ant. + 2% Bor.

Hun.=Huntite/hydromagnesite, Ant.= Antimony (III) Oxide and Bor.=Boric Acid

## 3.5 Characterization of Composites and Reinforcing Materials

### 3.5.1 Particle Size Distribution

Before and after milling process, the particle size distribution of huntite/hydromagnesite and antimony (III) oxide minerals was determined using particle size analyzer which uses light scattering techniques to measure hydrodynamic size of nanoparticles. The particle size distribution was measured using Malvern Zeta Sizer Nano ZS90. Water was used as a dispersant and the temperature was set to 25 °C.

### 3.5.2 X-Ray Diffractometer (XRD)

XRD is a powerful technique used to uniquely identify the crystalline phases present in materials and measure the structural properties (strain state, grain size, epitaxy, phase composition, preferred orientation and defect structure) of these phases. XRD is non-contact and non-destructive. The regular array of atoms in a crystalline material forms a 3D diffraction grating for waves with a wavelength around that of the distance between the atoms. When waves enter a crystal, they are scattered in all directions by the atoms. In certain directions, these waves can interfere destructively. In other directions, constructive interference will occur resulting in peaks in X-ray intensity. The diffraction pattern that results is a map of the reciprocal lattice of the crystal and can be used to determine the structure of the crystal. Bragg's law is the basis for crystal diffraction:

$$n\lambda=2.d.\sin\theta \quad (3.1)$$

where  $n$  is an integer known as the order of diffraction,  $\lambda$  is the X-ray wavelength is the spacing between two consecutive scattering planes and  $\theta$  is the angle between the atomic planes and the incident (and diffracted) X-ray beam (Ahmed & Jackson, 2009). Figure 3.2 illustrates diffraction of x-rays by planes of atoms.

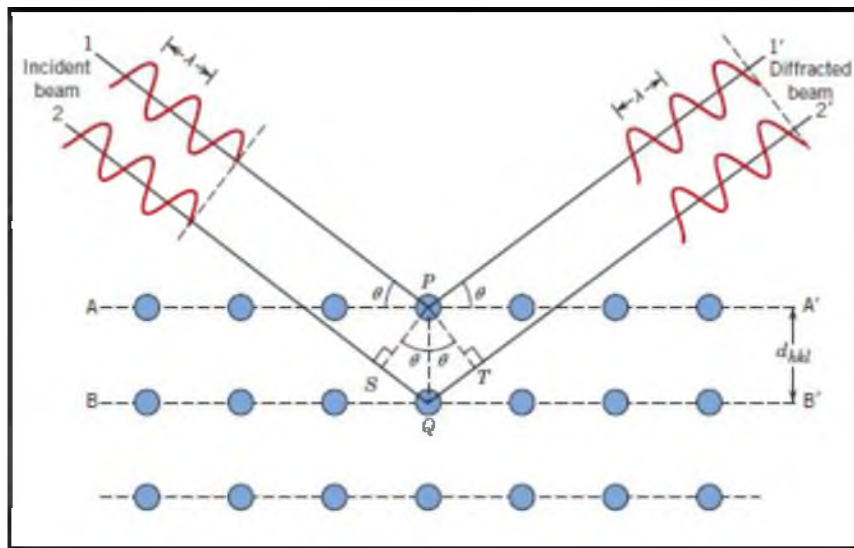


Figure 3.2 Diffraction of x-rays by planes of atoms (A–A' and B–B') (Callister, 2007).

Bragg's law is necessary but not sufficient condition for diffraction by real crystals. It specifies when diffraction will occur for unit cells having atoms positioned only at cell corners. Nonetheless, atoms situated at other sites (e.g., face and interior unit cell positions as with FCC and BCC) act as extra scattering centers, which can produce out-of-phase scattering at certain Bragg angles. The net result is the absence of some diffracted beams that, according to Bragg's law, should be present.

Schematic diagram of an X-ray diffractometer is presented in Figure 3.3 The diffractometer is an apparatus used to determine the angles at which diffraction occurs for specimens. A specimen S in the form of a flat plate is supported so that rotations about the axis labelled O are possible; this axis is perpendicular to the plane of the page. The monochromatic x-ray beam is generated at point T, and the intensities of diffracted beams are detected with a counter labelled C in the figure. The specimen, x-ray source, and counter are all coplanar (Callister, 2007).

Composites and reinforcing materials were analyzed by means of XRD with a grazing angle attachment and an incident angle of  $1^\circ$  (Thermo-Scientific, ARL-K $\alpha$ ). X-Ray radiation of Cu-K $\alpha$  was set at 45 kV and 44 mA with a scanning speed of  $2^\circ/\text{min}$ .

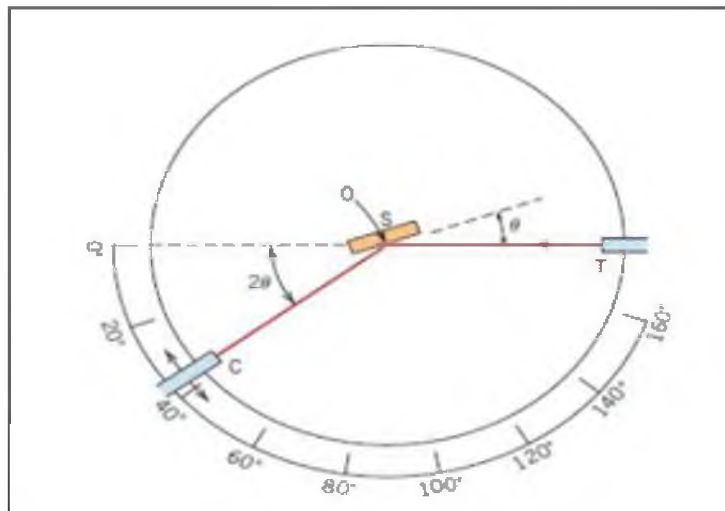


Figure 3.3 Schematic diagram of an x-ray diffractometer; T: x-ray source, S: specimen, C: detector, and O: the axis around which the specimen and detector rotate (Callister, 2007).

### 3.5.3 X-Ray Photoelectron Spectroscopy (XPS)

X-ray photoelectron spectroscopy (XPS) is a quantitative spectroscopic technique that measures the elemental composition, empirical formula, chemical state and electronic state of the elements that exist within a material. XPS spectra are obtained by irradiating a material with a beam of X-rays while simultaneously measuring the kinetic energy and number of electrons that escape from the top 1 to 10 nm of the material being analyzed (Figure 3.4). XPS requires ultra-high vacuum (UHV) conditions. It can be also used to analyze the surface chemistry of a material in its "as received" state, or after some treatment, for example: fracturing, cutting or scraping in air or UHV to expose the bulk chemistry, ion beam etching to clean off some of the surface contamination, exposure to heat to study the changes due to heating, exposure to reactive gases or solutions, exposure to ion beam implant, exposure to ultraviolet light.

XPS detects all elements with an atomic number ( $Z$ ) of 3 (lithium) and above. It cannot detect hydrogen and helium, because the diameter of these orbitals is so small, reducing the catch probability to almost zero. It is routinely used to analyze all solid materials (Crist, B.V., 2011). In this study, composites and reinforcing materials were analyzed as to characterize elemental via XPS (Thermo-Scientific,

Al-K $\alpha$ ). The device was calibrated according to gold 4f<sub>7/2</sub>. 10<sup>-8</sup> mbar under vacuum was studied and from a single point was done 20 scanning. Pass energy and energy step size were determined as 150 eV and 1 eV.

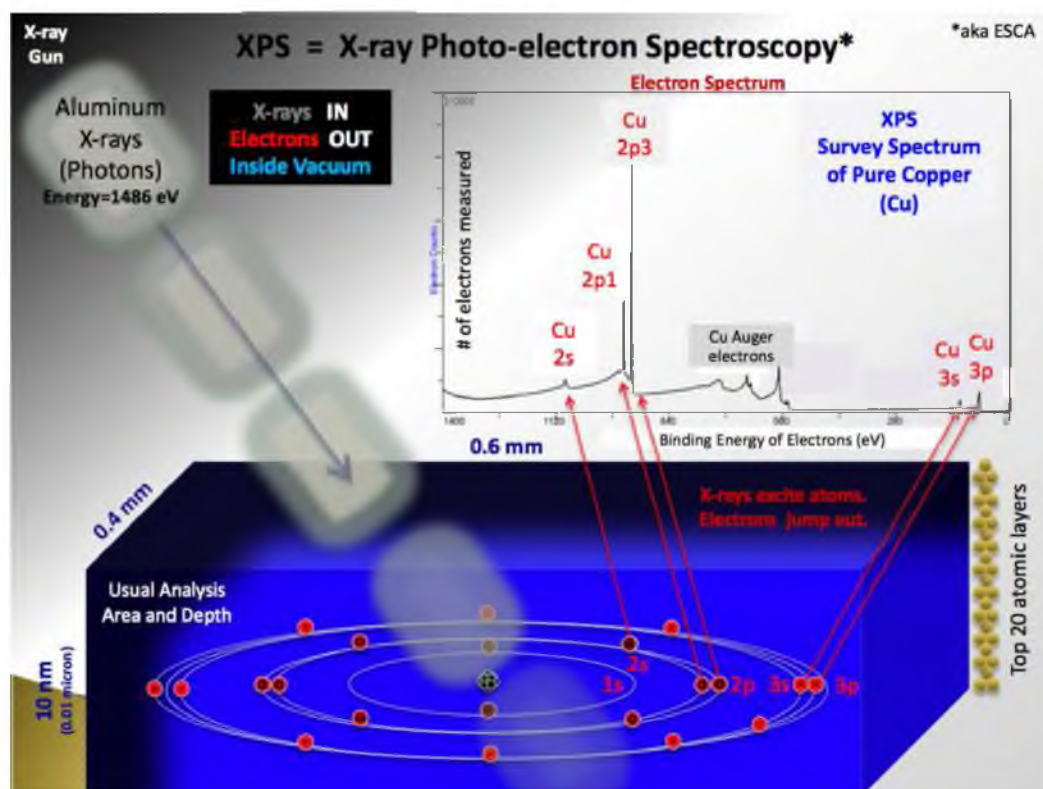


Figure 3.4 Rough schematic of XPS physics (Crist, 2011)

### 3.5.4 Fourier Transform Infrared Spectroscopy (FT-IR)

FT-IR is a powerful tool for identifying types of chemical bonds in a molecule by producing an infrared absorption spectrum that is like a molecular "fingerprint". Each different material is a unique combination of atoms, so two different compounds never produce the exact same infrared spectrum. Therefore, infrared spectroscopy can result in qualitative analysis of every different kind of material. By interpreting the infrared absorption spectrum, the chemical bonds in a molecule can be determined. In principle, molecular bonds vibrate at various frequencies depending on the elements and the type of bonds. For any given bond, there are several specific frequencies at which it can vibrate. According to quantum mechanics, these frequencies correspond to the ground state (lowest frequency) and several excited

states (higher frequencies). One way to cause the frequency of a molecular vibration to increase is to excite the bond by having it absorb light energy. For any given transition between two states the light energy (determined by the wavelength) must exactly equal the difference in the energy between the two states. The energy corresponding to these transitions between molecular vibrational states is generally 1-10 kilocalories/mole which corresponds to the infrared portion of the electromagnetic spectrum. The results are generally plotted as a function transmittance or absorbance versus wavelength. The conversion between transmittance to absorbance data is:  $A = \log (1/T)$  where A is absorbance and T is transmittance.

In addition to qualitative analysis, the size of the peaks in the spectrum is a direct indication of the amount of material present. With suitable software algorithms, infrared is also an excellent tool for quantitative analysis.

The technique of Attenuated Total Reflectance (ATR) has in recent years revolutionized solid and liquid sample analyses because it combats the most challenging aspects of infrared analyses namely sample preparation and spectral reproducibility. An ATR accessory operates by measuring the changes that occur in a totally internally reflected infrared beam when the beam comes into contact with a sample as indicated in Figure 3.5.

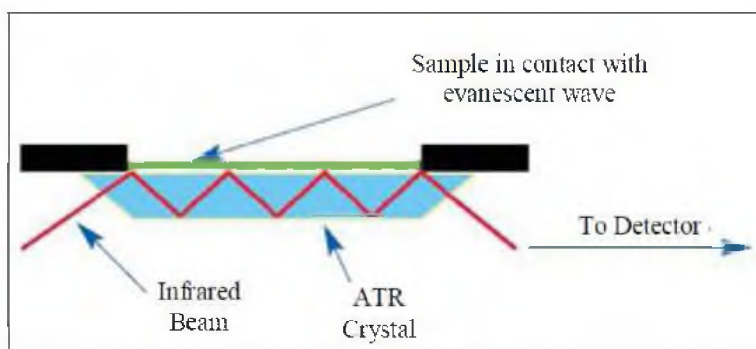


Figure 3.5 Schematic representation of an ATR system (Birlik, 2011)

The infrared spectra of the samples were recorded with a Perkin Elmer Spectrum BX instrument equipped with ATR apparatus in the spectra range between 4000 and



650  $\text{cm}^{-1}$  with a resolution of 4  $\text{cm}^{-1}$ . All of the samples were characterized by FT-IR by which % absorbance as a function of wave number curves can be obtained.

### ***3.5.5 Scanning Electron Microscopy (SEM)***

Scanning electron microscopy (SEM) is one of the most common analytical methods to examine surface morphology of the solid-state specimen. In SEM, a tiny high-energy electron beam is scanned across the sample surface. Series of radiations can be produced in terms of the interaction between the electron beam and the sample. Normally, two types of radiation are utilized for image formation: primary backscattered electrons and secondary electrons. Backscattered electrons reveal the compositional and topographical information of the specimen. The secondary electron images produce a depth of field which shows the surface topography. The signal modulation of the two types of radiation is viewed as images in the cathode ray tube (CRT) and provides the morphology, surface topology and composition of the specimen surface.

In this study, the surfaces of composites coatings/paints were examined by using JEOL JSM-6060 instrument operating at an accelerating voltage of 8-10 kV. Surfaces were coated with gold to be conductive. Materials were examined under 1000X and 5000X magnification.

### ***3.5.6 Differential Thermal Analysis-Thermogravimetry (DTA-TG)***

Thermal methods are based upon the measurement of the dynamic relationship between temperature and some property of the system such as mass and heat absorbed by or evolved from it. Differential Thermal Analysis (DTA) and Thermogravimetry (TG) are the most important thermal methods used in characterization of materials. In DTA the heat absorbed or emitted by a system is observed by measuring the temperature difference  $\Delta T$  between the sample and an inert reference material (generally alumina powder), as the temperature of both is increased at a constant rate. TG analysis is concerned with the change in weight of a

material as its temperatures changes. Many series of thermal analysis techniques can be combined with other non-thermal technique for valuable multiple-parameter information as in our DTA/TG system. The thermal behaviours of pure dye and composite coatings/paints were evaluated to observe decomposition and phase formation at a heating rate of 10 °C/min in the temperature range of 25-600 °C under air atmosphere by using DTA/TG machine (DTG-60H Shimadzu).

### ***3.5.7 Surface Profilometer (Roughness)***

Composite sample surface's profiles were investigated with a surface profilometer Mitutoyo SJ-301, in order to quantify the roughness. Whilst the historical notion of a profilometer was a device similar to a phonograph that measures a surface as the surface is moved relative to the contact profilometer's stylus, this notion is changing with the emergence of numerous non-contact profilometer techniques.

### ***3.5.8 Mechanical Tests***

Hardness is defined as the characteristic ability of a material to resist penetration or abrasion by other bodies. It has been nearly two centuries since the first hardness test was developed by Mohs in 1822. In that time, the state of the art has progressed from using reference materials to rank scratch relative resistance to the application of contact mechanics principles using instrumented, automated systems to probe mechanical properties on the nanometre scale.

Indentation testing is a simple method that consists essentially of touching the material of interest whose mechanical properties such as elastic modulus and hardness. Nanoindentation is simply an indentation test in which the length scale of the penetration is measured in nanometres ( $10^{-9}$  m) rather than microns ( $10^{-6}$  m) or millimetres ( $10^{-3}$  m), the latter being common in conventional hardness tests (Wheeler, 2009).

Nanoindentation hardness tests are generally made with either spherical or pyramidal indenters. Consider a Vickers indenter with opposing faces at a semi-angle of  $\theta = 68^\circ$  and therefore making an angle  $\beta = 22^\circ$  with the flat specimen surface. For a particular contact radius  $a$ , the radius  $R$  of a spherical indenter whose edges are at a tangent to the point of contact with the specimen is given by  $\sin \beta = a/R$ , which for  $\beta = 22^\circ$  gives  $a/R = 0.375$ . It is interesting to note that this is precisely the indentation strain<sup>1</sup> at which Brinell hardness tests, using a spherical indenter, are generally performed, and the angle  $\theta = 68^\circ$  for the Vickers indenter was chosen for this reason (Fisher, 2009).

The Berkovich indenter, in Figure 3.6 (a), is generally used in small-scale indentation studies and has the advantage that the edges of the pyramid are more easily constructed to meet at a single point, rather than the inevitable line that occurs in the four-sided Vickers pyramid. The face angle of the Berkovich indenter normally used for nanoindentation testing is  $65.27^\circ$ , which gives the same projected area-to-depth ratio as the Vickers indenter. Originally, the Berkovich indenter was constructed with a face angle of  $65.03^\circ$ , which gives the same actual surface area to depth ratio as a Vickers indenter. The tip radius for a typical new Berkovich indenter is on the order of 50–100 nm. This usually increases to about 200 nm with use. The Knoop indenter, in Figure 3.6 (b), is a four-sided pyramidal indenter with two different face angles. Measurement of the unequal lengths of the diagonals of the residual impression is very useful for investigating anisotropy of the surface of the specimen. The indenter was originally developed to allow the testing of very hard materials where a longer diagonal line could be more easily measured for shallower depths of residual impression. The cube corner indenter, Figure 3.6 (c), is finding increasing popularity in nanoindentation testing. It is similar to the Berkovich indenter but has a semi-angle at the faces of  $35.26^\circ$  (Berkovich, 1951).

The Berkovich indenter is used routinely for nanoindentation testing because it is more readily fashioned to a sharper point than the four-sided Vickers geometry, thus ensuring a more precise control over the indentation process. The mean contact

pressure is usually determined from a measure of the contact depth of penetration,  $h_c$  in such that the projected area of the contact is given by;

$$A = 3\sqrt{3}h_c^2 \tan^2\theta \quad (3.2)$$

which for  $\theta = 65.27^\circ$ , evaluates to:

$$\begin{aligned} A &= 24.494h_c^2 \\ &\approx 24.5h_c^2 \end{aligned} \quad (3.3)$$

and hence the mean contact pressure, or hardness, is:

$$H = \frac{P}{24.5h_c^2} \quad (3.4)$$

The original Berkovich indenter was designed to have the same ratio of actual surface area to indentation depth as a Vickers indenter and had a face angle of  $65.0333^\circ$ .

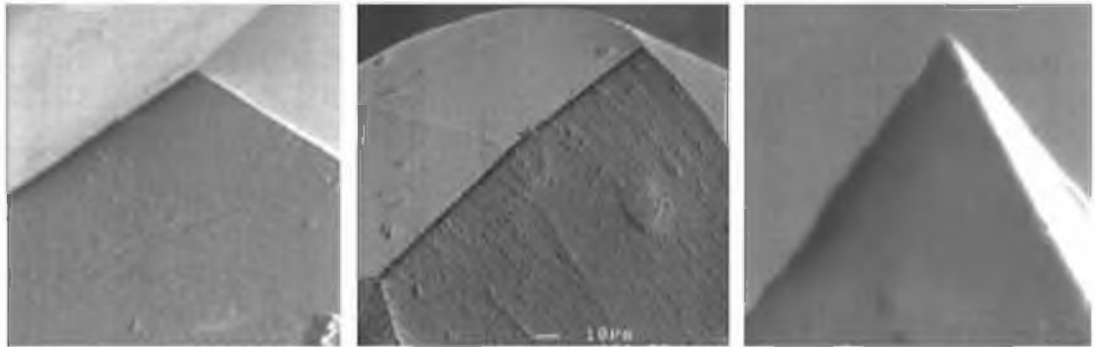


Figure 3.6 SEM images of the tips of (a) Berkovich, (b) Knoop, and (c) cube-corner indenters used for nanoindentation testing. The tip radius of a typical diamond pyramidal indenter is in the order of 100 nm (Fischer, 2009).

For the calculation of modulus based on elastic contact theory, there are some differences in view of its indentation deformation. Figure 3.7 depicts the schematic representation of loading versus displacement during nanoindentation. In the figure,  $S$  represents the contact stiffness while  $h_c$  is the contact depth (Oliver & Pharr, 1992).

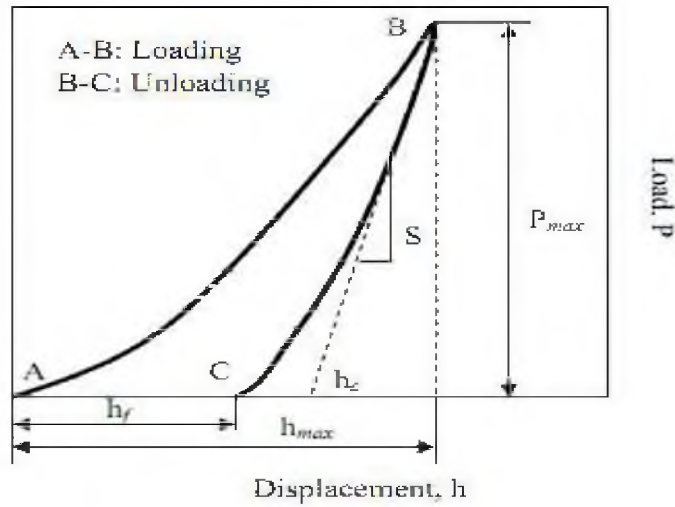


Figure 3.7 A schematic representation of load versus displacement during nanoindentation (Oliver & Pharr, 1992).

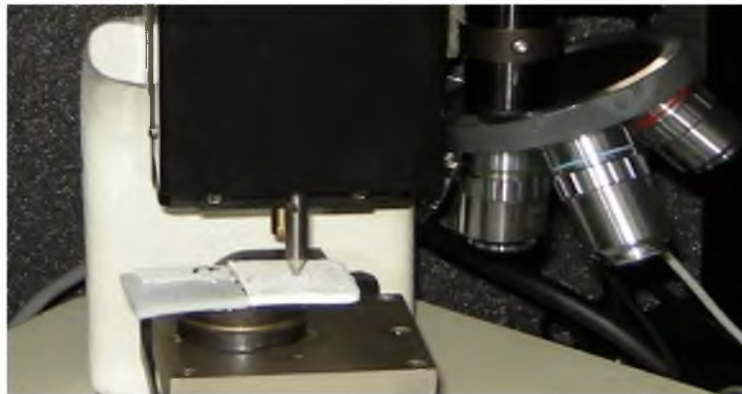


Figure 3.8 Nanoindentation system

Nanoindentation measurements were performed using a nanoindentation system (IBIS, Fischer-Cripps Laboratories, Australia) (see Figure 3.8). We have used a three-side pyramid (Berkovich) diamond indenter. The area function, which is used to calculate contact area  $A_c$  from contact depth  $h_c$ , was carefully calibrated by using a fused silica sample, prior to the experiments. Samples were stuck on a low contraction resin and cut in 2 x 2 cm. Loads of 2, 4, 8, 16 and 20 mN were used for the tests.

### 3.6 Flame Retardant Test

Needle-flame testing simulates the effect of a small flame which may result from fault conditions, in order to assess by a simulation technique the fire hazard. It is applicable to electrotechnical equipment, its sub-assemblies and components and to solid electrical insulating materials or other combustible materials. In this study, in order to determine the flame retardant properties of composite materials, the obtained samples were tested during 3 minutes via the candle-flame test method (according to IEC 62441 standard) in the needle-flame test machine (under the terms of the test IEC 60695-11-5) shown in Figure 3.9.



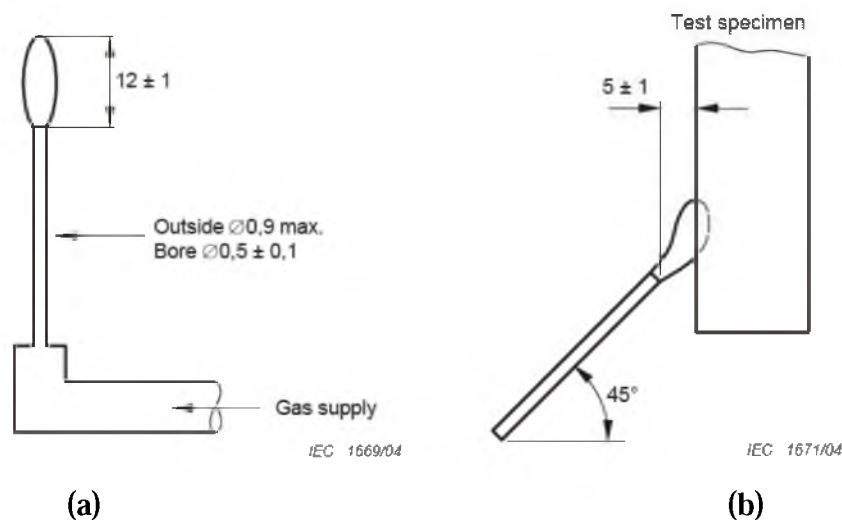
Figure 3.9 Needle flame test machine

According to IEC 60695-11-5 testing standards;

- The burner to produce the test flame have to consist of a tube at least 35 mm long with a bore of  $0.5 \text{ mm} \pm 0.1 \text{ mm}$  and an outer diameter not exceeding 0.9 mm.
- The burner has to be supplied with butane or propane gas having a purity of at least 95 %. There have to be no air admitted to the burner tube.
- With the axis of the burner in the vertical position, the gas supply is adjusted so that the length of the flame is  $12 \text{ mm} \pm 1 \text{ mm}$ , when viewed in subdued light against a dark background (see Figure 3.10 a). The test time for the

temperature to increase from  $100\text{ }^{\circ}\text{C} \pm 5\text{ }^{\circ}\text{C}$  to  $700\text{ }^{\circ}\text{C} \pm 3\text{ }^{\circ}\text{C}$  have to be  $23,5\text{ s} \pm 1,0\text{ s}$ .

If the test specimen drips molten or flaming material during the application of the flame, the burner is tilted up to  $45^{\circ}$  from the vertical to prevent material from dripping into the burner tube while maintaining an  $8\text{ mm} \pm 1\text{ mm}$  spacing between the centre of the top of the burner and the remaining portion of the test specimen, ignoring any strings of molten material. The tip of the burner tube was positioned at a distance of  $5\text{ mm} \pm 0,5\text{ mm}$  from the candle flame accessible area (see Figure 3.10 b), with the burner tube in  $45^{\circ}$  position. The centre-line of the burner was positioned within the candle flame accessible area.



The test flame has to remain stationary for 3 min even if the surface melts or shrinks away from the flame. If any flaming does not exceed 3 min after the removal of test flame, including flaming of materials that may have dropped from the individual item, the test flame has to be moved to another candle flame accessible area and the procedure is repeated until each relevant surface within the candle flame accessible area has been tested.

## CHAPTER FOUR

### RESULTS AND DISCUSSION

#### 4.1 Particle Size Distribution

The most important parameters in the intended production of nanocomposite materials are particle size distribution and homogeneous dispersion in the polymeric matrix since the total particle surface increases with decreasing particle size. Therefore surfaces interactions of nanoparticles with each other increase so that the polymer matrix composites have a higher efficiency than larger grained powders.

Before and after milling process, particle size distribution of flame retardant reinforcing materials which were milled via Fritsch pulverisette 7 are shown in Figures 4.1 and 4.2. As a result of the particle size analysis, whilst huntite/hydromagnesite minerals were average 739 nm before milling, it was nearly 121 nm after milling as presented in Figure 4.1. Similarly, while antimony (III) oxide mineral was approximately 1058 nm before milling, it was found to be 141 nm after milling process (Figure 4.2). In these results, we provide a greater surface area and a lower surface roughness.

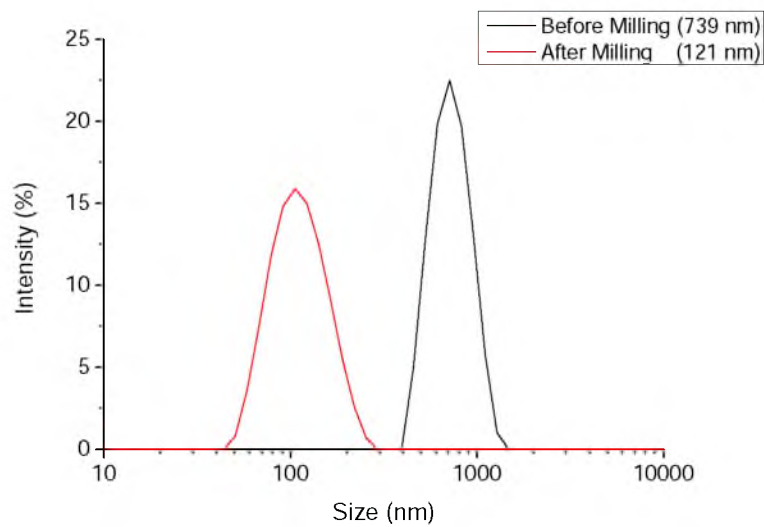


Figure 4.1 Particle size distribution of huntite/hydromagnesite powder mineral after and before milling process



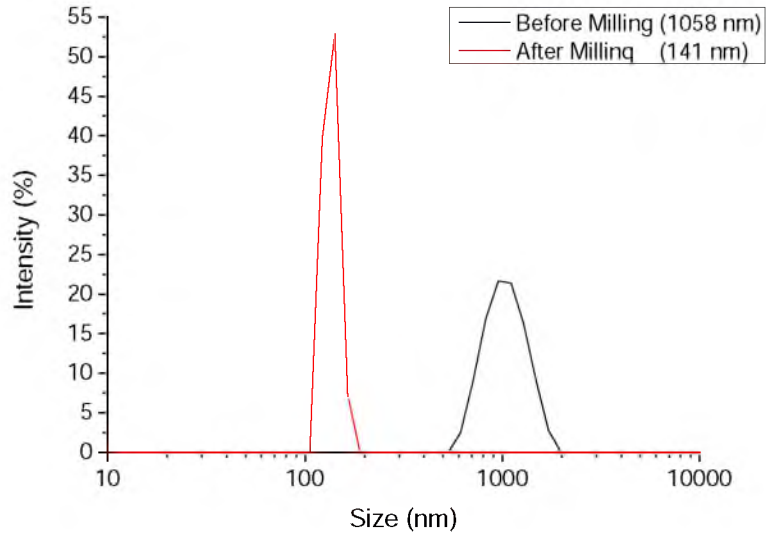


Figure 4.2 Particle size distribution of antimony (III) oxide mineral after and before milling process

## 4.2 Phase Analysis

XRD pattern of huntite/hydromagnesite mineral powder is presented in Figure 4.3. It is found from this result that the basic minerals are hydromagnesite ( $\text{Mg}_4(\text{OH})_2(\text{CO}_3)_3 \cdot 3\text{H}_2\text{O}$ ) and huntite ( $\text{Mg}_3\text{Ca}(\text{CO}_3)_4$ ) in the raw huntite/hydromagnesite mineral which is a flame retardant material. As demonstrated in the literature (Kirschbaum, 2001), an average mineralogical composition, based on XRD and chemical analysis data of current ores is as follows huntite (46%), hydromagnesite (46%), magnesite (4%), aragonite (3%), calcite (1%). The current study is similar to Kirschbaum's research. In this study, magnesite, aragonite and calcite phases are not found as impurities which influence flame retardant properties. Likely, XRD pattern of antimony (III) oxide mineral powder is shown in Figure 4.4. It is clear that antimony (III) oxide which was analyzed was determined to be 100%.

A sample was selected from each category in Table 3.2 and composite coatings/paints were analyzed by XRD. Phase analyses of these coatings/paints are illustrated in Figures 4.5 and 4.6. It should be noted that, as a result of this analysis, calcite, titanium oxide and aluminum hydroxide minerals are determined. This result clarifies the structure of the plastic dye phase as explained beforehand. Inasmuch as

the amount of reinforcing material in the matrix is very low in the samples, their XRD patterns were not detected clearly. As may be expected, the results of XPS analysis confirm the results strongly related phase.

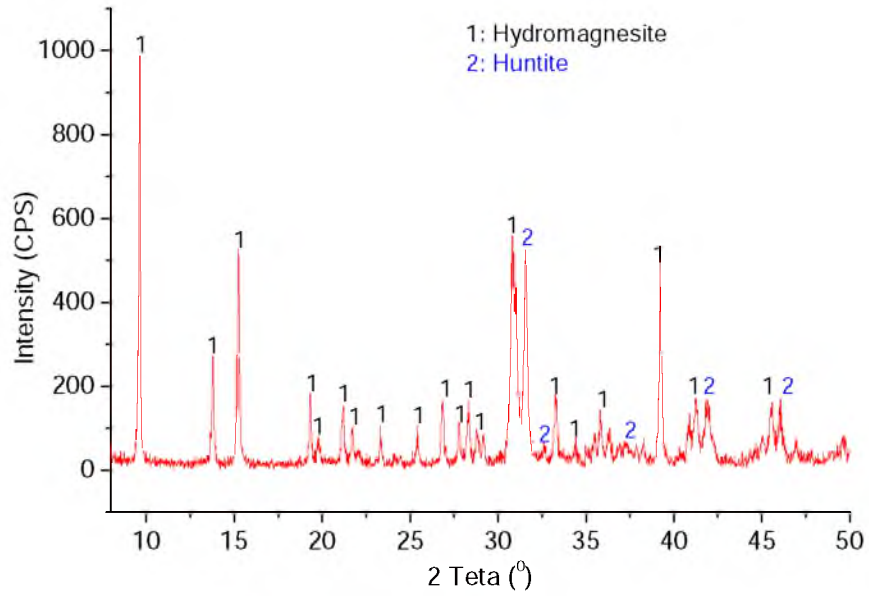


Figure 4.3 XRD pattern of huntite/hydromagnesite mineral

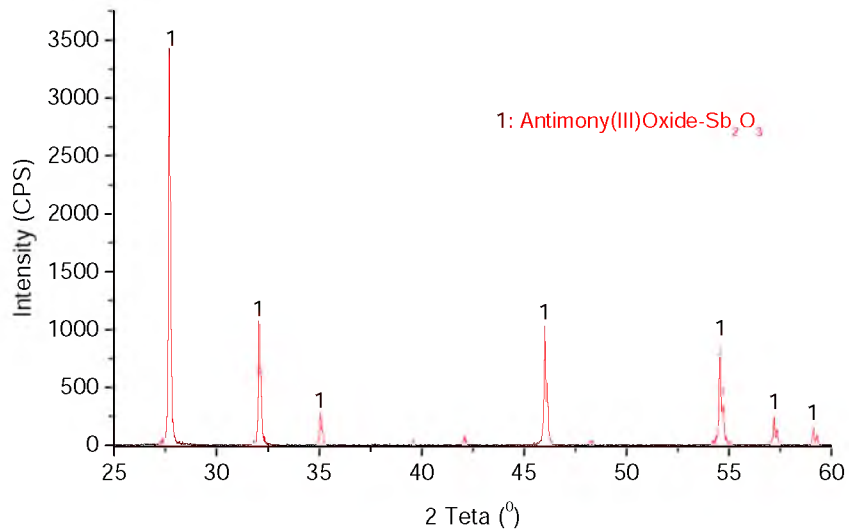


Figure 4.4 XRD pattern of antimony (III) oxide powder

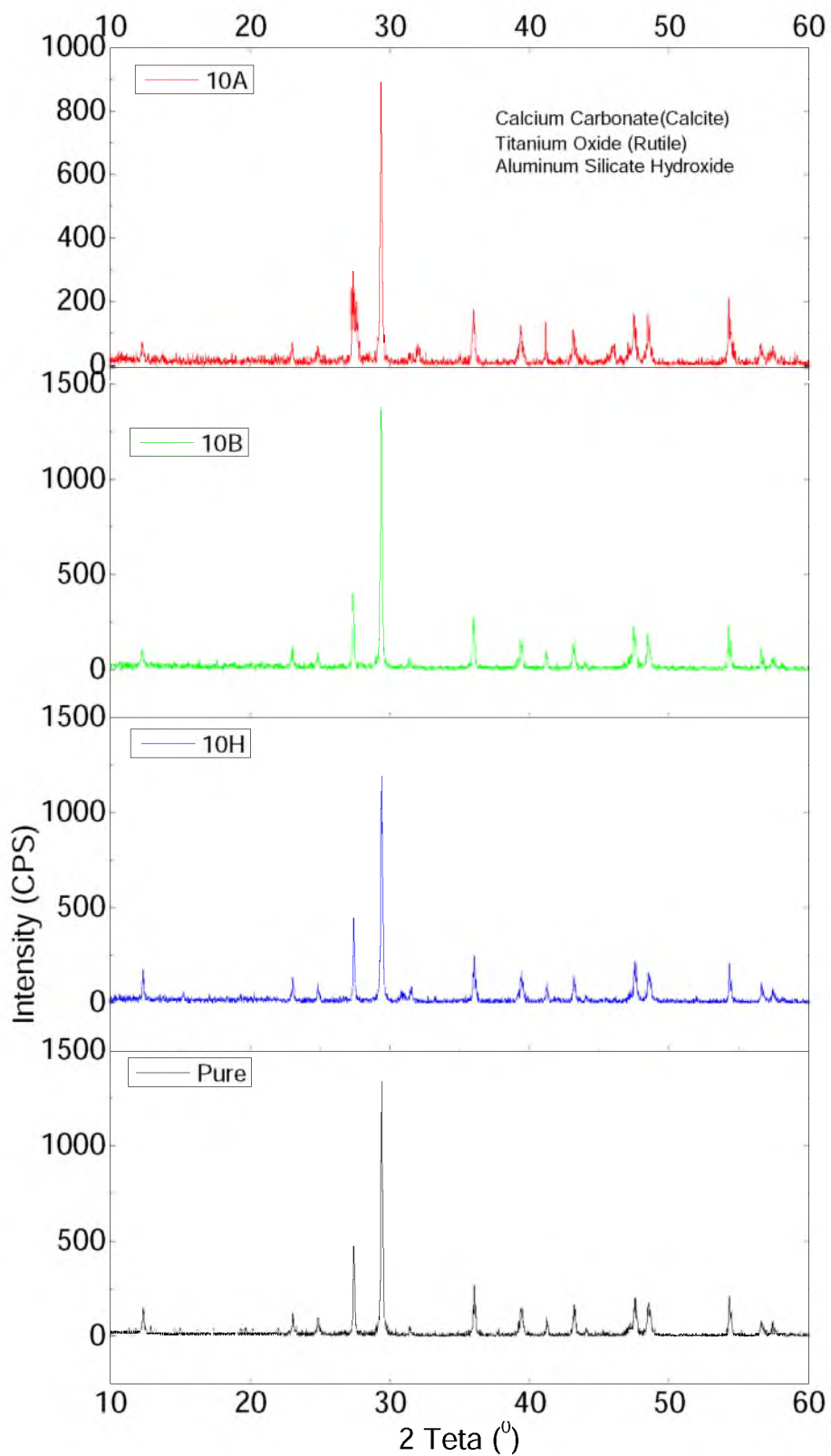


Figure 4.5 XRD patterns of pure, 10H, 10B and 10A samples

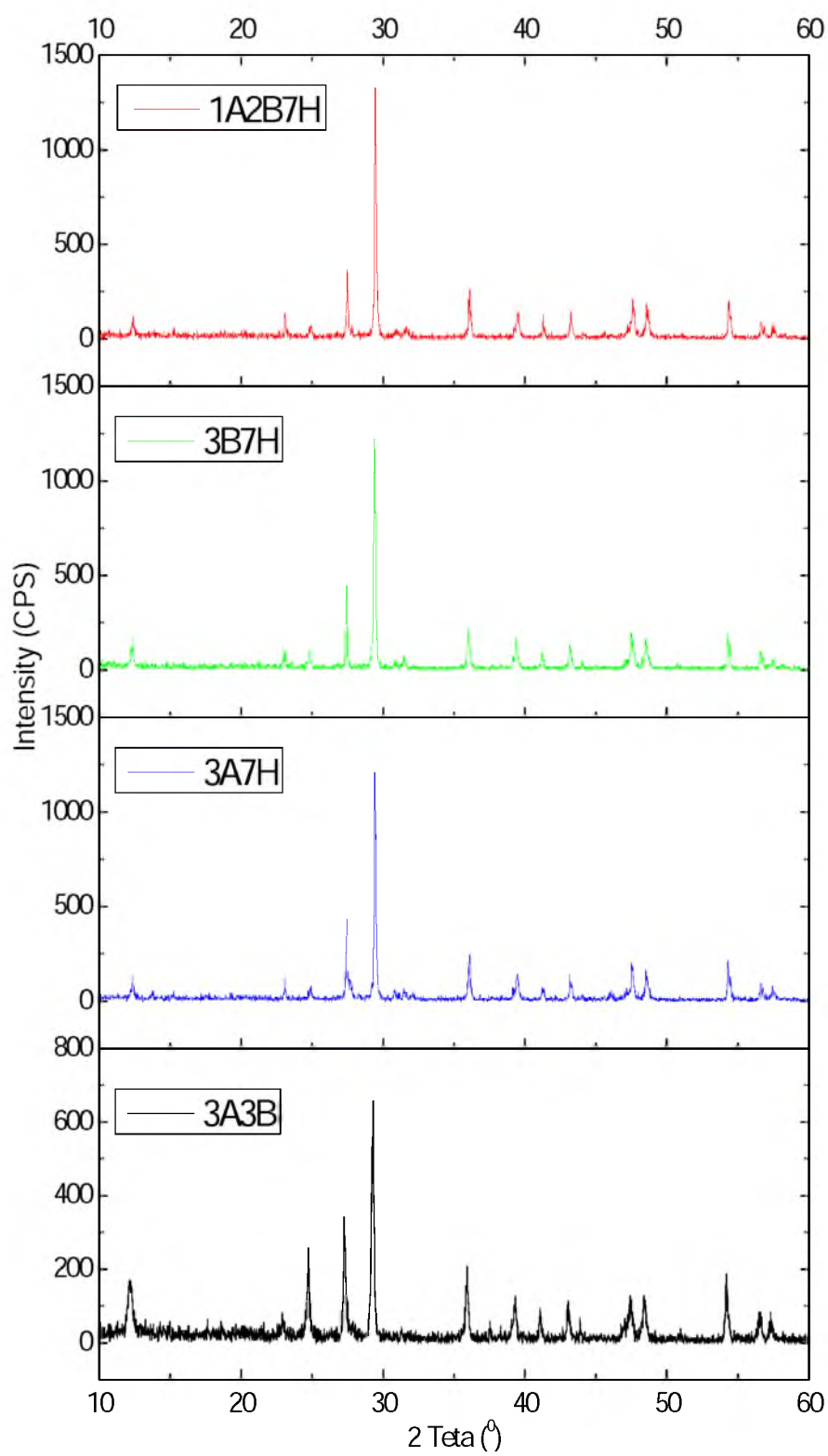


Figure 4.6 XRD patterns of 3A3B, 3A7H, 3B7H and 1A2B7H samples

### 4.3 Elemental Analysis

Elemental analyses of reinforcing materials and composite coatings/paints were determined with the help of XPS. The XPS analysis of huntite/hydromagnesite mineral is shown in Figure 4.7 a. Once the result was analyzed, it was determined to be Mg, C, O and Ca elements which belong to huntite/hydromagnesite mineral. XPS

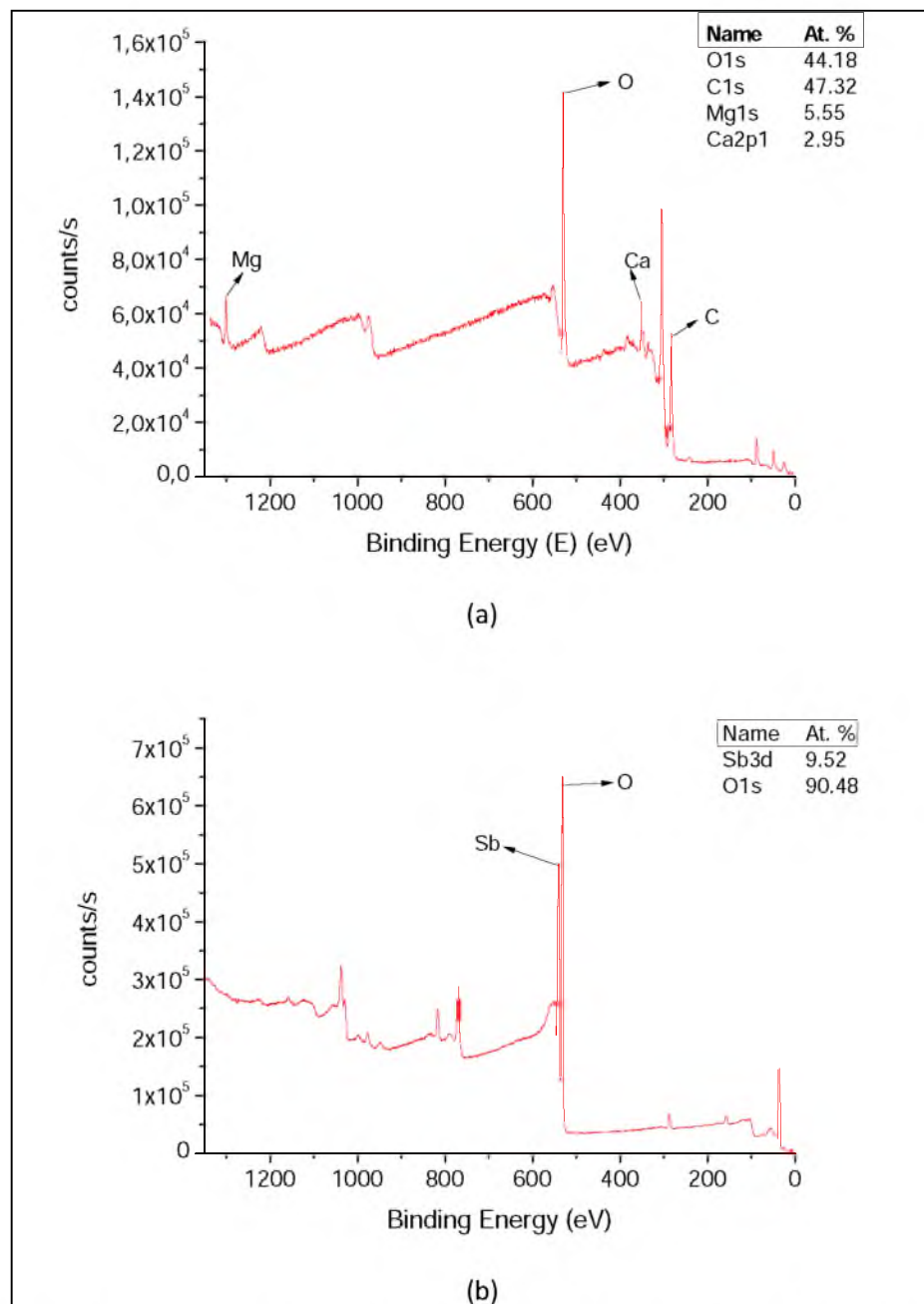


Figure 4.7 XPS results of (a) huntite/hydromagnesite mineral and (b) antimony (III) oxide powders

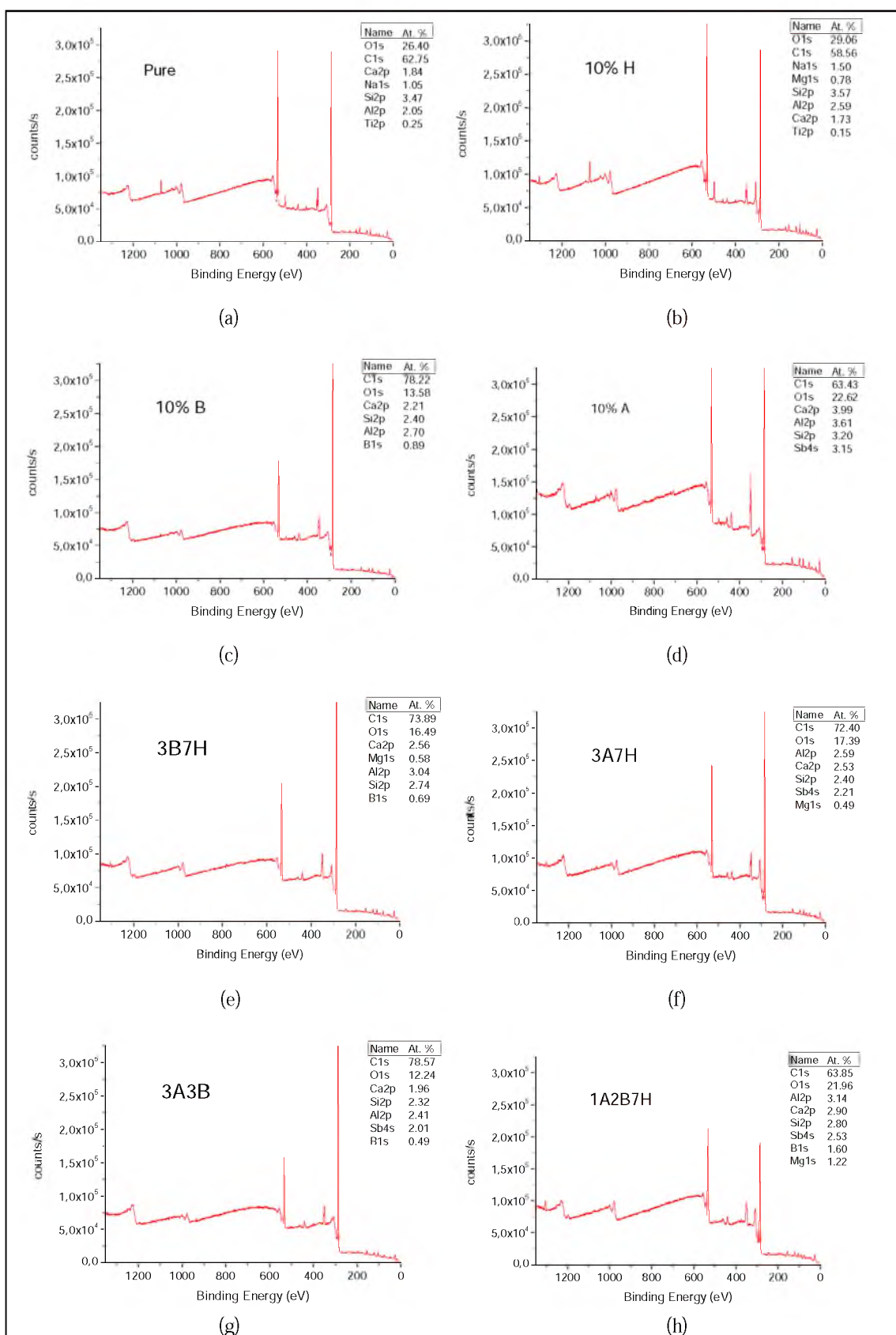


Figure 4.8 XPS results of (a) pure, (b) 10%H, (c) 10%B, (d) 10%A, (e) 3B7H, (f) 3A7H, (g) 3A3B and (h) 1A2B7H samples

analysis of antimony (III) oxide is denoted in Figure 4.7 b. It should be noted that, analysis result detected, the presence of Sb and O elements were detected to belong to antimony (III) oxide. Elemental analysis results of composite coatings/paints are depicted in Figure 4.8. Elemental analysis results of composites which were selected from each category in Table 3.2 were detected. Elements of both dye material and reinforcing materials were detected in all results.

#### 4.4 FT-IR Analysis

FT-IR spectra of pure dye and huntite/hydromagnesite, antimony (III) oxide, boric acid single, binary and ternary reinforced composite coatings/paints are given in Figure 4.9. In these experiments, the analysis was carried out in the band range of 600 and 4000  $\text{cm}^{-1}$ . Generally speaking from the composite samples, it is important to realize that the high intensity bands at 1400  $\text{cm}^{-1}$  and 870  $\text{cm}^{-1}$  may be related with  $\text{CO}_3^{-2}$  groups in the dye. Bands at 1000-1200  $\text{cm}^{-1}$  may be related with C-O bonds which come from binder or pigments in dye. It is also important to express that bands at 1700-1800  $\text{cm}^{-1}$  are related with C=O bonds which may come from binder in dye. Bands at 2300-2400  $\text{cm}^{-1}$  may be related to  $\text{CO}_2$  in air. FT-IR analyses of coatings/paints are only to show the peaks of dye material.

The most striking feature of these characteristics is that there does not exist interaction between reinforcing minerals such as huntite/hydromagnesite, antimony (III) oxide, boron based materials and pure dye in the composite samples. As stated previously, these reinforced materials do not influence pure dye in the composite samples. As a consequence, single, binary and ternary reinforced composite materials are not reacted from pure dye. Because of this reason, the position and intensity of the band peaks do not alter considerably as shown in Figure 4.9.



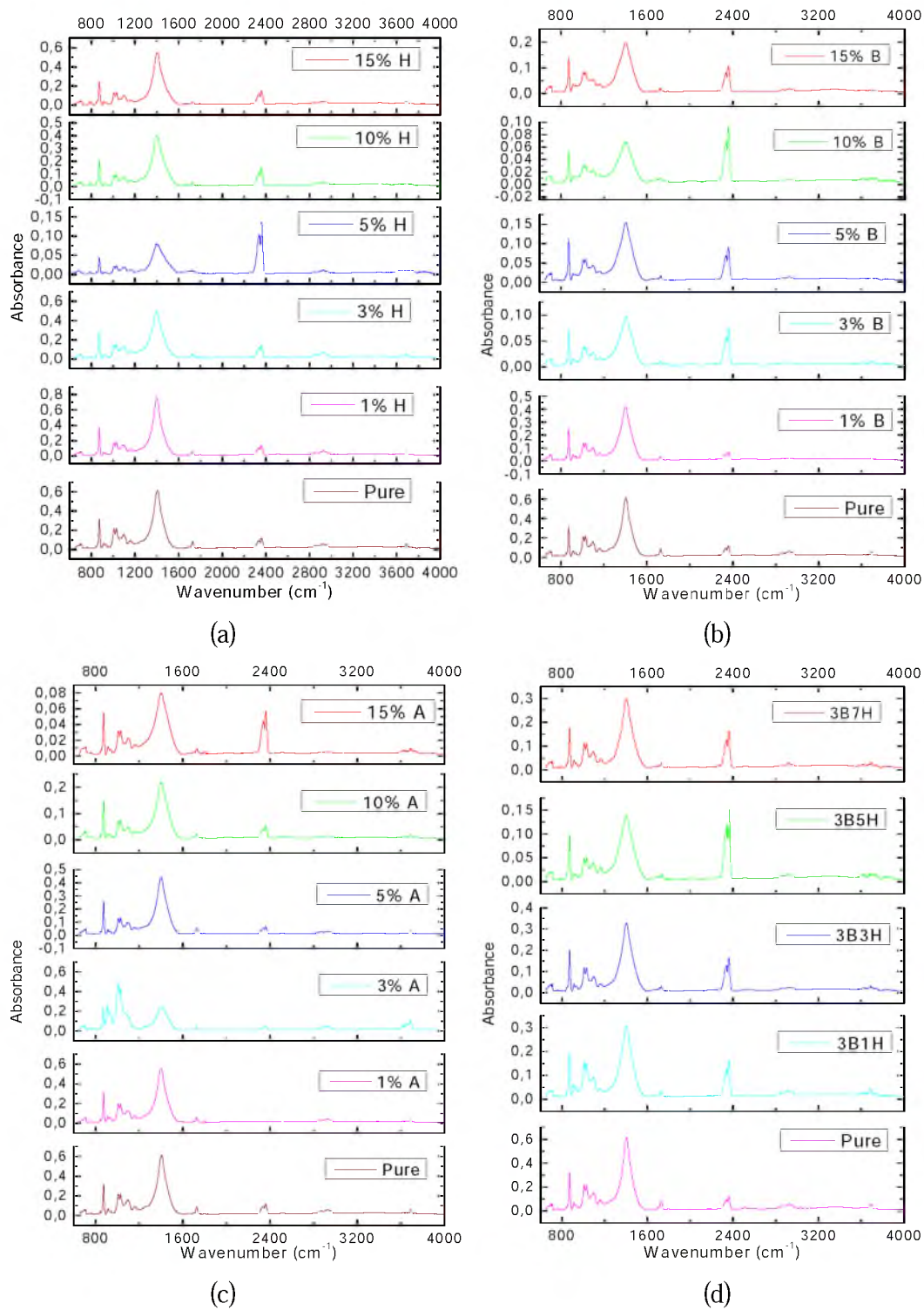
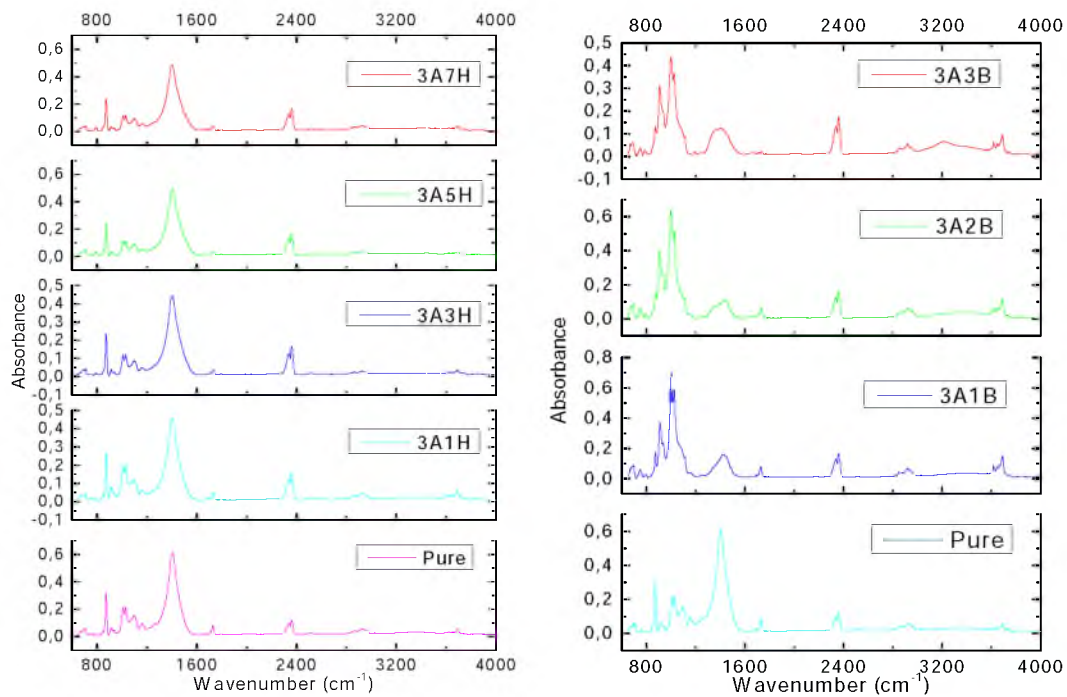


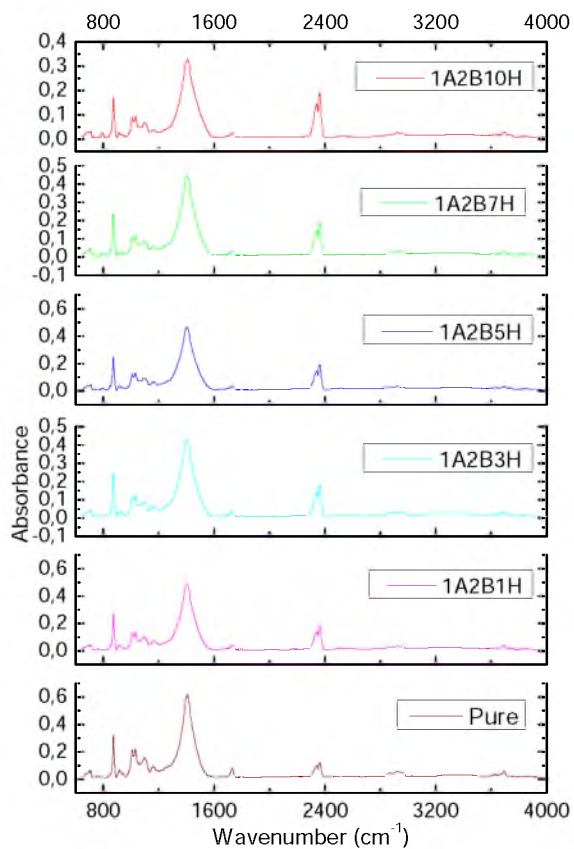
Figure 4.9 FT-IR analysis of (a) 10%H, (b) 10%B, (c) 10%A and (d) 3B7H composite samples





(e)

(f)



(g)

Figure 4.9 continued, FT-IR analysis of (e) 3A7H, (f) 3A3B and (g) 1A2B7H composite samples

## 4.5 SEM Analysis

In order to examine the surface properties of composite coatings/paints and control whether reinforcing materials homogeneously disperse in dye, SEM micrographs at different magnifications were taken and shown in Figure 4.10. When the results were analyzed, composite coatings/paints on plastic substrates are more rough and tough than pure dye and the presences of micro-cracks were also observed. We also observed the presence of reinforced materials in composites. The results of this investigation show that even though pure substrate and pure paint possess very smooth surfaces, huntite/hydromagnesite, antimony (III) oxide, boric acid single, binary and ternary reinforced composite coatings/paints reinforced composite coatings possess rough surfaces on account of mineral particles. It can be expressed that smaller the size of the mineral denser and smoother the composite material. We have a good agreement with literature (Yılmaz, 2013) and summarized here in details. Note that boric acid based reinforced composite coatings are smoother than that of huntite/hydromagnesite and antimony (III) oxide. This is due to the fact that boric acid can easily dissolve in solvents. Whereas antimony (III) oxide cannot be dissolved in any solvent owing to stable structure. As it was mentioned above, this will positively affect to increase the flame retardancy property of the material. Currently these attempts are being made to harmonise denser the composite coatings and to finalise a novel opportunity in the flame retardancy results.

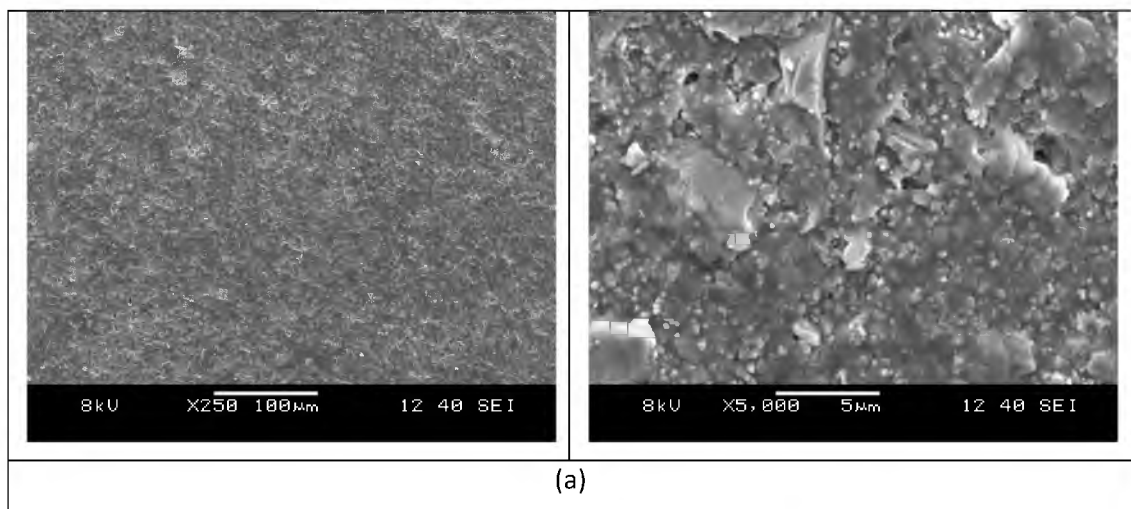


Figure 4.10 SEM micrographs of (a) pure dye at 100X and 5000X magnifications.

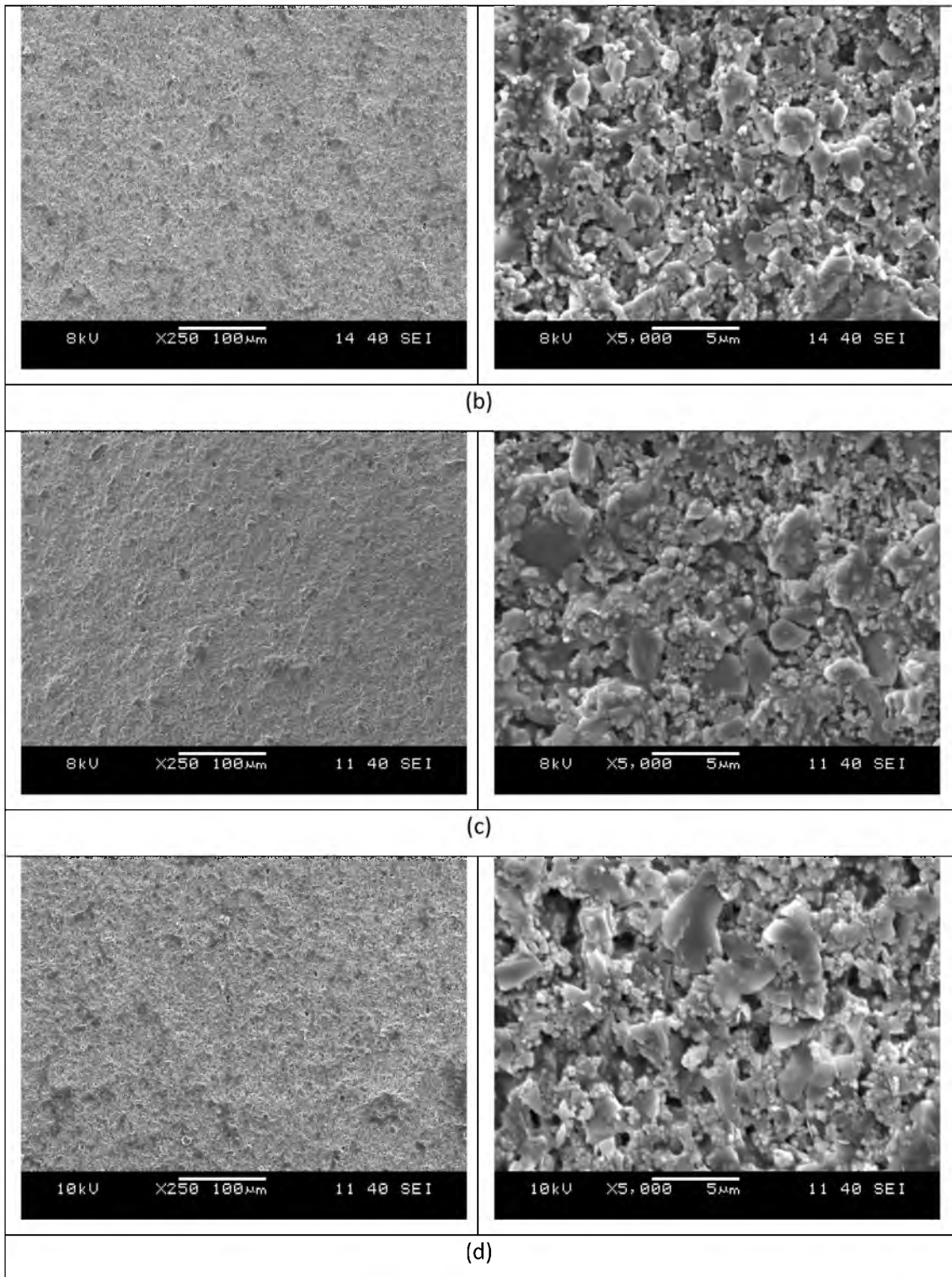


Figure 4.10 continued, SEM micrographs of (b) 10%H, (c) 10%B and (d) 10%A samples at 100X and 5000X magnifications.

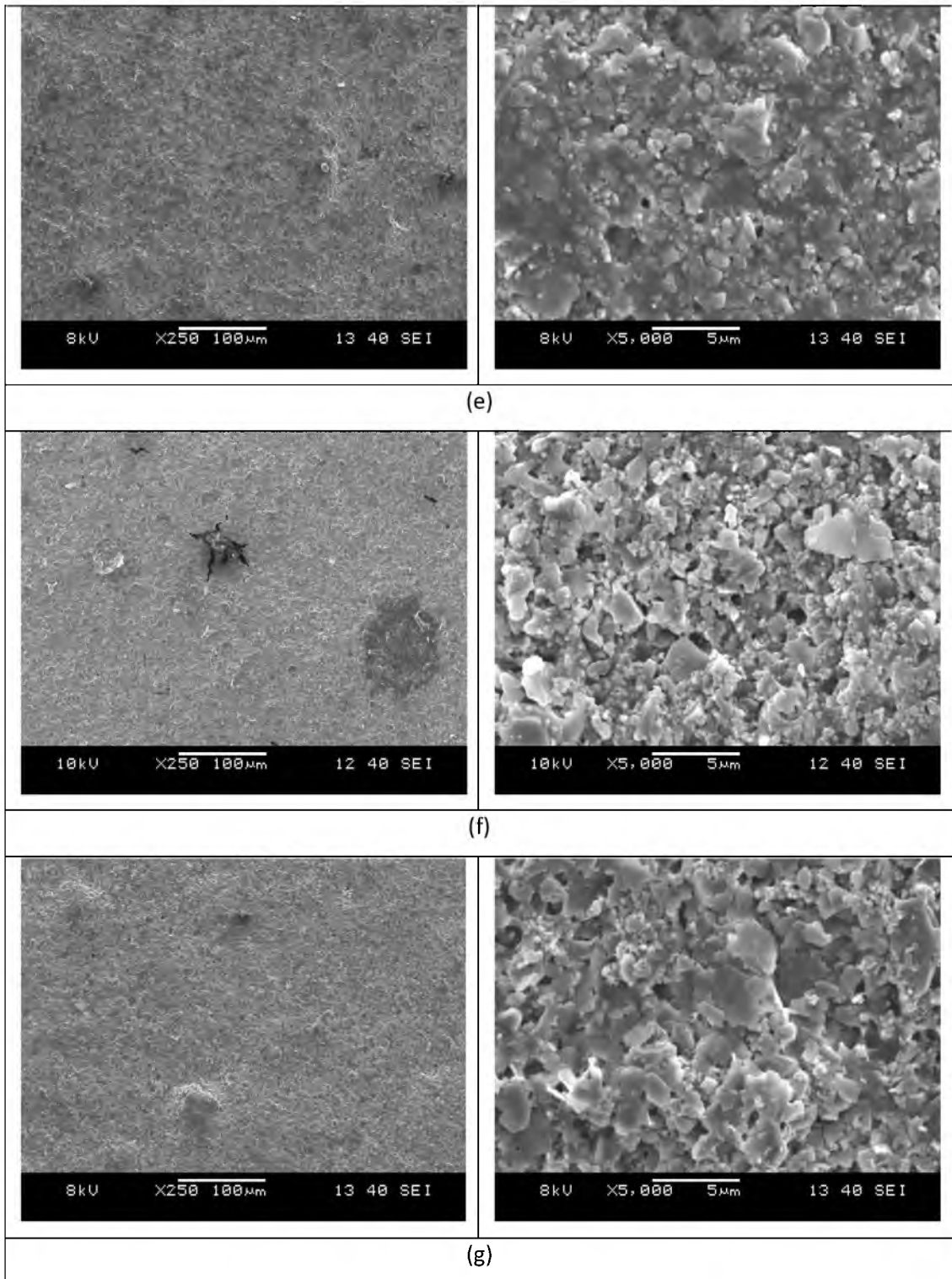


Figure 4.10 continued, SEM micrographs of (e) 3B7H, (f) 3A7H and (g) 3B3A samples at 100X and 5000X magnifications.

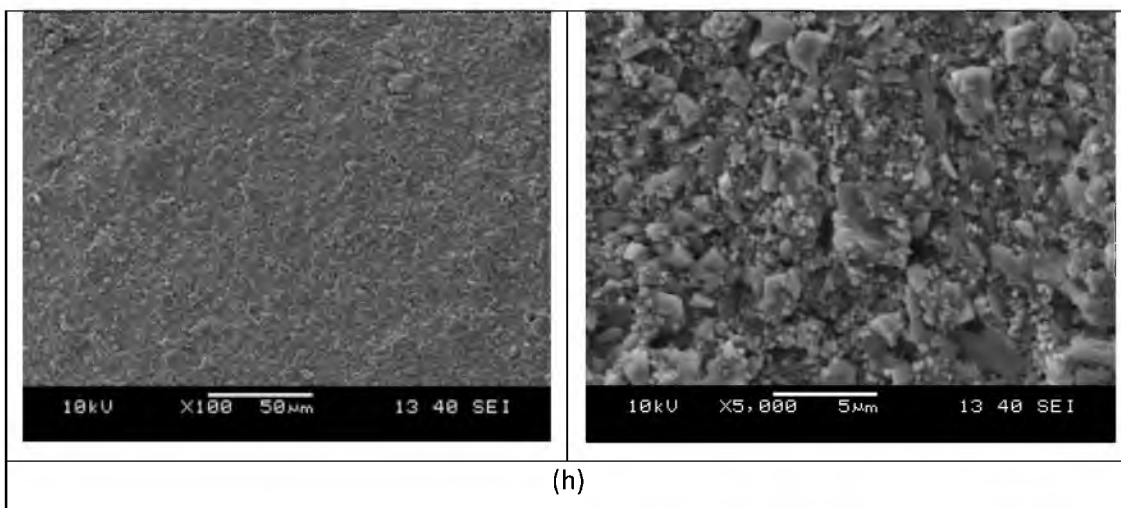


Figure 4.10 continued, SEM micrographs of (h) 1A2B7H at 100X and 5000X magnifications.

#### 4.6 DTA-TG Analysis

Now that exothermic and endothermic reactions are significant in regard to flame retardancy properties, DTA-TG analysis was carried out to investigate the thermal behaviours of pure dye and the huntite/hydromagnesite, antimony (III) oxide and boric acid reinforced composite materials. DTA-TG analyses are performed by heating up at the rate of 10 °C/min at temperatures between 25 °C and 600 °C under air.

DTA and TG curves of huntite/hydromagnesite, antimony (III) oxide and boric acid reinforced composite materials are depicted in Figure 4.11. It can be seen from Figure 4.11 that there are three thermal reactions including solvent removal, combustion of carbon based materials and thermal decomposition. The first thermal phenomenon starts at 90 °C and ends at 140 °C, corresponding to removal of water and OH groups. After removal of water and OH groups, the combustion of carbon based materials containing in pure paint takes place at temperatures between 150 °C and 400 °C. The third phenomenon is thermal decomposition of minerals in the pure paint and reinforced materials. This generally occurs at temperatures between 400 °C and 600 °C. It is difficult to separately state decomposition phenomena of the individual components of huntite/hydromagnesite, antimony (III) oxide and boric acid in optimum samples because it is a mixture of  $Mg_4(OH)_2(CO_3)_3 \cdot 3H_2O$ ,



Mg<sub>3</sub>Ca(CO<sub>3</sub>)<sub>4</sub>, Sb<sub>2</sub>O<sub>3</sub> and H<sub>3</sub>BO<sub>3</sub>. By TGA analysis of the samples, as demonstrated in Figure 4.11, the weight losses occur, it is indicated that the decomposition of mineral occurs at temperatures between 25 °C and 600 °C. Char yield of all samples was found to be approximately 77 %.

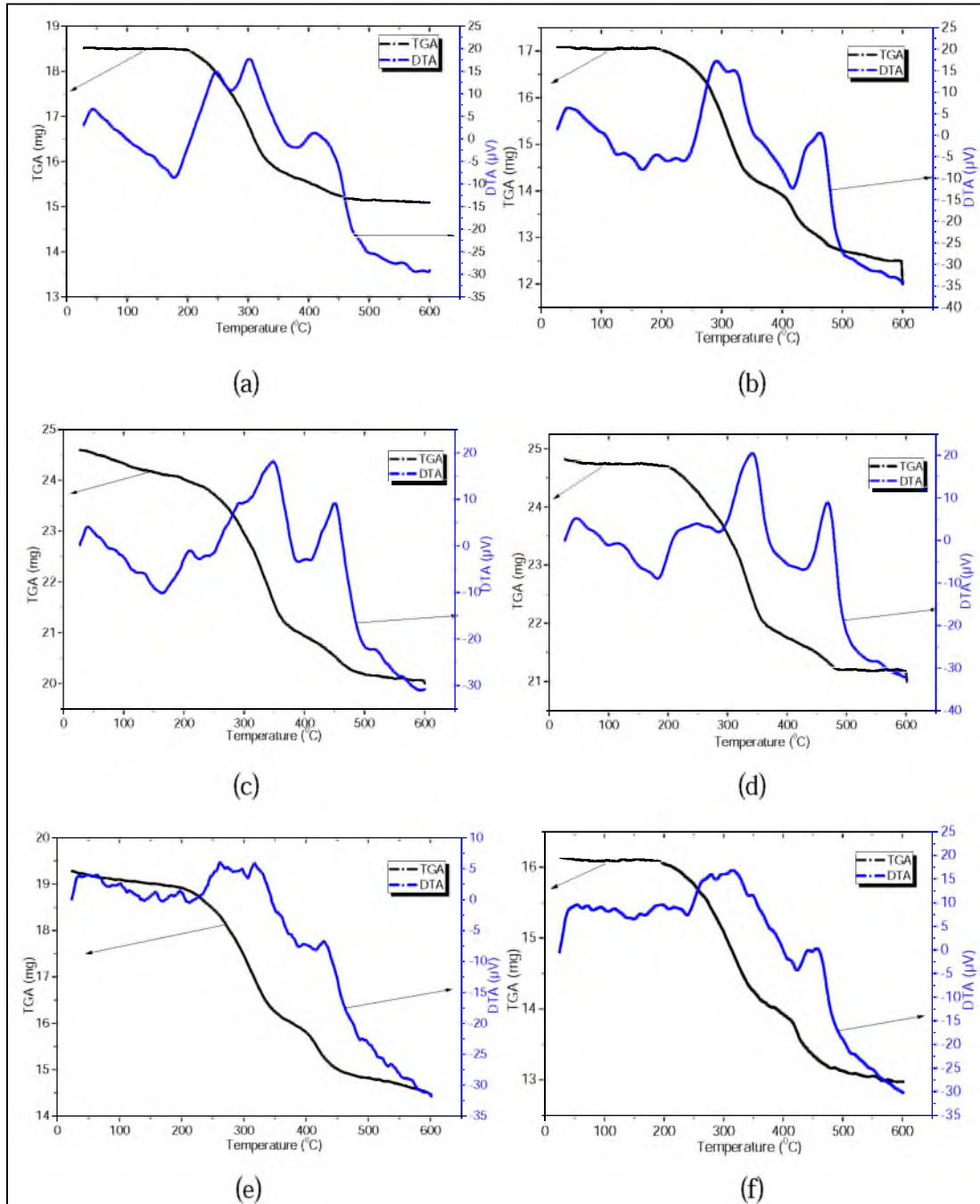


Figure 4.11 Thermal behaviours of (a) pure, (b) 10%H, (c) 10%B, (d) 10%A, (e) 3B7H and (f) 3A7H samples

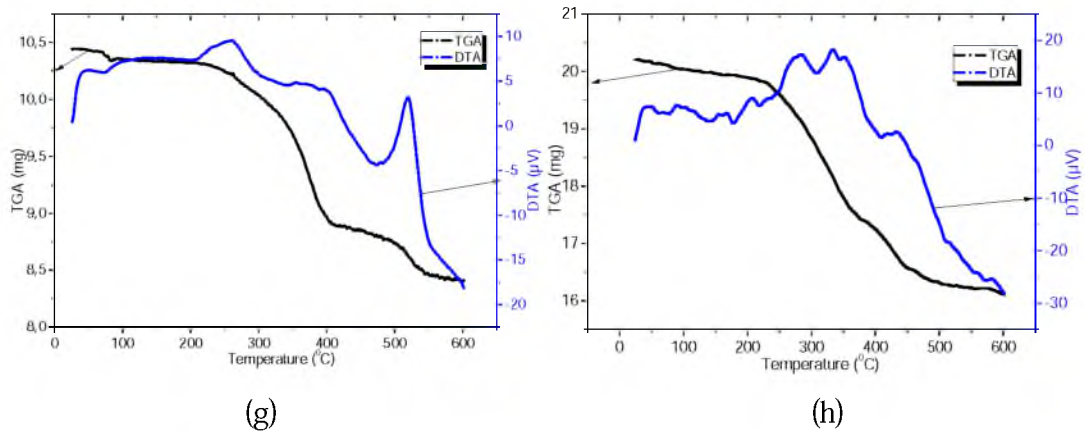


Figure 4.11 continued, Thermal behaviours of (g) 3A3B and (h) 1A2B7H samples

More specifically, Figure 4.11.a shows thermal behaviour of pure paint material. In this case, there are three thermal reactions for DTA. The first thermal phenomenon which is removal of water and OH groups occurs at nearly 90-130 °C. At temperatures between 174 °C and 373 °C, combustion of carbon based materials in pure paint occurs and heat absorption is 14.71 J. This is very high value in terms of flame retardancy because the combustion peak is very large. After this phenomenon, thermal decomposition takes place at temperature between 373 °C and 476 °C, and heat absorption is 4.20 J. It is believed that  $\text{Al}(\text{OH})_3$  and  $\text{CaCO}_3$  decompose into  $\text{Al}_2\text{O}_3 + \text{H}_2\text{O}$  and  $\text{CaO} + \text{CO}_2$  in the pure paint respectively. For TGA analysis of the sample, it is indicated that the decomposition of mineral occurs at temperatures between 25 °C and 600 °C. Char yield was found to be 81.52 %.

For huntite/hydromagnesite mineral reinforced paint, it can be seen from Figure 4.11.b that there are three thermal reactions for DTA. The first thermal phenomenon starts at 90 °C and ends at 130 °C, again corresponding to removal of water and OH groups. At temperatures between 239 °C and 357 °C, the combustion of carbon based materials occurs, heat absorption is 8.21 J. Upon compared with pure dye, this value decreases from 14.71 J to 8.21 J indicating that huntite/hydromagnesite mineral improves flame retardancy behaviour in pure paint. At temperatures between 415 °C and 503 °C, decomposition of minerals occurs, heat absorption is 5.46 J. As well as decomposition of  $\text{Al}(\text{OH})_3$  and  $\text{CaCO}_3$  in pure paint,  $\text{Mg}_4(\text{OH})_2(\text{CO}_3)_3 \cdot 3\text{H}_2\text{O}$ ,  $\text{Mg}_3\text{Ca}(\text{CO}_3)_4$  reinforced materials decompose in the composite sample at the

mentioned temperature range.  $\text{H}_2\text{O}$  and OH groups in  $\text{Mg}_4(\text{OH})_2(\text{CO}_3)_3 \cdot 3\text{H}_2\text{O}$  are strongly important to obtain flame retardant properties in the composite coatings/paints on plastic substrates. For TGA analysis of the samples, as denoted in Figure 4.11.b, it is indicated that the combustion and decomposition of pure paint and mineral occur at temperatures between 25 °C and 600 °C. Note that char yield was found to be 73.07 %.

For boric acid reinforced composites, it is clear from Figure 4.11.c that there are three thermal reactions for DTA as the same as previous samples. The first thermal phenomenon starts at 77 °C and ends at 140 °C and second phenomenon starts at 250 °C and ends at 390 °C, heat absorption is 3.95 J corresponding to combustion of carbon based materials in the composite samples. A clear improvement can be seen in flame retardant properties. For TGA analysis of the samples, as given in Figure 4.11.c, it is explained that the combustion and decomposition of composite material occur at temperatures between 25 °C and 600 °C. It can be noticed that char yield was found to be 81.52 %.

As for antimony (III) oxide reinforced paint, it can be seen from Figure 4.11.d that there are three thermal reactions for DTA. The first thermal phenomenon starts at 90 °C and ends at 140 °C, again corresponding to removal of water and OH groups. At temperatures between 286 °C and 383 °C, combustion of antimony (III) oxide reinforced paint occurs, heat absorption is 5.85 J. Upon compared with pure paint and huntite/hydromagnesite reinforced paint, heat absorption values decrease to 5.85 J suggesting that antimony (III) oxide increases flame retardancy behaviour. For TGA analysis of the samples, (see Figure 4.11.d), it is said that the decomposition of mineral occurs at temperatures between 25 °C and 600 °C. Char yield was found to be 85.35 %.

As in the case of huntite/hydromagnesite-boric acid, huntite/hydromagnesite-antimony (III) oxide and antimony (III) oxide-boric acid binary reinforced composites, they are obviously clear from Figures 4.11.e, 4.11.f and 4.11.g that there are three thermal reactions for DTA. The first thermal phenomenon starts at 75 °C



and ends at 140 °C, corresponding to removal of water and OH groups. At temperatures between 239 °C and 349 °C, combustion of carbon based materials occurs, heat absorption is 2.5 J. It is worth noting that a synergistical development in binary system can be seen in flame retardant properties. As for TGA analysis of the samples, it is indicated that the combustion and decomposition of paint and reinforced minerals occur at temperatures between 25 °C and 600 °C. It can be concluded that char yield was found to be 81 %.

A comparative representation of the performance of huntite/hydromagnesite-antimony (III) oxide-boric acid ternary reinforced composites was given in Figure 4.11.h showing DTA and TGA curves. It was also found here that there are three thermal reactions, the first thermal phenomenon starts at 77 °C and ends at 140 °C. Second phenomenon which contains a small combustion peak starts at 251°C and ends at 304 °C, heat absorption is 1.04 J. It is important to point out that a synergistical effect in ternary system can be seen in flame retardant properties. This synergistical effect cause thermal stable in the composite structure. As in case of the synergistical improvement of huntite/hydromagnesite- antimony (III) oxide-boric acid ternary reinforced composites, a great result was achieved as shown in Figure 4.11.h. The third thermal effect starts at 412 °C and ends at 510 °C. In this case, heat release is 2.48 J. For TGA analysis of the samples, as depicted in Figure 4.11.h at temperatures between 25 °C and 600 °C, char yield was found to be 80 %.

#### **4.7 Surface Roughness**

Surface roughness is critical to the efficient design of the composite paints. The smooth surfaces are desirable in all paints. In this study, surface roughness analyses of samples were investigated with a surface profilometer. The optimum samples selected from Table 3.2 were preferred for surface roughness analyses. When surface roughness results in Table 4.1 were examined, average values are in the range of 1 and 2 µm. The roughness values of some samples are lower than pure coating (see Table 4.1). Note that boric acid based reinforced composite coatings gave much

better results. This is because boric acid was added into the dye as aqueous solution and this provided us to achieve a smoother surface.

Table 4.1 Surface roughness values of pure and reinforced composite coatings/paints

Sample code	R <sub>a</sub> (µm)
Pure	1,65
10H	1,72
10B	1,17
10A	1,80
3B7H	1,92
3A7H	1,77
3A3B	1,35
1A2B7H	1,70

#### 4.8 Mechanical Properties

The applied load (P), penetration depth ( $h_t$ ), hardness (H) and modulus of elasticity (E) values belong to mechanical tests of pure and composite coatings/paints on plastic substrates were illustrated in Table 4.2. Nanoindentation tests were performed with five different loads. Samples were measured with different penetration depths ranging from 1-5 µm. An increase in penetration depth was generally observed with increasing of load.

Upon evaluating nanoindentation results, huntite/hydromagnesite-boric acid binary reinforced composite coatings (3B7H coded samples) possess the highest hardness and modulus of elasticity as mechanical properties. These results were illustrated in Figures 4.12 and 4.13. Inasmuch as boric acid is added as an aqueous solution in the matrix and consequently it is homogenously distributed in the composite paints. Because of this reason, boric acid reinforcement improved mechanical properties. Hardness and modulus of elasticity values of boric acid reinforced composite coating (10B coded sample) were also observed to have high values. This results is a proof of increased mechanical strength with the addition of boric acid solution. Hardness and modulus of elasticity values of

huntite/hydromagnesite-boric acid binary and huntite/hydromagnesite-antimony (III) oxide-boric acid (3A7H and 1A2B7H coded samples) reinforced composite coatings are close to the obtained results of pure coating. Nevertheless, pure coating is higher than these at some loads. Unlike these, hardness and modulus of elasticity results of antimony (III) oxide, huntite/hydromagnesite and antimony (III) oxide-boric acid (10A, 10H and 3A3B coded samples) coatings are found to be medium values as shown in Table 4.2, Figures 4.12 and 4.13 (H=0.05-0.10 GPa).

Tablo 4.2 Mechanical properties of pure and reinforced composite coatings/paints

Sample	P (mN)	h <sub>t</sub> (μm)	E (GPa)	H (GPa)	Sample	P (mN)	h <sub>t</sub> (μm)	E (GPa)	H (GPa)
<b>Pure</b>	4	2,05	1,95	0,05	<b>3B7H</b>	4	0,95	6,17	0,22
	8	2,28	1,30	0,05		8	1,19	11,14	0,27
	12	2,64	2,68	0,08		12	2,29	6,46	0,10
	16	4,72	1,01	0,04		16	2,2	7,90	0,15
	20	5,29	0,78	0,04		20	1,87	8,60	0,29
<b>10H</b>	4	1,48	3,11	0,08	<b>3A7H</b>	4	0,95	1,58	0,03
	8	2,42	2,40	0,06		8	1,19	1,32	0,02
	12	2,60	3,27	0,08		12	2,29	2,34	0,04
	16	3,20	2,79	0,07		16	2,2	1,06	0,03
	20	3,40	3,07	0,08		20	1,87	2,63	0,05
<b>10B</b>	4	0,93	8,14	0,22	<b>3A3B</b>	4	1,43	2,89	0,09
	8	2,07	4,69	0,08		8	1,86	5,46	0,1
	12	2,22	6,67	0,11		12	2,31	4,64	0,11
	16	2,76	5,58	0,98		16	3,01	3,74	0,08
	20	2,23	8,25	0,18		20	2,49	6,16	0,15
<b>10A</b>	4	1,41	2,58	0,10	<b>1A2B7H</b>	4	1,98	1,76	0,04
	8	2,52	2,43	0,06		8	2,71	1,93	0,05
	12	2,78	2,67	0,08		12	4,66	0,78	0,03
	16	3,01	3,48	0,08		16	5,18	0,31	0,11
	20	3,68	2,80	0,07		20	4,92	1,57	0,04

Huntite/hydromagnesite-boric acid and boric acid reinforced composite coatings/paints (3B7H and 10B coded samples) were detected as the most durable materials as mechanical point of view. As might be expected, boric acid added coatings/paints protects from external effects such as impact, scratches, deformation

to the coating/paint surface and it shows a better performance than others. In contrast, antimony (III) oxide added composite coating/paint no effect on mechanical

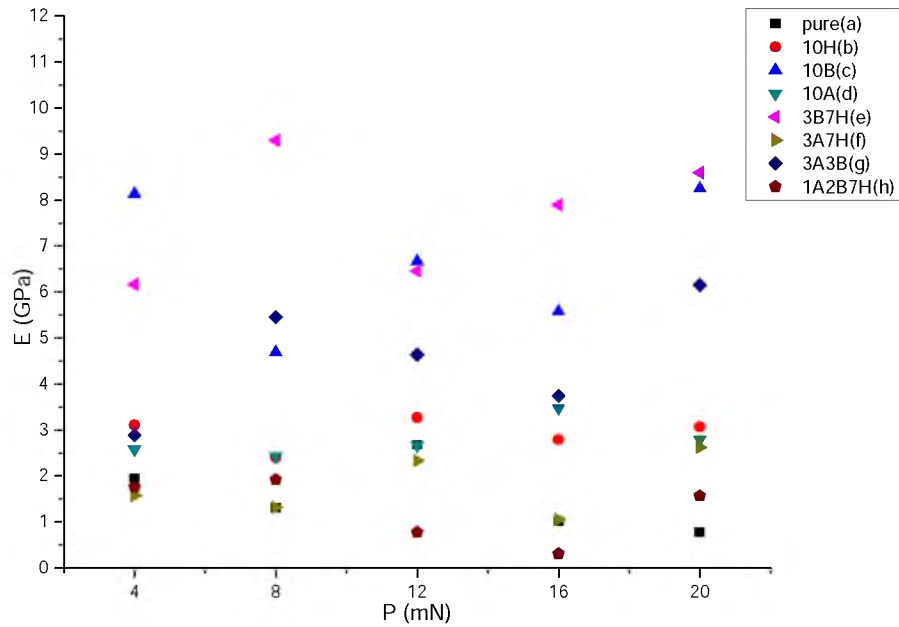


Figure 4.12 Elasticity modulus of (a) pure dye, (b) 10%H, (c) 10%B, (d) 10%A, (e) 3B7H, (f) 3A7H, (g) 3B3H and (h) 1A2B7H samples

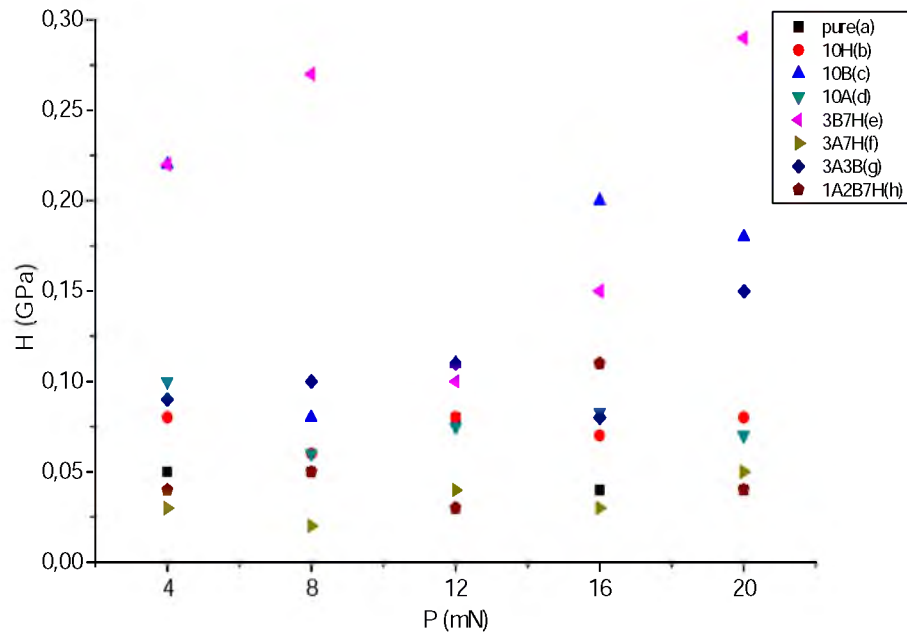


Figure 4.13 Hardness of (a) pure dye, (b) 10%H, (c) 10%B, (d) 10%A, (e) 3B7H, (f) 3A7H, (g) 3B3H and (h) 1A2B7H samples

strength was detected because of wettability problem between oxide particle and pure dye. It is believed that the composite coatings containing boric acid include good wettability in the structure. It should be kept in mind that the liquid state of boric acid covers other particles such as huntite/hydromagnesite and antimony (III) oxide very well in the composite coating/paint structure.

#### **4.9 Flame Retardant Properties**

To see how the flame retardancy is formed in the composite coatings/paints, let us focus on flame retardant tests which are very important. In this context, all samples in Table 3.2 after the preparation of test conditions corresponding to IEC 60695-11-5 needle flame testing standard were performed according to IEC 62441 candle flame testing standard (flame is applied for 180 seconds on sample). At the end of the test, if coatings/paints are not burnt or melt dripping during 180 seconds, it is in accordance with the standards. If coatings/paints are burnt or melt dripping during 180 seconds, it is not accordance with the standards. All results are illustrated with pictures in Table 4.3 after the flame retardancy tests. Pure coating/paint observed combustion after flame applied 110 sec. and after ignition was taken back and continued to combustion. After the flame was extinguished, a big hole was observed on the plastic material. After pure coating/paint also started to combustion, black smoke was observed and this event is to show the presence of CO gas. Therefore complete combustion event did not happen, and this is an undesirable situation for pure dye coatings/paints on plastic substrate.

While flame during 180 sec. was applied to 1, 3, 5, 10 and 15 % huntite/hydromagnesite reinforced composite coating/paint, it was not observed not only combustion but also melt dripping and occurred char layer on the surface. Note that formation of char layer is desirable during the combustion process. Char layers occurred in the combustion region both insulates heat and extinguishes flame by stopping oxygen between ignition and surface. In the all coatings/paints containing huntite/hydromagnesite mineral white smoke was observed in comparison to pure materials during the experiments and it shows CO<sub>2</sub> release and also complete

combustion occurs. This event is really important. Most of the deaths that occurred because of the fires are usually caused by the lack of complete combustion of CO poisoning caused by gas. Therefore, huntite/hydromagnesite mineral which was used in dye is both environmentally friendly and an extremely important mineral due to reduction in the amount of CO. It was not observed any deformation on the structure of this type of the composite coatings.

Table 4.3 Flame retardancy results of pure and the reinforced composite coatings/paints




Sample Code	Flame Application Time(s)	Melt Dripping	Char	Ignition Time(s)	Samples After Flame Application
Pure	110	Yes	No	110	
1H	180	No	Yes	Not Ignited	
3H	180	No	Yes	Not Ignited	

Table 4.3 continued, Flame retardancy results of pure and the reinforced composite coatings/paints






5H	180	No	Yes	Not Ignited	
10H	180	No	Yes	Not Ignited	
15H	180	No	Yes	Not Ignited	
1B	120	Yes	120		
3B	180	Yes	Yes	Not Ignited	

Table 4.3 continued, Flame retardancy results of pure and the reinforced composite coatings/paints






5B	180	Yes	Yes	Not Ignited	
10B	180	Yes	Yes	Not Ignited	
15B	180	Yes	Yes	Not Ignited	
1A	130	Yes	No	130	
3A	180	No	Yes	Not Ignited	



Table 4.3 continued, Flame retardancy results of pure and the reinforced composite coatings/paints






5A	180	Yes	Yes	Not Ignited	
10A	180	Yes	Yes	Not Ignited	
15A	180	Yes	Yes	Not Ignited	
3A1H	180	No	Yes	Not Ignited	
3A3H	180	No	Yes	Not Ignited	

Table 4.3 continued, Flame retardancy results of pure and the reinforced composite coatings/paints

3A5H	180	No	Yes	Not Ignited	
3A7H	180	No	Yes	Not Ignited	
3B1H	180	No	Yes	Not Ignited	
3B3H	180	No	Yes	Not Ignited	
3B5H	180	No	Yes	Not Ignited	

Table 4.3 continued, Flame retardancy results of pure and the reinforced composite coatings/paints










3B7H	180	No	Yes	Not Ignited	
3A1B	180	No	Yes	Not Ignited	
3A2B	180	No	Yes	Not Ignited	
3A3B	180	No	Yes	Not Ignited	
1A2B1H	180	No	Yes	Not Ignited	

Table 4.3 continued, Flame retardancy results of pure and the reinforced composite coatings/paints

1A2B3H	180	No	Yes	Not Ignited	
1A2B5H	180	No	Yes	Not Ignited	
1A2B7H	180	No	Yes	Not Ignited	
1A2B10H	180	No	Yes	Not Ignited	

After the applied flame tests to coatings/paints containing only antimony (III) oxide and only boric acid, it was examined that the coatings/paints which contain 1 % antimony (III) oxide and 1 % boric acid burned. In all other coatings/paints was not observed combustion phenomenon. All of these materials occurred melt dripping and plastic substrate materials deformed. This phenomenon is not a desired result in the plastic materials. Huntite/hydromagnesite-antimony (III) oxide, huntite/hydromagnesite-boric acid, antimony (III) oxide-boric acid binary and huntite/hydromagnesite-antimony (III) oxide-boric acid ternary reinforced composite

coatings/paints on the plastic substrates did not burn after the flame tests. In these tests, char layer occurred on the composite coatings/paints. As a result of this process melt dripping was not observed. Flame retardant test results of these materials were extremely excellent. Deformation was not observed on plastic materials. Upon evaluating the experiments, the best results were obtained in the huntite/hydromagnesite-boric acid reinforced composite coatings/paints on the plastic substrates.

## CHAPTER FIVE

### CONCLUSIONS AND FUTURE PLANS

#### 5.1 General Results

Fire retardant materials provide a comprehensive source of information on all aspects of fire retardancy, emphasizing the burning behaviour and flame retarding properties of polymeric materials. It covers combustion, flame retardants, smoke and toxic products in general, and material-specific aspects of combustion in relation to textiles, composites, and bulk polymers. Flame retardant materials increase the initial resistance to ignition and are able to effectively slow down burning rates which in turn are proportioned to the rate of smoke and toxic gas built up. Therefore potential escape time increases. Paints used in many areas of daily life are used with the aim of creating in surface protection and decorative designs of materials. These paints contain material susceptible to fire such as polymeric binders, organic solvents. Because of this reason, paints easily burn.

In this study, flame retardant properties of plastic paint material were investigated and developed. With this respect, the composite materials were obtained by adding different amounts of environmentally friendly (halogen-free) and nanosized flame retardant materials such as huntite/hydromagnesite, antimony (III) oxide and boric acid to paint material. The following successful results are obtained from the experimental works:

1. In order to obtain lower surface roughness and higher efficiency, reinforcing materials such as huntite/hydromagnesite and antimony (III) oxide minerals were milled at rate of 750 rpm at room temperature for 120 minutes in air. Before and after milling process, particle size distribution of huntite/hydromagnesite minerals was average 739 nm before milling, it was nearly 121 nm after milling. While antimony (III) oxide mineral was approximately 1058 nm before milling, it was found to be 141 nm after milling process. In these results, we provide a greater surface area and a lower surface roughness.

2. Composite coatings/paints were prepared by reinforcing flame retardant nanoparticles at different ratios into the water-based white dye as single, binary and ternary components. The materials were stirred for 30 minutes and at 1000 rpm with the magnetic stirrer to homogenize dye-mineral mixture. Prepared composite materials were applied on plastic substrate by a paint gun and were dried at 60 °C for 90 minutes in oven.
3. XRD pattern of huntite/hydromagnesite mineral powder analyzed as huntite ( $\text{Mg}_3\text{Ca}(\text{CO}_3)_4$ ) and hydromagnesite ( $\text{Mg}_4(\text{OH})_2(\text{CO}_3)_3 \cdot 3\text{H}_2\text{O}$ ). XRD pattern of antimony (III) oxide mineral powder which was analyzed was determined to be 100%. Phase analyses of analyzed composite coatings/paints showed calcite, titanium oxide and aluminum hydroxide minerals. The amount of reinforcing material in the matrix is very low, and thus their XRD patterns were not detected.
4. XPS analysis of huntite/hydromagnesite mineral showed to be Mg, C, O and Ca elements which belong to huntite/hydromagnesite mineral. XPS analysis of antimony (III) oxide illustrated to presence of Sb and O elements which belong to antimony (III) oxide.
5. It was found that the high intensity bands at  $1400\text{ cm}^{-1}$  and  $870\text{ cm}^{-1}$  may be related with  $\text{CO}_3^{2-}$  groups in the dye. Bands at  $1000\text{-}1200\text{ cm}^{-1}$  may be related with C-O bonds which come from binder or pigments in dye. It is also important to express that bands at  $1700\text{-}1800\text{ cm}^{-1}$  are related with C=O bonds which may come from binder in dye. Bands at  $2300\text{-}2400\text{ cm}^{-1}$  may be related to  $\text{CO}_2$  in air. FT-IR analyses of coatings/paints are only to show the peaks of dye material. Single, binary and ternary reinforced composite materials are not reacted from pure dye.
6. It is clear that the composite coatings/paints on plastic substrates are more rough and tough than pure dye. Even though pure substrate and pure paint possess very smooth surfaces, huntite/hydromagnesite, antimony (III) oxide, boric acid single, binary and ternary reinforced composite coatings/paints reinforced composite

coatings possess rough surfaces on account of mineral particles. It can be expressed that smaller the size of the mineral denser and smother the composite material.

7. As for DTA-TG analysis, there are three thermal reactions including solvent removal, combustion of carbon based materials and thermal decomposition of minerals. The first thermal phenomenon starts at 90 °C and ends at 140 °C, corresponding to removal of water and OH groups. After removal of water and OH groups, the combustion of carbon based materials containing in pure paint takes place at temperatures between 150 °C and 400 °C. The third phenomenon is thermal decomposition of minerals in the pure paint and reinforced materials. This generally occurs at temperatures between 400 °C and 600 °C. By TGA analysis of the samples, in terms of weight losses, it is indicated that the decomposition of mineral occurs at temperatures between 25 °C and 600 °C. Total weight loss of all samples was found to be approximately 23 %. A synergistical effect in huntite/hydromagnesite-antimony (III) oxide-boric acid ternary reinforced composites was obtained in flame retardant properties. This synergistical effect cause thermal stability in the composite structure.
8. Surface roughness is critical to the efficient design of the composite paints. The smooth surfaces are desirable in all paints. Average values are in the range of 1 and 2 μm. The roughness values of some samples are lower than pure coating. Boric acid based reinforced composite coatings gave much better results. This is because boric acid was added into the dye as aqueous solution and this provided us to achieve a smoother surface.
9. Huntite/hydromagnesite-boric acid and boric acid reinforced composite coatings/paints (3B7H and 10B coded samples) were detected as the most durable materials. Boric acid added coatings/paints protects from external effects such as impact, scratches, deformation to the coating/paint surface and it shows a better performance than others. In contrast, antimony (III) oxide added composite coating/paint no effect on mechanical strength was detected because of wettability



problem between oxide particle and pure dye. The composite coatings containing boric acid bring about good wettability in the structure.

10. As for flame retardancy properties, after pure coating/paint started to burn, black smoke was observed and this event is to show the presence of CO gas. Therefore complete combustion event did not happen, and this is an undesirable situation for pure dye coatings/paints on plastic substrate. While flame during 180 sec. was applied to 1, 3, 5, 10 and 15 % huntite/hydromagnesite reinforced composite coating/paint, it was not observed not only combustion but also char layer in the surface and melt dripping. In the all coatings/paints containing huntite/hydromagnesite mineral white smoke was observed in comparison to pure materials during the experiments and it shows output of CO<sub>2</sub> and also complete combustion occurs. After the applied flame tests to coatings/paints containing only antimony (III) oxide and only boric acid, it was examined that the coatings/paints which contain 1 % antimony (III) oxide and 1 % boric acid burned. In all other coatings/paints combustion phenomenon was not observed. All of these materials occurred melt dripping and plastic substrate materials deformed. This phenomenon is not a desired result in the plastic materials. Huntite/hydromagnesite-antimony (III) oxide, huntite/hydromagnesite-boric acid, antimony (III) oxide-boric acid binary and huntite/hydromagnesite-antimony (III) oxide-boric acid ternary reinforced composite coatings/paints on the plastic substrates did not burn after the flame tests. In these tests, char layer occurred on the composite coatings/paints. As a result of this process melt dripping was not observed. Flame retardant test results of these materials were extremely excellent. Deformation was not observed on plastic materials. Upon evaluating the experiments, the best results were obtained in the huntite/hydromagnesite-boric acid reinforced composite coatings/paints on the plastic substrates.

## 5.2 Future Plans

Investigation and development of flame retardancy properties of different type paints will be planned. In order to obtain lower surface roughness and better

efficiency in coatings/paints system, it is desirable to decrease size of the reinforced powders by extending time of the milling process and to plan usage of nanoscaled reinforced materials instead of pigment materials during production of paints. It is aimed that their flame retardancy behaviour will improve with reducing the amount of reinforced material content in the composite coatings/paints. To develop flame retardant properties of the composite materials, different reinforced materials such as zinc borate and bentonite will be used. Finally, production of flame retardant paints as industrial scale will be planned in the future.

## REFERENCES

- Ahmed, W. & Jackson, M. (2009). *Emerging nanotechnologies for manufacturing*. USA: Elsevier.
- Alexander, B. M. & Charles, A. W. (2007). *Flame retardant polymer nanocomposites*. New Jersey:Wiley.
- Berkovich, E.S., (1951). *Three-faceted diamond pyramid for micro-hardness testing*. Industrial Diamond Review.
- Bertelli, G., Costa, L., Fenza, S., Marchetti, E., Camino, G., Locatelli, R., (1988). Thermal behavior of brominmetal fire retardant systems. *Polymer Degradation and Stability*, 20(3-4), 295-314.
- Bie, F. (2002). The crucial question in fire protection. *Engineering Plastic*. 92(2), 27-29.
- Birlik, I. (2011). *Synthesis of superconducting films and improvement of their flux pinning properties with barium zirconate nanoparticles using chemical solution deposition method*. Ph.D. Thesis. Dokuz Eylul University, Izmir
- Boryniec, S., Przygocki, W. (2001) Polymer combustion processes, 3: Flame retardants for polymeric materials. *Progress in Rubber and Plastics Technology*, 17, 127-148.
- Bulewicz, E. M., Padley, P. J., (1971). Photometric observations on the behaviour of tin in premixed H<sub>2</sub> + O<sub>2</sub> + N<sub>2</sub> flames. *Transactions of the Faraday Society*, 67, 2337-2347.
- Callister, W. D. (2007). *Materials science and engineering* (7th ed.). United States of America: John Willey & Sons.

- Camino, G. (1987). Mechanism of fire retardancy in chloroparaffin-polymer mixtures. *In Developments in Polymer Degradation*, Grassie, N., Ed., London, U.K.: Elsevier Applied Sciences
- Castrovinci, A., Lavaselli, M., Camino, G., (2008). *Recycling and disposal of flame retarded materials*. In *Advances in Fire Retardant Materials*. Horrocks, A. R. Price, D., Eds., Boca Raton: CRC.
- Charles A. W. & Alexander B. M. (2010). *Fire retardancy of polymeric materials*. Parkway: CRC Press.
- Crist, B.V., (2011). *X-ray photoelectron spectroscopy*. Retrieved June 10, 2010, from [http://en.wikipedia.org/wiki/X-ray\\_photoelectron\\_spectroscopy](http://en.wikipedia.org/wiki/X-ray_photoelectron_spectroscopy)
- Costa, L., Camino, G., Luda, D., Cortemiglia, P., (1990). *Fire and Polymers*, 425, *ACS Symposium*, Washington DC.
- Costa, L., Goberti, P., Paganetto, G., Camino, G., Sgarzi, P. (1990). Thermal behaviour of chlorine-antimony fire-retardant systems. *Polymer Degradation and Stability*, 30(1), 13–28.
- Dieter S., (1998). *Paints, coatings and solvents*. Werner Freitag (ed.). 2. completely rev. ed. Weinheim. New York: Basel: Cambridge: Tokyo: Wiley-VCH.
- Dufton, P.W., (2003). *Flame retardants for plastics market report*. Birmingham: Rapra Technology Limited
- Efra, (2012). *Flame retardants integral to fire safety*. Retrieved August 15, 2012, from <http://www.cefic-efra.com/index.php>

- Fang Z., Song P., Tong L. & Guo Z. (2008). Thermal degradation and flame retardancy of polypropylene/C<sub>60</sub> nanocomposite. *Thermochimica Acta*, 473, 106-108.
- Fenimore, C.P., Martin, F.J., (1966). *Modern Plastics*. 44, 141.
- Fink, U., (2004). The market situation, in: J. Troitzsch, Ed., *Plastics flammability handbook*. Carl Hanser Verlag, Munich, Germany, 8–32.
- Fisher-Cripps, A. C. (2009). *Nanoindentation*, 3rd, Fischer-Cripps Laboratories Private company., Australia
- G. Pal & H. Macskasy. (1991). Their behavior in fires. *Plastics*. Elsevier, New York.
- Georlette, P., Simons, J., Costa, L. (2000). Halogen-containing fire-retardant compounds, in: (A.F. Grand and C.A. Wilkie, Eds.), *Fire Retardancy of Polymeric Materials*. New York: Marcel Dekker.
- Hastie, J. W., (1973). Mass spectrometric studies of flame inhibition: Analysis of antimony trihalides in flames, *Combustion and Flame*, 21, 49–54.
- Henrist, C., Mathieua, J. P., Vogelsb, C., Rulmonta A., Clootsa R. (2003). Morphological study of magnesium hydroxide nanoparticles precipitated in dilute aqueous solution. *Journal of Crystal Growth*, 249, 321–330.
- Hirschler, M. M. (2000). *Chemical aspects of thermal decomposition*, in: (A.F. Grand and C.A. Wilkie, Eds.), *Fire Retardancy of Polymeric Materials*. New York: Marcel Dekker.
- Horrocks, A. R. & Price, D. (Eds). (2001). *Fire retardant materials*. Cambridge: CRC Press.

- Huggett, C., (1980). Estimation of rate of heat release by means of oxygen consumption measurements. *Fire Materials*, 4 (2), pp. 61–65.
- Hull T.R., (2008). Challenges in fire testing: Reaction to fire tests and assessment of fire toxicity. *In Advances in Fire Retardant Materials*, D. Price and A.R. Horrocks (eds.), Cambridge: Woodhead Publishing Ltd.
- Iji, M., Serizawa, S., (1998). Silicone derivatives as new flame retardants for aromatic thermoplastics used in electronic devices. *Polymer Advanced Technology*. 9, 543–600.
- Innes J. D., (1996). Flame retardants and their market applications. *Flame retardants—101: basic dynamics, past efforts create future opportunities*. Baltimore: Fire Retardant Chemicals Association; 61–69.
- Joseph, A. & Serbaroli, J. R. (2006). A primer on flame retardants for thermoplastics. *Plastics Engineering Magazine*.
- Kuan C., Hsin W., Chen C., Yuen S., Kuan H. & Chiang C. (2008). Synthesis, characterization, flame retardance and thermal properties of halogen-free expandable graphite/PMMA composites prepared from sol–gel method. *Polymer Degradation and Stability*, 93, 1357-1363.
- Kirschbaum, G. (2001). Minerals on fire, Flame retardants look to mineral solutions. *3rd Minerals in Compoundings Conference, IMIL-AMI Joint Conference*. 8-10 April 2001.
- Laoutid, F., Bonnaud, L. Alexandre, M. Lopez-Cuesta, J. M. & Dubois P. (2009). New prospects in flame retardant polymer materials From fundamentals to nanocomposites. *Materials Science and Engineering*. 63, 100–125.

- Levchik, G.F., Levchik, S.V., Selevich, A.F., Lesnikovich, A.I., (1995). The effect of ammonium pentaborate on combustion and thermal decomposition of polyamide. *Flame Retardant Materials*, 3, 34–39.
- Levchik, S., Wilkie, C.A. (2000). *Char formation*, in: (A.F. Grand and C.A. Wilkie, Eds.), *Fire Retardancy of Polymeric Materials*. New York: Marcel Dekker
- Lewin, M., Weil, E.D., (2001). Mechanisms and modes of action in flame retardancy of polymers, in: A.R. Horrocks and D. Price, Eds., *Fire Retardant Materials*. Cambridge: Woodhead Publishing.
- Lomakin, S. M., Zaikov, G. E., (2003). Polyhalogenated flame retardants and dioxins, *Journal of Environmental Protection and Ecology*, 4(1), 95–119.
- Lum, R. M. (1977). Antimony oxide-PVC synergism: Laser pyrolysis studies of the interaction mechanism, *Journal of Polymer Science: Polymer Chemistry Edition*, 15(2), 489–497.
- Lyons, J. W. (1970). *The Chemistry and uses of fire-retardants*, New York: Wiley-Interscience.
- Manor-Orit, G. P. (2005). Flame retardants and the environment. *Speciality Chemicals.*, 25(7).
- Martin, C., Hunt, B.J., Ebdon, J.R., Ronda, J.C. & Cadiz, V. (2006). Synthesis, crosslinking and flame retardance of polymers of boron-containing difunctional styrenic monomers. *Reactive & Functional Polymers*, 66, 1047-1054.
- Martin, F. J., Price, K. R., (1968). Flammability of epoxy resins, *Journal of Applied Polymer Science*, 12(1), 143–158.

- Nishihara, H., Suda, Y., Sakuma, T., (2003). Halogen- and phosphorus-free flame retardant PC plastic with excellent moldability and recyclability. *Journal of Fire Sciences*. 21, 451–464.
- Oliver, W.C. & Pharr, G.M., (1992). An improved technique for determining hardness and elastic modulus using load and displacement sensing indentation experiments. *Materials Research Society*, 7, 1564-1583.
- Pearce, E.M., Shalaby, S.W., Barker, R.H. (1975). Retarding combustion of polyamides, in: M. Lewin, S.M. Atlas, and E.M. Pearce, Eds., *Flame-Retardant Polymeric Materials*, 1. New York: Plenum Press.
- Pitts, J.J. Scott, P.H. Powell, D.G. (1970). Thermal decomposition of antimony oxychloride and mode in flame retardancy. *Journal of Cellular Plastics*., 6, 35–37.
- Price, D., Gao, F., Milnes, G.J., Eling, B., Lindsay, C.I. and McGrail, T.P., (1999). Laser pyrolysis/time-of-flight mass spectrometry studies pertinent to the behavior of flame retarded polymers in real fire situations. *Polymer Degradation and Stability*., 64, 403–410 .
- Rothon, R. (2003). *Particulate-filled polymer composites*. Rapra Technology Limited.
- Sain M., Park S.H., Suhara F. & Law S. (2004). Flame retardant mechanical properties of natural fibre-PP composites containing magnesium hydroxide. *Polimer Degradation and Stability*, 83, 363-367.
- Shui, Y. L. & Ian, H. (2002) Recent developments in the chemistry of halogen-free flame retardant polymers. *Progress in Polymer Science*, 27, 1661–1712.



- Song, L., Hu, Y., Lin, Z., Xuan, S., Wang, S., Chen, Z. & Fan, W. (2004), Preparation and properties of halogen-free flame-retarded polyamide 6/organoclay nanocomposite. *Polymer Degradation and Stability*, 86, 535-540.
- Stevenson, D., Lee, V., Stein, D., Shah, T. (2002). Flame retardant formulations for HIPS and polyolefins using chlorinated paraffins, in: *Proceedings of the Spring International Conference on Fire Safety Conference*, San Antonio, Texas.
- Szabo, A., Marosfoi, B., Anna, P., and Marosi, Gy., (2009). Complex micro-analysis assisted design of fire retardant nanocomposites. *Flame Retardancy of Polymers: New Strategies and Mechanisms*, T.R. Hull and B.K. Kandola (eds.), The Royal Society of Chemistry, Cambridge, 74–91.
- Van, D.W. (1975). Some basic aspects of flame resistance of polymeric materials. *Polymer*, 16, 615–620.
- Weber, M. (1999). Mineral flame retardants, Overview & future trends. *Euromin '99, European Minerals & Markets, Nice, IMIL Conference*.
- Weil, E., (1975). Additivity, synergism and antagonism in flame retardancy, in: W.C. Kuryla and A.J. Papa, Eds., *Flame Retardancy of Polymeric Materials*, New York: Marcel Dekker.
- Weil, E.D. (1999). Synergists, adjuvants and antagonists in flame retardant systems, in: A.F. Grand and C.A. Wilkie, Eds., *Fire Retardancy of Polymeric Materials*. Marcel Dekker, New York, 115–145.
- Weil, E.D., Lewin, M., Rao, D., (2004). A search for an interactive flame retardant system for ethylene–vinyl acetate, in: *Proceedings of the 15th Conference on Recent Advances in Flame Retardancy of Polymeric Materials*, Stamford, Connecticut.

- Wheeler, J. M., (2009). *Nanoindentation under dynamic conditions*. Ph.D. Thesis, Clare College, University of Cambridge, England
- Xanthos, M. (2004). *Functional fillers for plastic*. New York: Wiley-VCH.
- Yang, Y., Shi, X., Zhao, R., (1999). Flame retardancy behavior of zinc borate. *Journal of Fire Sciences*. 17, 355–361.
- Yılmaz, A. H. (2007). *Use of huntite and hydromagnesite mineral in plastic materials as a flame retardant*. Msc Thesis. Dokuz Eylül University, Izmir
- Yılmaz, A. H. & Çelik, E. (2010). Use of huntite/hydromagnesite mineral in plastic materials as a flame retardant. *Polymer Composites*. 31, 1692–1700.
- Yılmaz, A. H. (2013). *The fabrication and technical applications of multifunctional materials*. Ph.D. Thesis. Dokuz Eylül University, Izmir.